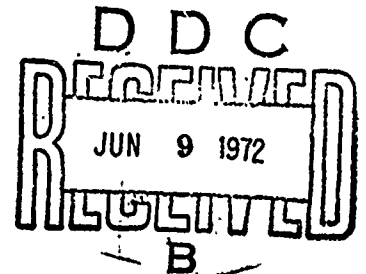


AD 742943

NAVAL POSTGRADUATE SCHOOL

Monterey, California



THESIS

STATISTICAL RELATIONS
BETWEEN SALINITY, TEMPERATURE
AND SPEED OF SOUND IN THE UPPER OCEAN

by

Harry Augustus Seymour, Jr.

Thesis Advisor:

H. Medwin

Thesis Co-Advisor:

N. E. Boston

March 1972

Reproduced by
NATIONAL TECHNICAL
INFORMATION SERVICE
Springfield, Va. 22151

Approved for public release; distribution unlimited.

Security Classification

DOCUMENT CONTROL DATA - R & D

(Security classification of title, body of abstract and indexing annotation must be entered when the overall report is classified)

1. ORIGINATING ACTIVITY (Corporate author) Naval Postgraduate School Monterey, California 93940		2a. REPORT SECURITY CLASSIFICATION Unclassified	
		2b. GROUP	
3. REPORT TITLE Statistical Relations Between Salinity, Temperature and Speed of Sound in the Upper Ocean			
4. DESCRIPTIVE NOTES (Type of report and, inclusive dates) Master's Thesis; March 1972			
5. AUTHOR(S) (First name, middle initial, last name) Harry Augustus Seymour, Jr.			
6. REPORT DATE March 1972		7a. TOTAL NO. OF PAGES 109	7b. NO. OF REFS 16
8a. CONTRACT OR GRANT NO.		9a. ORIGINATOR'S REPORT NUMBER(S)	
b. PROJECT NO.			
c.		9b. OTHER REPORT NO(S) (Any other numbers that may be assigned this report)	
d.			
10. DISTRIBUTION STATEMENT Approved for public release; distribution unlimited.			
11. SUPPLEMENTARY NOTES		12. SPONSORING MILITARY ACTIVITY Naval Postgraduate School Monterey, California 93940	
13. ABSTRACT - In situ measurements of salinity and temperature fluctuations at depths to 14 meters indicate distinct dependences at different times of the day. The variance of the salinity fluctuations decreased with increasing depth, but was greater just after sunrise than just prior to sunset. The variance of the temperature fluctuations decreased with increasing depth just prior to sunset, but increased with depth immediately after sunrise. The correlation length of the sound index of refraction was calculated by using the variance of the sound velocity fluctuations, and the variance of sound amplitude modulation in the theory of Mintzer. This analysis shows that microstructure patch size increases approximately linearly with depth. The power spectral densities of the salinity, temperature and sound velocity fluctuations show peaks of energy corresponding to dominant ocean wave frequencies.			

Security Classification

14.

KEY WORDS

LINK A

LINK B

LINK C

ROLE

WT

ROLE

WT

ROLE

WT

Salinity
 Temperature
 Sound Velocity
 Variance
 Correlation Length
 Power Spectral Density
 Temporal Correlation

Statistical Relations
Between Salinity, Temperature
and Speed of Sound in the Upper Ocean

by

Harry Augustus Seymour, Jr.
Lieutenant, United States Navy
B.S., United States Naval Academy, 1965

Submitted in partial fulfillment of the
requirements for the degree of

MASTER OF SCIENCE IN OCEANOGRAPHY

from the
NAVAL POSTGRADUATE SCHOOL
March 1972

Author

Harry Augustus Seymour, Jr.

Approved by:

William H. Stebbins
Thesis Advisor

Noel Gordon
Thesis Co-Advisor

Walter F. Lipps
Chairman, Department of Oceanography

William H. Clancy
Academic Dean

ABSTRACT

In situ measurements of salinity and temperature fluctuations at depths to 14 meters indicate distinct dependences at different times of the day. The variance of the salinity fluctuations decreased with increasing depth, but was greater just after sunrise than just prior to sunset. The variance of the temperature fluctuations decreased with increasing depth just prior to sunset, but increased with depth immediately after sunrise. The correlation length of the sound index of refraction was calculated by using the variance of the sound velocity fluctuations, and the variance of sound amplitude modulation in the theory of Mintzer. This analysis shows that microstructure patch size increases approximately linearly with depth. The power spectral densities of the salinity, temperature and sound velocity fluctuations show peaks of energy corresponding to dominant ocean wave frequencies.

TABLE OF CONTENTS

I.	INTRODUCTION	11
	A. HISTORY	11
	B. SIGNIFICANCE OF PROBLEM	12
	C. OBJECTIVES OF THIS RESEARCH	13
II.	EXPERIMENTAL PROCEDURE	14
	A. OCEANOGRAPHIC ENVIRONMENT	14
	1. Location	14
	2. Time of Year	14
	3. Meteorological, Oceanographic, and Biological Conditions at Time of Project	14
	B. EQUIPMENT USED DURING EXPERIMENT	16
	1. Bissett-Berman STD Model 9006	16
	2. Thermistors (3)	18
	3. Ramsay Corporation Mark I SVTD	18
	4. Wave Height Sensors	18
	5. Particle Velocity Sensor	19
	6. High Pass Filter #1 - Krohn-Hite Model 3340	19
	7. Band Pass Filter #2 - Krohn-Hite Model 330-A	19
	8. Band Pass Filter #3 - Velocimeter	19
	9. Amplifier #1: Preston Scientific Model 8300 xwb	19
	10. Amplifier #2: Preston Scientific Model 8300 xwb	19
	11. Amplifier #3: Hewlett-Packard Model 2470	19
	12. Amplifier #4: Hewlett-Packard Model 2470	19

13.	Amplifier #5: Hewlett-Packard Model 2470	20
14.	Amplifier #6: Hewlett-Packard Model 2470	20
15.	Sangamo Magnetic Tape Recorder Model 3500	20
C.	EXPERIMENTAL CONFIGURATION	20
1.	Schematics	20
2.	Geometry of Sensors	24
III.	DATA CUMULATION AND RUN DESCRIPTION	29
IV.	DATA REDUCTION	30
A.	INTRODUCTION	30
B.	MAGNETIC TAPE TO STRIP-CHART RECORDING	30
C.	ANALOG TO DIGITAL TAPE	32
D.	CONVERSION OF TAPED DIGITAL DATA TO DATA CARDS	32
V.	DATA ANALYSIS	34
A.	INTRODUCTION	34
B.	STATISTICAL PROGRAMMING	34
C.	STATISTICAL ANALYSIS	36
1.	Introduction	36
2.	Variance of Oceanographic Fluctuations	36
3.	Variance of Temperature Fluctuations	37
4.	Variance of Salinity Fluctuations	43
5.	Probability Density Function Results	44
6.	Normalized Autocorrelation Function	44
7.	Power Spectral Density	44

VI.	PARAMETRIC INTERRELATIONS BETWEEN SALINITY, TEMPERATURE, AND SOUND VELOCITY	48
	A. INTRODUCTION	48
	B. DERIVATION OF THEORETICAL SOUND VELOCITY VARIANCE FROM WILSON'S EQUATION	48
	1. Wilson's Equation	48
	2. Computation of Variance	48
	3. Dropping the Term, $\text{var}(T^2)$, as Negligible Yields the Final Result	48
VII.	CONCLUSIONS	52
VIII.	RECOMMENDATIONS FOR FURTHER STUDY	53
	APPENDIX A GENERAL DESCRIPTION OF BISSETT-BERMAN MODEL 9006 SALINITY, TEMPERATURE AND DEPTH MONITORING SYSTEM	54
	APPENDIX B DATA CUMULATION AND RUN DESCRIPTION	56
	COMPUTER OUTPUT	59
	COMPUTER PROGRAM A	97
	COMPUTER PROGRAM B	103
	BIBLIOGRAPHY	104
	INITIAL DISTRIBUTION LIST	106
	FORM DD 1473	108

LIST OF TABLES

I.	Values of Variance as Computed From Power Spectral Densities	38
II.	Values of Variance as Computed Directly From Time Series Data	38
III.	Values of Salinity as Determined From Nansen Cast Samples	58

LIST OF FIGURES

1.	NUC Oceanographic Research Tower	15
2.	Bathythermograph Traces	17
3.	Bissett-Berman STD Flow Diagram	21
4.	Ramsay Sound Velocimeter Flow Diagram	22
5.	Thermistor Flow Diagram	23
6.	Geometrical Relationships Between Sensors	25
7.	Geometrical Separations Between Oceanographic Sensors and Acoustic Source	26
8.	Bissett-Berman STD Model 9006	27
9.	STD Relationship With Other Sensors	27
10.	STD and Other Sensors	28
11.	STD and Other Sensors	28
12.	Representative Oceanographic Fluctuations	31
13.	Plot of Temperature Variance Versus Time of Day	40
14.	Plot of Salinity Variance Versus Time of Day	41
15.	Plot of Sound Velocity Variance Versus Time of Day	42
16.	Salinity Histogram	45
17.	Sound Velocity Histogram	46
18.	Temporal Correlation of Thermistor 1 Run 3	59
19.	Temporal Correlation of Thermistor 2 Run 3	60
20.	Temporal Correlation of Salinity Run 3	61
21.	Temporal Correlation of Thermistor 2 Run 4	62
22.	Temporal Correlation of Salinity Run 4	63

23.	Temporal Correlation of Sound Velocity Run 4	64
24.	Temporal Correlation of Thermistor 1 Run 5	65
25.	Temporal Correlation of Thermistor 2 Run 5	66
26.	Temporal Correlation of Salinity Run 5	67
27.	Temporal Correlation of Sound Velocity Run 5	68
28.	Temporal Correlation of Thermistor 1 Run 6	69
29.	Temporal Correlation of Salinity Run 6	70
30.	Temporal Correlation of Sound Velocity Run 6	71
31.	Temporal Correlation of Thermistor 1 Run 8	72
32.	Temporal Correlation of Salinity Run 8	73
33.	Temporal Correlation of Sound Velocity Run 8	74
34.	Temporal Correlation of Thermistor 1 Run 9	75
35.	Temporal Correlation of Salinity Run 9	76
36.	Temporal Correlation of Thermistor 1 Run 10	77
37.	Temporal Correlation of Salinity Run 10	78
38.	Power Spectral Density of Thermistor 1 Run 3	79
39.	Power Spectral Density of Thermistor 2 Run 3	80
40.	Power Spectral Density of Salinity Run 3	81
41.	Power Spectral Density of Thermistor 2 Run 4	82
42.	Power Spectral Density of Salinity Run 4	83

43.	Power Spectral Density of Sound Velocity Run 4	84
44.	Power Spectral Density of Thermistor 1 Run 5	85
45.	Power Spectral Density of Thermistor 2 Run 5	86
46.	Power Spectral Density of Salinity Run 5	87
47.	Power Spectral Density of Sound Velocity Run 5	88
48.	Power Spectral Density of Thermistor 1 Run 6	89
49.	Power Spectral Density of Salinity Run 6	90
50.	Power Spectral Density of Sound Velocity Run 6	91
51.	Power Spectral Density of Thermistor 1 Run 8	92
52.	Power Spectral Density of Sound Velocity Run 8	93
53.	Power Spectral Density of Thermistor 1 Run 9	94
54.	Power Spectral Density of Thermistor 1 Run 10	95
55.	Power Spectral Density of Salinity Run 10	96

ACKNOWLEDGEMENT

The author wishes to express his appreciation to his two thesis advisors Dr. Herman Medwin and Dr. Noel E. Boston for their guidance and assistance throughout the project.

The author would also like to thank LCDR Gail Griswold of the Pt. Mugu Oceanographic Detachment, Mr. Dana Maberry of the Naval Postgraduate School, and Mr. Dale Good of the Naval Undersea Research and Development Center all of whom played integral roles necessary to the successful completion of the project.

The author would also like to acknowledge the support of the Navy Ship Systems Command, as well as the Office of Naval Research which funded the project under ONR Contract P.O. 2-0012.

Finally, but not to the least degree, the author would like to thank his wife for the many hours she spent typing the several drafts of this manuscript.

I. INTRODUCTION

A. HISTORY

The study of sound propagation in the ocean and the effects of oceanographic parameters (particularly temperature) on it has been the subject of considerable research since early World War II. Wilson [Ref. 1] formulated an equation describing the relationships between sound velocity, temperature and pressure in distilled water, and then extended his work to an oceanic regime by utilizing filtered seawater diluted with distilled water to obtain desired salinity dependence [Ref. 2]. Since Wilson's efforts in this field, many investigators have attempted to revise the sound speed equation with newer techniques and theory. The reasons for revised formulations included, among others, the use of new type velocimeters [Ref. 3] the suspicion that standard sea water did not maintain a standard salinity to sound speed relationship [Ref. 4], the desire to obtain simpler expressions, and the use of a more realistic range of values for the oceanographic parameters [Ref. 5].

While these investigations into the parametrical relationships to sound velocity were proceeding, other investigators attempted to measure the magnitude of the fluctuations of the important parameters affecting sound propagation in seawater. Liebermann [Ref. 6] studied the effects of temperature inhomogeneities on sound propagation. He found that thermal inhomogeneities do have an effect on the scattering,

intensity, and refraction of the sound transmission. Shonting [Ref. 7] also measured the thermal microstructure, his results indicating the importance and magnitudes of temperature fluctuations in the ocean environment.

B. SIGNIFICANCE OF PROBLEM

The characteristics of sound propagation in a deep ocean environment (defined in this paper as the depth below the thermocline) are well known and predictable. This is due to the fact that in the deep water regime the fluctuations of temperature and salinity are minor. As a result of this predictability, sound is used properly and constructively in deep waters. For the United States Navy this specifically relates to optimum usage of sound in the field of anti-submarine warfare.

However the propagation of sound in the shallow ocean environment and in the near surface region is not as predictable, and as a result seriously hinders the user and the planner in their efforts to utilize sound to its best advantage. The near surface region usually plays a part in long range propagation of sound.

Sound velocity amplitude and phase in the region between sound source and sound receiver change in the near surface regions. They change due to small scale variations in oceanographic parameters including possibly the presence of microbubbles and organic content in the regime.

C. OBJECTIVES OF THIS RESEARCH

The main motivation in this research was to statistically describe the oceanic parameters of temperature and salinity, and to relate their statistics to the statistics of sound velocity in a near surface environment. It was hoped to obtain enough data to enable one to draw conclusions concerning the variation of the fluctuations with respect to depth and time of day. If such concrete conclusions could be reached in the near surface region, then the users of sound either in oceanographic research or in present anti-submarine warfare would be afforded new tools with which to update the state-of-the-art in sound use and understanding.

II. EXPERIMENTAL PROCEDURE

A. OCEANOGRAPHIC ENVIRONMENT

1. Location

Due to its advantageous location of being rigidly fixed in a shallow water environment the N.U.C. Oceanographic Research Tower, approximately one mile off Mission Beach, California, was chosen as the location for the project. It allows for continuous data accumulation and monitoring as well as some analysis in a near laboratory controlled environment.

Figure 1 is an illustration of the tower. It is fixed by supporting pins driven 63 feet into the ocean floor. Electrical power is supplied from shore thereby guaranteeing stable voltage and frequency. The tower is located in 60 feet (18 m) of water with a sandy bottom and is free of water traffic most of the time. The upper level of the two level tower was the location for electronic support equipment. The lower was for handling equipment.

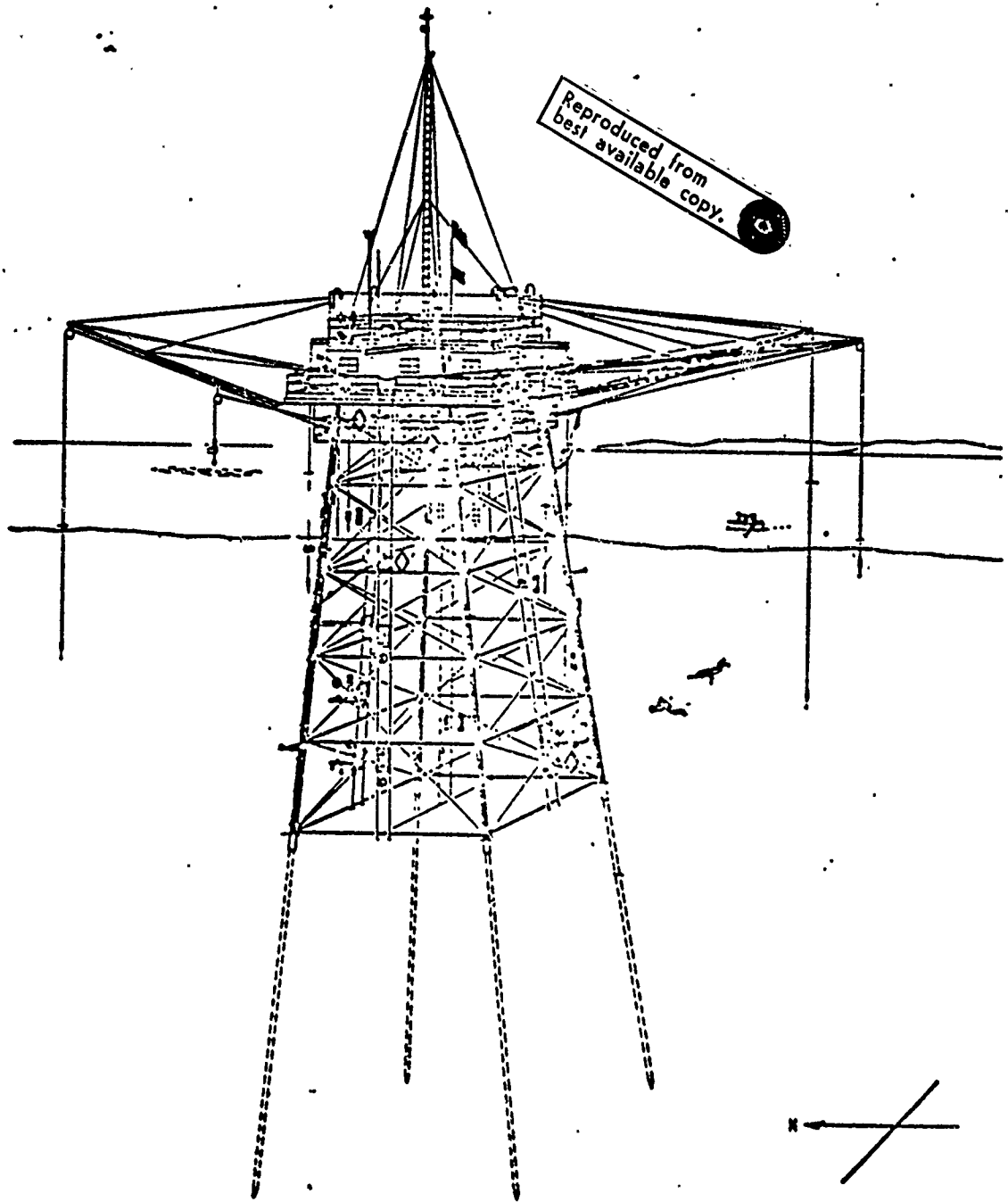
2. Time of Year

The experiment was conducted from the afternoon of 21 October 1971 through the morning of 22 October 1971.

3. Meteorological, Oceanographic, and Biological

Conditions at Time of Project

- a. Weather State: clear to light haze
- b. Wind: 21 October - 300-320 from 7 to 9 kts
22 October - 065-110 from 2 to 8 kts



Reproduced from
best available copy.

FIGURE 1. NUC Oceanographic Research Tower.

c. Wind Waves: 0 to $\frac{1}{2}$ ft from crest to trough
d. Swell: 2 ft from Northwest
e. Bubbles: 1 square foot in vicinity of tower stanchions during all runs. During run #4 bubbles were present on the surface in patches of size 20 ft by 2 ft near vicinity of tower.

f. Biologics

(1) Seaweed. Small amount of sea grass on surface during run #4.

(2) Animal Life. Seal in vicinity during run #6, porpoise and seals in vicinity during runs 7 and 8.

g. Temperature Structure: thermocline varied from depths between 40 ft to 60 ft below the surface (see Fig. 2)

h. Salinity: Nansen Cast results, as determined from Hytech model 621 salinometer, found in Table III.

B. EQUIPMENT USED DURING EXPERIMENT

1. Bissett-Berman STD Model 9006

a. Temperature Sensor

- (1) Time Constant: 0.35 sec
- (2) Output: 0 - 10 mv DC
- (3) Temperature Range Used: 14 - 19° C
- (4) Accuracy: $\pm 0.02^\circ$ C

b. Salinity Sensor

- (1) Time Constant: 0.35 sec
- (2) Output: 0 - 10 mv DC

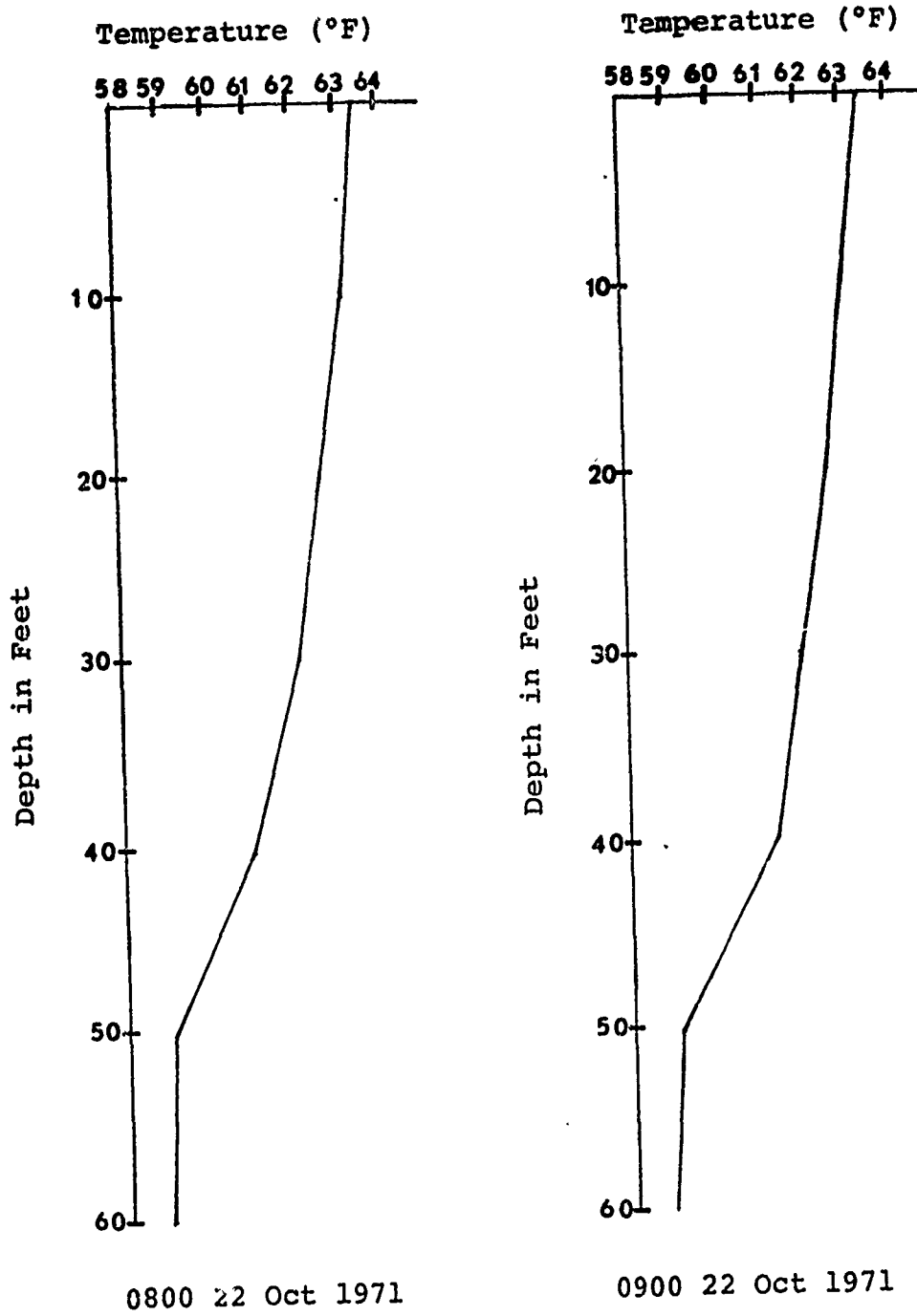


FIGURE 2. Bathythermograph Traces.

(3) Salinity Range Used: 37.5 - 39.5 ppt
(before correction)

(4) Accuracy: ± 0.03 ppt

c. Detailed Description Found in Appendix A

2. Thermistors (3)

a. Time Constant: 150 milliseconds

b. Output: .0553 volts per °C

c. Temperature Range: Thermistors nulled using Wheatstone Bridge Circuit prior to start of each run.

d. For further description see NPS thesis of LCDR Duchock, March 1972.

3. Ramsay Corporation Mark I SVTD

a. Time Constant: 160 microseconds

b. Output: 0 - 10 v DC

c. Sound Velocity Range: 1400 - 1600 m/sec

d. Accuracy: ± 0.01 m/sec

e. For further description see NPS thesis of LCDR Duchock, March 1972.

4. Wave Height Sensors

a. Baylor Wave Profile Recorder System

(1) Output: 50 millivolts per foot of height

(2) Accuracy: 1% or reading

(3) For further description see NPS thesis of LT Bordy, March 1972.

b. Interstate Electronics Corporation Pressure Wave Gauge

(1) Output: .25 v/psi

(2) Accuracy: 2% of reading

5. Particle Velocity Sensor

a. Engineering Physics Company Electromagnetic

Current Meter

(1) Output: variable voltage per meter/second

(2) Accuracy: 1% of full scale reading

b. For further description see NPS thesis of LT

Bordy, March 1972.

6. High Pass Filter #1 - Krohn-Hite Model 3340

a. Gain: 0dB

b. High Pass Filter Cutoff: 0.01 HZ

7. Band Pass Filter #2 - Krohn-Hite Model 330-A

a. Gain: 0dB

b. Low Pass Cutoff: 0.02 HZ

High Pass Cutoff: 2000 HZ

8. Band Pass Filter #3 - Velocimeter

a. Gain: 0dB

b. Low Pass Cutoff: 0.02 HZ

High Pass Cutoff: 2000 HZ

9. Amplifier #1: Preston Scientific Model 8300 xwb

a. Gain: 500

10. Amplifier #2: Preston Scientific Model 8300 xwb

a. Gain: 1

11. Amplifier #3: Hewlett-Packard Model 2470

a. Gain: 30

12. Amplifier #4: Hewlett-Packard Model 2470

a. Gain: 100

13. Amplifier #5: Hewlett-Packard Model 2470

a. Gain: 100

14. Amplifier #6: Hewlett-Packard Model 2470

a. Gain: varied 100-300

15. Sangamo Magnetic Tape Recorder Model 3500

a. 14 channel with 11 channels allocated for oceanographic parameter data were utilized.

b. Channel Allocation:

- (1) Ramsay Temperature Sensor (not used)
- (2) Ramsay Velocimeter
- (3) Bissett-Berman Salinometer
- (4) Turbulent Velocity (horizontal component)
- (5) Turbulent Velocity (vertical component)
- (6) Baylor Wave Height
- (7) Sound Amplitude Modulation
- (8) Pressure Wave Height
- (9) Thermistor #1
- (10) Bissett-Berman Temperature (not used)
- (11) Thermistor #2
- (12) Thermistor #3
- (13) Sound Phase Modulation
- (14) Voice (not used)

C. EXPERIMENTAL CONFIGURATION

1. Schematics

- a. Bissett-Berman STM - See Fig. 3
- b. Ramsay Velocimeter - See Fig. 4
- c. Temperature Thermistors - See Fig. 5

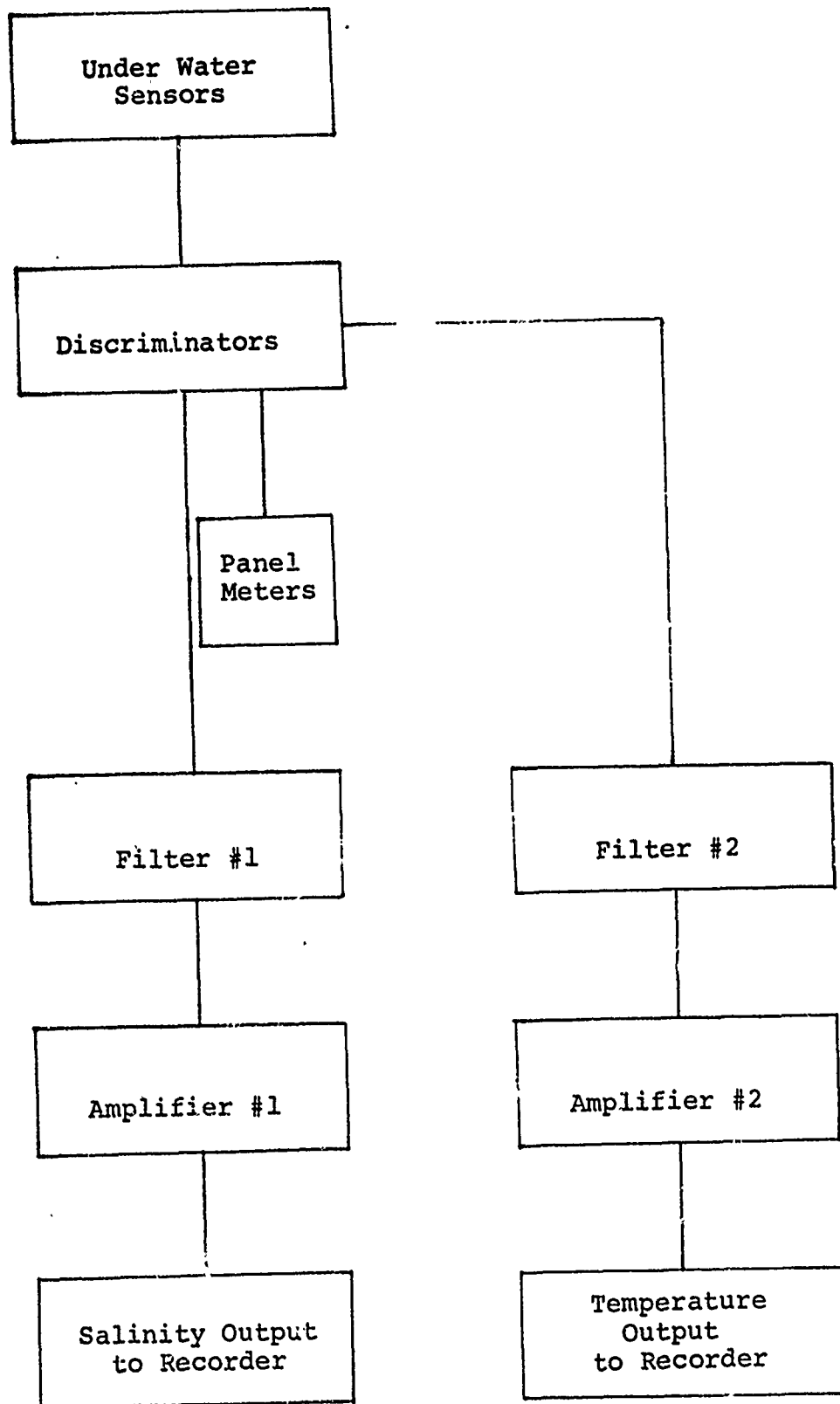


FIGURE 3. Bissett-Berman STD Flow Diagram.

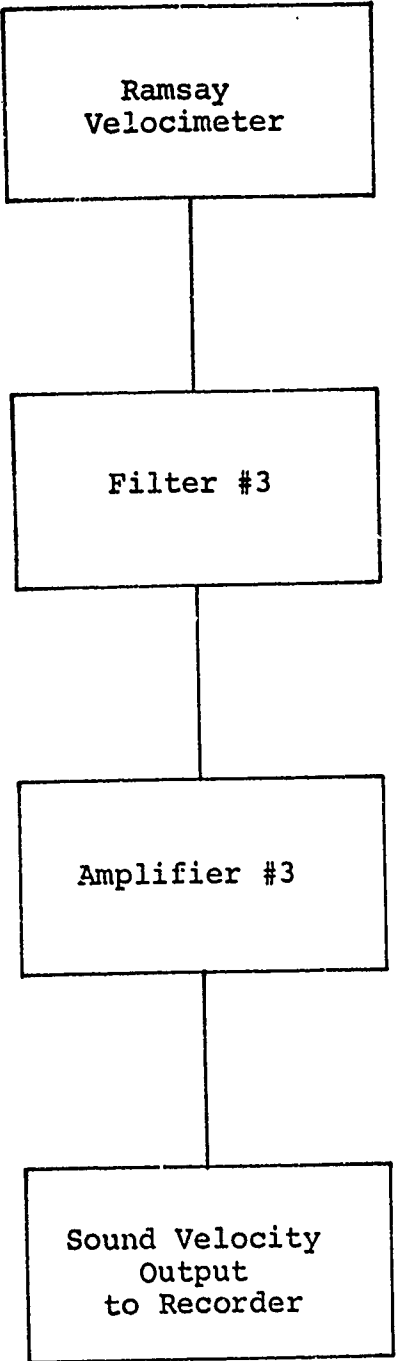


FIGURE 4. Ramsay Sound Velocimeter Flow Diagram.

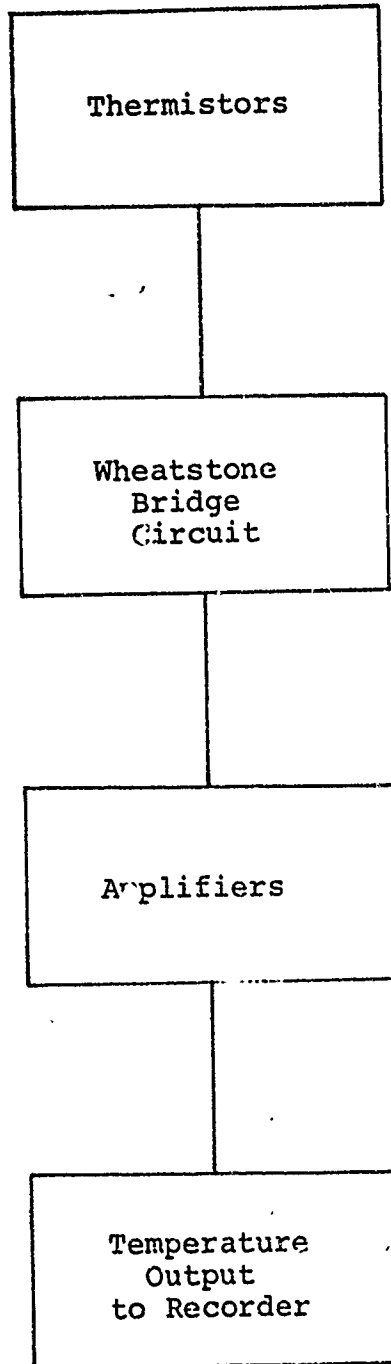


FIGURE 5. Thermistor Flow Diagram.

2. Geometry of Sensors

The sensors' geometric relationships were deemed to be of major importance in view of potential acoustical and physical interferences which could have had an adverse effect on the experimental results. In addition to the attempt to describe the oceanic regime in terms of the oceanic parameters two acousticians simultaneously conducted experiments related to sound amplitude modulation, sound dispersion, and phase fluctuations. (See NPS thesis of LCDR W. J. Smith, Jr., December 1971 and thesis of LCDR Juerger Rautmann, December 1971.)

In order to reduce the effects of mutual interference between the sensors especially in the path of sound propagation between hydrophone and receiver, a physical separation of the sensors was mandatory. The geometrical separations between the sensors as shown in Figs. 6, 7 were used. Photographs of the Bissett-Berman STD and the geometrical relationships of the other sensors to it appear in Figs. 8-11.

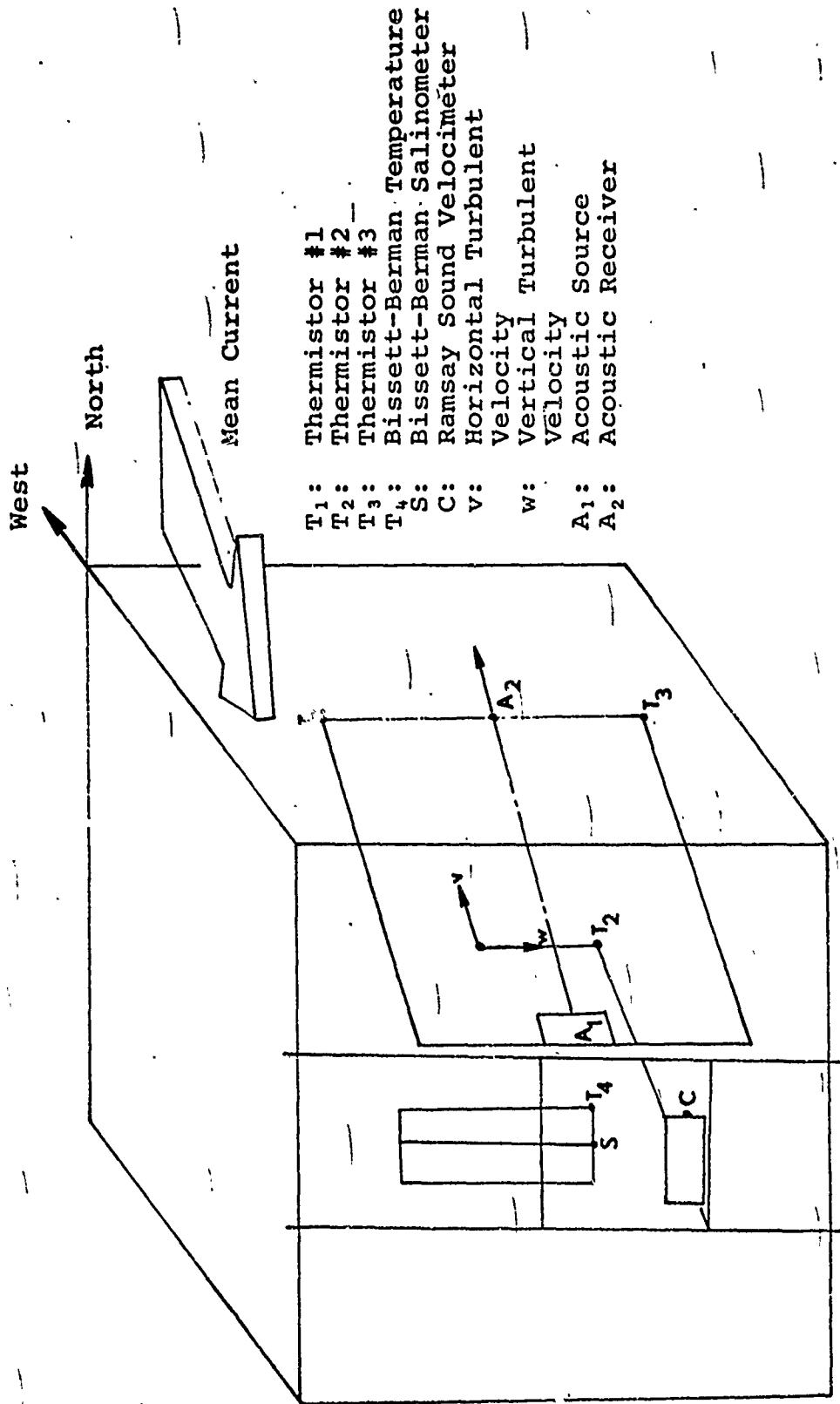


FIGURE 6. Geometrical Relationships Between Sensors.

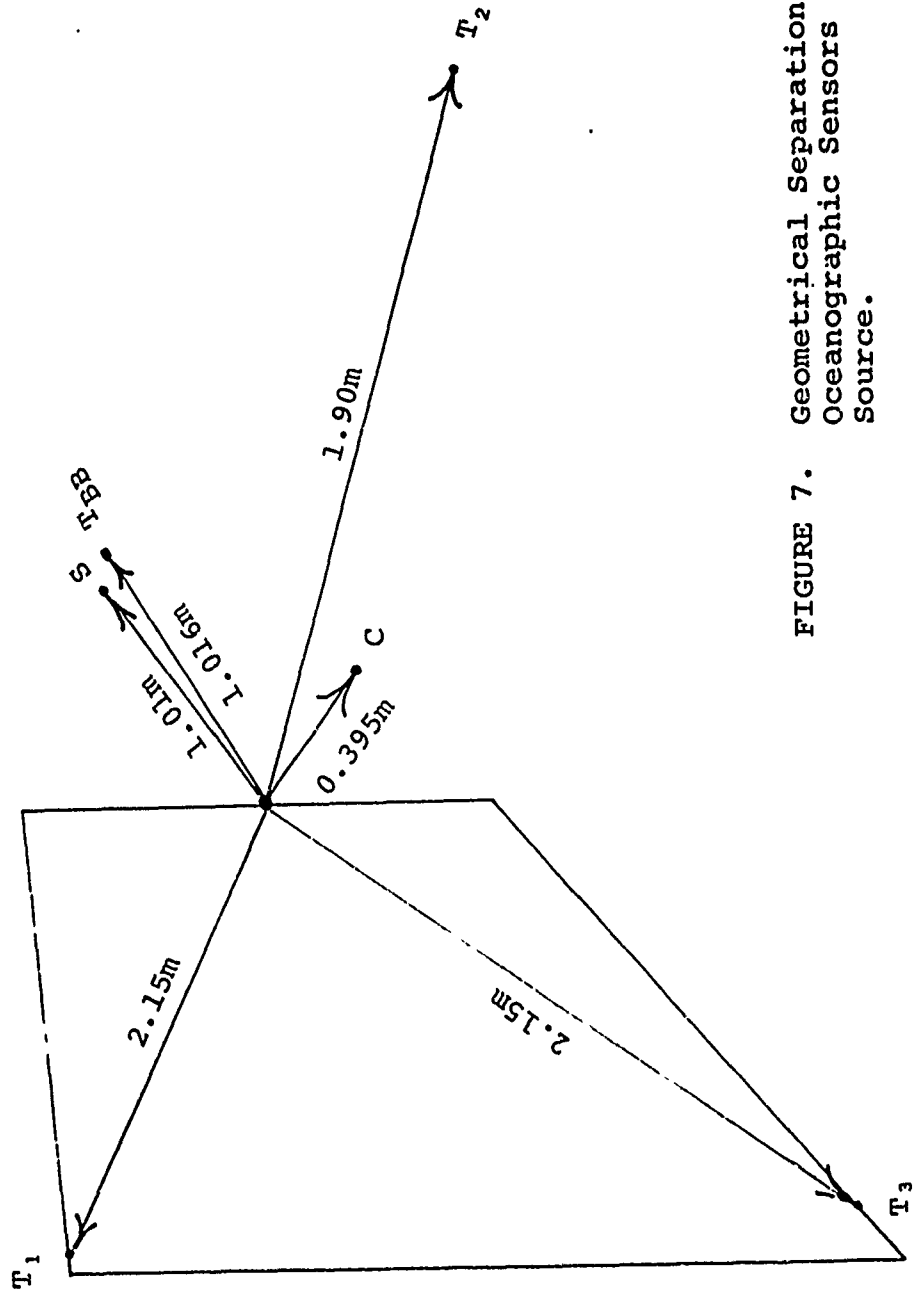


FIGURE 7. Geometrical Separations Between Oceanographic Sensors and Acoustic Source.



FIGURE 8.

Bisset-Berman
STD Model 9006.



FIGURE 9.

STD Relationship
With Other Sensors.

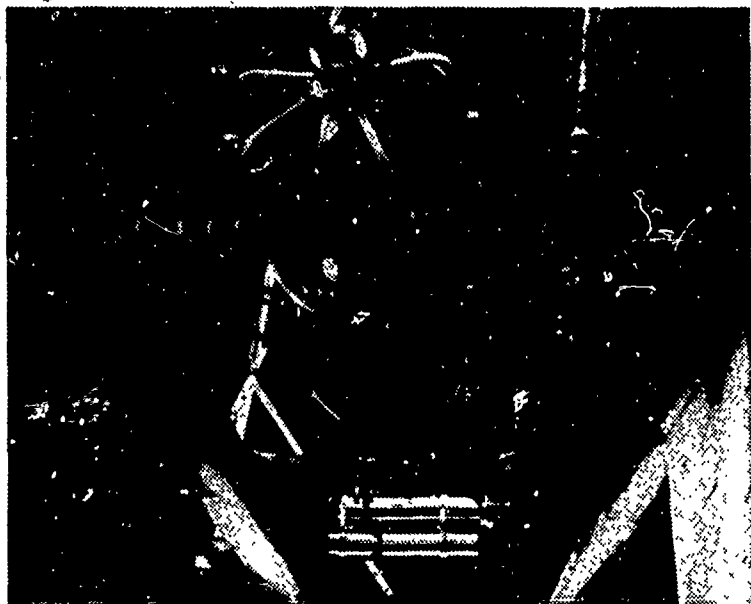


FIGURE 10.
STD and
Other Sensors.

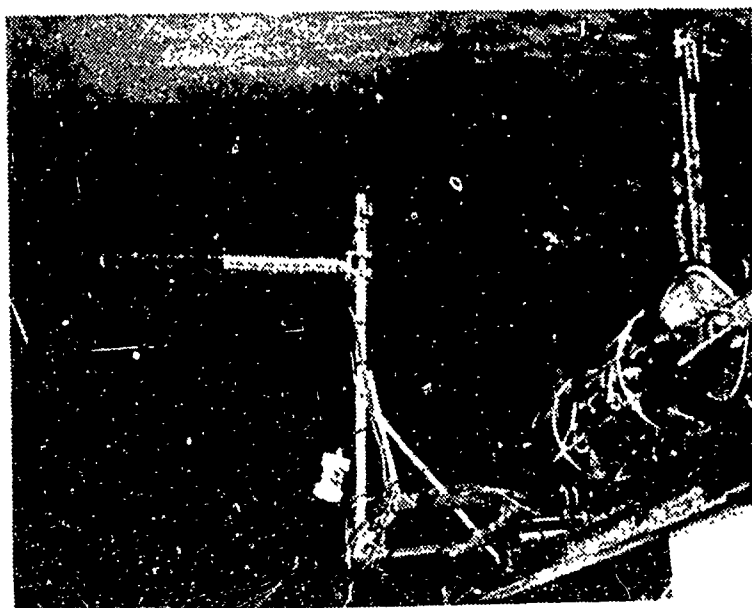


FIGURE 11.
STD and
Other Sensors.

III. DATA COLLECTION AND RUN DESCRIPTION

Data collection and run description will be found on page 56 under
Appendix B.

IV. DATA REDUCTION

A. INTRODUCTION

The analog data were recorded for each run on the Sangamo Model 3500 magnetic tape recorder operated at a speed of 1 7/8 ips using FM electronics. The recorded data were then transferred to a Brush Mark 200 Strip-Chart recorder. In some instances, in order to produce better resolution, the recorded data were transferred to a Brush Mark 2 Strip-Chart recorder through a Krohn-Hite Model 3340 filter set on low pass-max flat (see Fig. 12). The printed analog data were converted to digital data on magnetic tape using the Fleet Numerical Weather Central, Point Pinos, California tracing digitizer. The taped data were transferred to punched IBM data cards compatible for statistical analysis on an IBM 360-67 digital computer.

B. MAGNETIC TAPE TO STRIP-CHART RECORDING

The recorder playback speed was seven and one half inches per second, which is an increase of four times over the data collection speed. The strip-chart recorder was run at a speed of five millimeters per second. The speed differentials between the record, playback, and strip-chart phases were programmed in the IBM program used for data analysis. The sensitivity setting on the strip-chart recorder was important for data presentation and analysis. The sensitivity settings varied from run to run and with

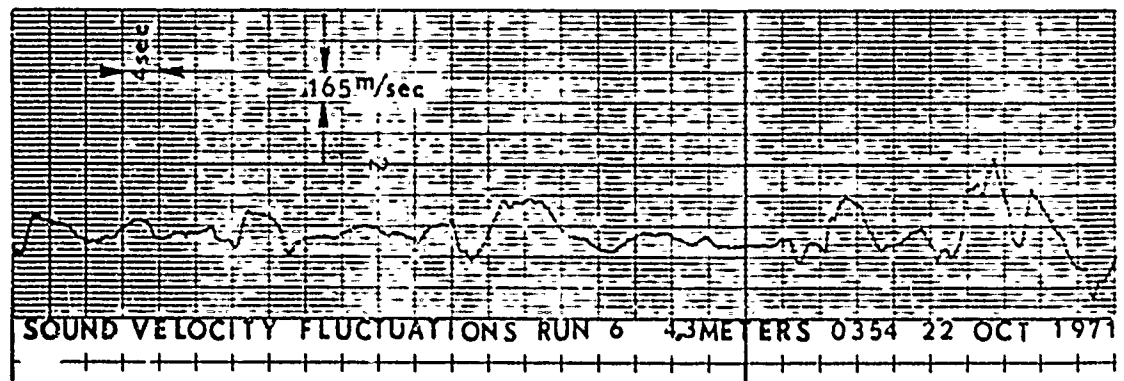
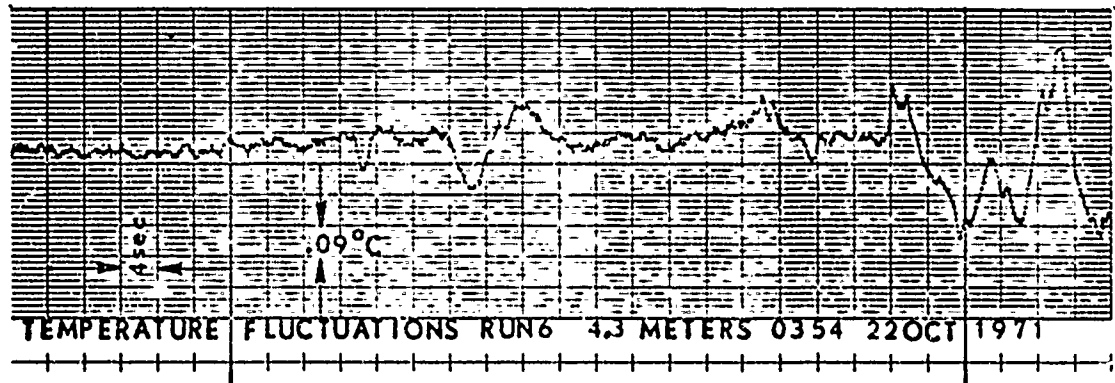
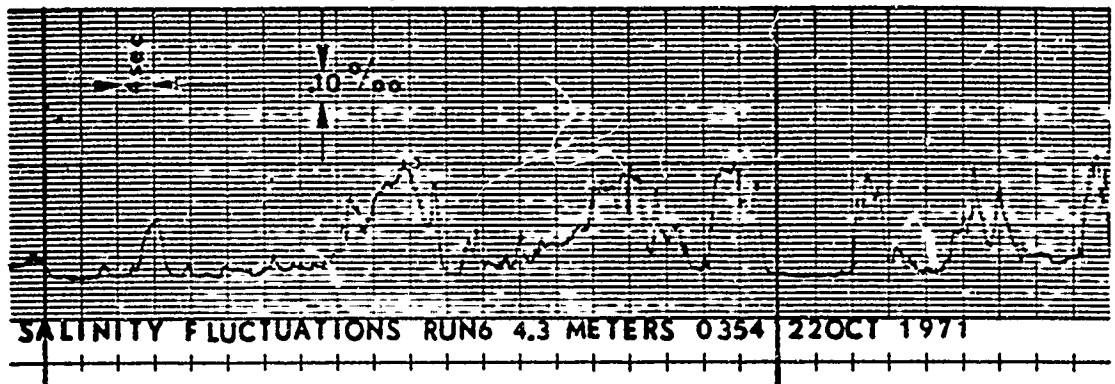


FIGURE 12. Representative Oceanographic Fluctuations.

each parameter. The settings used can be found in Appendix E.

C. ANALOG TO DIGITAL TAPE

In order to utilize the IBM 360 computer to determine the statistics of the fluctuations, the analog data on the strip-chart record had to be converted to digital form. In order to effect the conversion use was made of the Calma tracing digitizer at Fleet Numerical Weather Central's Point Pinos, California facility. The tracing digitizer transfers analog data to digital data on magnetic tape at a sampling rate of 100 samples per inch in both the x and y directions. The length of each run analyzed amounted to approximately the first nineteen minutes of the run while the number of data points varied depending upon the positioning of the strip chart on the digitizer. It was important for future correlations that the tracing of all parameters began at the same starting point. This was ensured by starting at the sharp line transient signaling the start of a particular run.

D. CONVERSION OF TAPED DIGITAL DATA TO DATA CARDS

Conversion of taped digital data to a form compatible for use on the IBM 360 Digital Computer, i.e. data card form, was accomplished using Fleet Numerical Weather Central's Computer Facility. Fourteen data points were recorded on each IBM card. The number of data points per

run varied depending on the positioning of the strip chart on the Calma Plotter at Point Pinos, but the average run produced approximately 5400 data points.

V. DATA ANALYSIS

A. INTRODUCTION

Attention was focused entirely on analysis of the statistics of the fluctuating parameters. Two arguments led to this method of analysis: first of all, the statistics of the oceanographic variables are important in determining the statistics of sound propagation. Since the major objective of the experiment was to define the medium in order to determine its effect upon the propagation of sound the statistical method of analysis was the natural approach. The second reason for using statistics as the major tool for analysis was due to the relatively wide separation between sensors which was required to prevent instrumental interactions. In order to enable one to discuss the interrelationships between spaced sensors it was necessary either to correct for the lack of identical point location or to consider the statistical relations, assuming that the medium was statistically homogeneous in the region of the sensors. The latter is the easier choice.

B. STATISTICAL PROGRAMMING

The programs used in the data analysis appear in Appendix C.

Program A analyzed the data for mean, variance, normalized autocorrelation function, and power spectral density. The standard Blackman-Tukey method was used to compute power spectral density with a Parzen window as the spectral

window. Program A was modified to compute variance by two methods. The first method calculated variance by integrating the power spectral density. A subroutine (aver) was then added to calculate variance directly from the time series data.

Program B was used to output data from which a histogram could be plotted of the number of times a particular value of a parameter occurred versus the value of that parameter.

In utilizing program A several important inputs were necessary:

NTS: number of data points

MLAG: number of time lags = 10% (NTS)

DT: time increment in seconds/sample. This parameter took into account the different driving speeds of the strip-chart recorder, playback and record modes of the tape recorder, and the analog-to-digital digitizer.

$$DT = \frac{1}{(5/4 \text{ mm/sec}) \left(\frac{\text{inch}}{25.4\text{mm}}\right) \left(\frac{100 \text{ samples}}{\text{inch}}\right)}$$

$$= 0.2032 \text{ sec/sample}$$

$$\Delta f: \text{ frequency increment} = \frac{1}{2 \text{ MLAG (DT)}}$$

FBHZ: lowest frequency

FEHZ: highest frequency = Nyquist Frequency

$$FEHZ = \frac{1}{2(.2032)} = 2.46 \text{ HZ}$$

Calibration factor: variable on each run

The raw data on the IBM cards had the units of inches. The calibration factor converted inches to volts per millimeter by incorporating the Brush recorder sensitivity setting into the program input thereby giving the data units of volts per inch. When each data point was multiplied by the calibration factor the results produced were in voltage units.

$$\text{C.F.} = \frac{\# \text{ volts}}{\text{millimeter}} \left(\frac{25.4 \text{ millimeters}}{\text{inch}} \right) = "x" \frac{\text{volts}}{\text{inch}}$$

C. STATISTICAL ANALYSIS

1. Introduction

In order to convert the program output in volts to the correct oceanographic units and values, conversion factors for sensor voltage sensitivities, amplification factors and filter gains were used. On location monitoring of the data combined with post-experimental review indicated some runs higher in quality and accuracy than others. For such reasons runs 3,4,5,6,7,9,10 were analyzed for salinity and temperature, and runs 4,5,6,8 for sound velocity. The conversion factors used were:

thermistors: 5.53 v/°C

salinity: 2.5v/‰

sound velocity: 1.5 v/ $\frac{\text{m}}{\text{sec}}$

2. Variances of Oceanographic Fluctuations

The values of the variances of the oceanographic parameters as computed by integrating the power spectral densities are indicated in Table I.

The values of the variances of the oceanographic parameters as computed directly from the time series data are listed in Table II.

It was noted that there was only a very slight difference between the values of variance computed by both methods. However the variances used in subsequent analysis were those computed directly from the data thereby ensuring a higher degree of accuracy. Additionally all subsequent analysis was performed using temperature data measured by thermistor #1 since the quality of the fluctuating signal from that sensor was the best and most consistent throughout all runs. (Thermistor #2 data used during run 4 since thermistor 2 was operating reliably at that time). Figures 13-15 are graphical displays of variances versus time of day with depths at which runs were made noted in parentheses.

A survey of the literature indicates that this experiment was unique in its attempt to establish statistical relationships between the described oceanographic parameters. As a result little direct comparison with previous results is possible.

3. Variance of Temperature Fluctuations

Two past investigators have studied temperature fluctuations in the near surface region on approximately the same time scale as was used in this experiment. Shonting used a double-beaded thermistor manufactured by Fenwall Electronics, Inc., Framingham, Massachusetts, to observe thermal microstructure. He conducted his measurements in the Bahamas in

Run	Time	Depth	Sound Vel. Variance	Temp #1 Variance	Temp #2 Variance	Salinity Variance
	21 OCT					
3	1616	9.0m	-	.0187(°C) ²	.0121(°C) ²	.0016(‰) ²
4	1648	13.9m	.0294(M/S) ²	.0167	-	.0013
5	1728	6.9m	.0003	.0230	.0002	.0023
	22 OCT					
6	0354	4.3m	.0072	.0052	-	.0044
8	0650	9.5m	.0023	.0013	-	.0110
9	0725	14.6m	-	.0076	-	.0065
10	0802	7.8m	-	.0017	-	.0002

TABLE I

Run	Time	Depth	Sound Vel. Variance	Temp #1 Variance	Temp #2 Variance	Salinity Variance
	21 OCT					
3	1616	9.0m	-	.0143(°C) ²	.0093(°C) ²	.0016(‰) ²
4	1648	13.9m	.0293(M/S) ²	.0129	-	.0012
5	1728	6.9m	.0003	.0184	.0002	.0023
	22 OCT					
6	0354	4.3m	.0072	.0042	-	.0041
8	0650	9.5m	.0021	.0010	-	.0111
9	0725	14.6m	-	.0059	-	.0059
10	0802	7.8m	-	.0013	-	.0002

TABLE II

August 1967. Analysis of his measurements taken between 1323-1400 indicated representative values of variance of approximately $25 \times 10^{-6} (\text{°C})^2$ at two meters depth and approximately $72 \times 10^{-8} (\text{°C})^2$ at 20 meters, a decrease of two orders of magnitude with depth down to 20 meters. Although the variance was much greater in the present experiment than in Shonting's, there was in the late afternoon period a one order of magnitude decrease in temperature variance with depth down to approximately 15 meters.

Liebermann also recorded temperature fluctuations in the near surface region at a depth of 50 meters. A rough calculation of variance from Liebermann's Fig. 1, which was given as a representative temperature record for July and August (time of day unreported) for the continental waters from Southern California to Alaska, resulted in a variance of approximately $17 \times 10^{-4} (\text{°C})^2$. This figure is somewhat closer to data of Fig. 13 but the lack of time of day information and depth dependence prevents conclusions from being drawn.

Due to the maximum temperature gradient being effected just prior to sunset the strongest fluctuations of temperature were noticed at all depths at that time. The variance decreased with increasing depth. However in the short period just after sunrise the temperature fluctuations were noticed to increase with depth. Sagar [Ref. 8] quotes, from a personal communication, Deacon, of the National Institute of Oceanography, as having observed this same situation.

FIGURE 13.

Plot of Temperature
Variance Versus Time
of Day (Depth in
Parentheses).

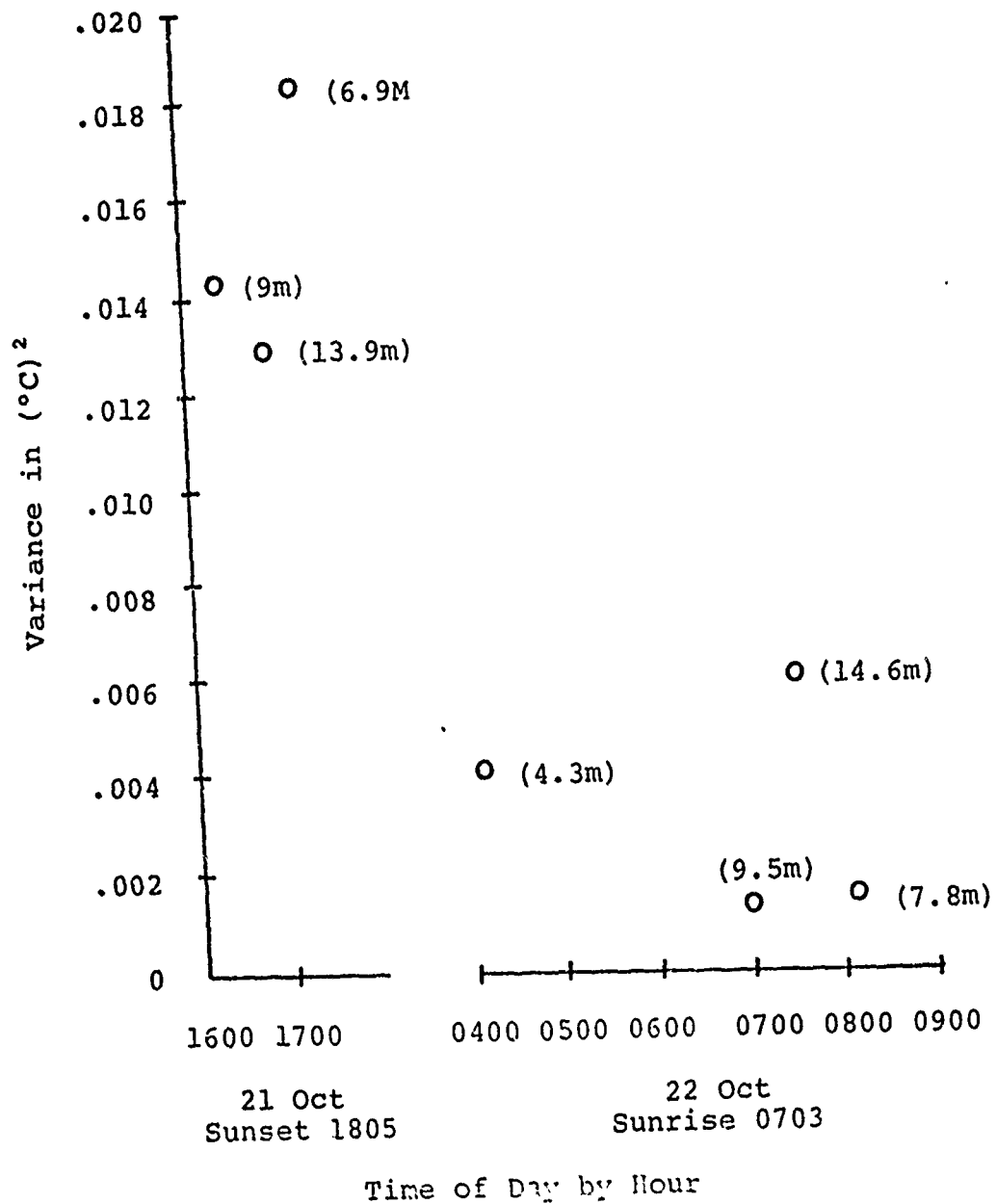


FIGURE 14.

Plot of Salinity
Variance Versus Time
of Day (Depth in
Parentheses).

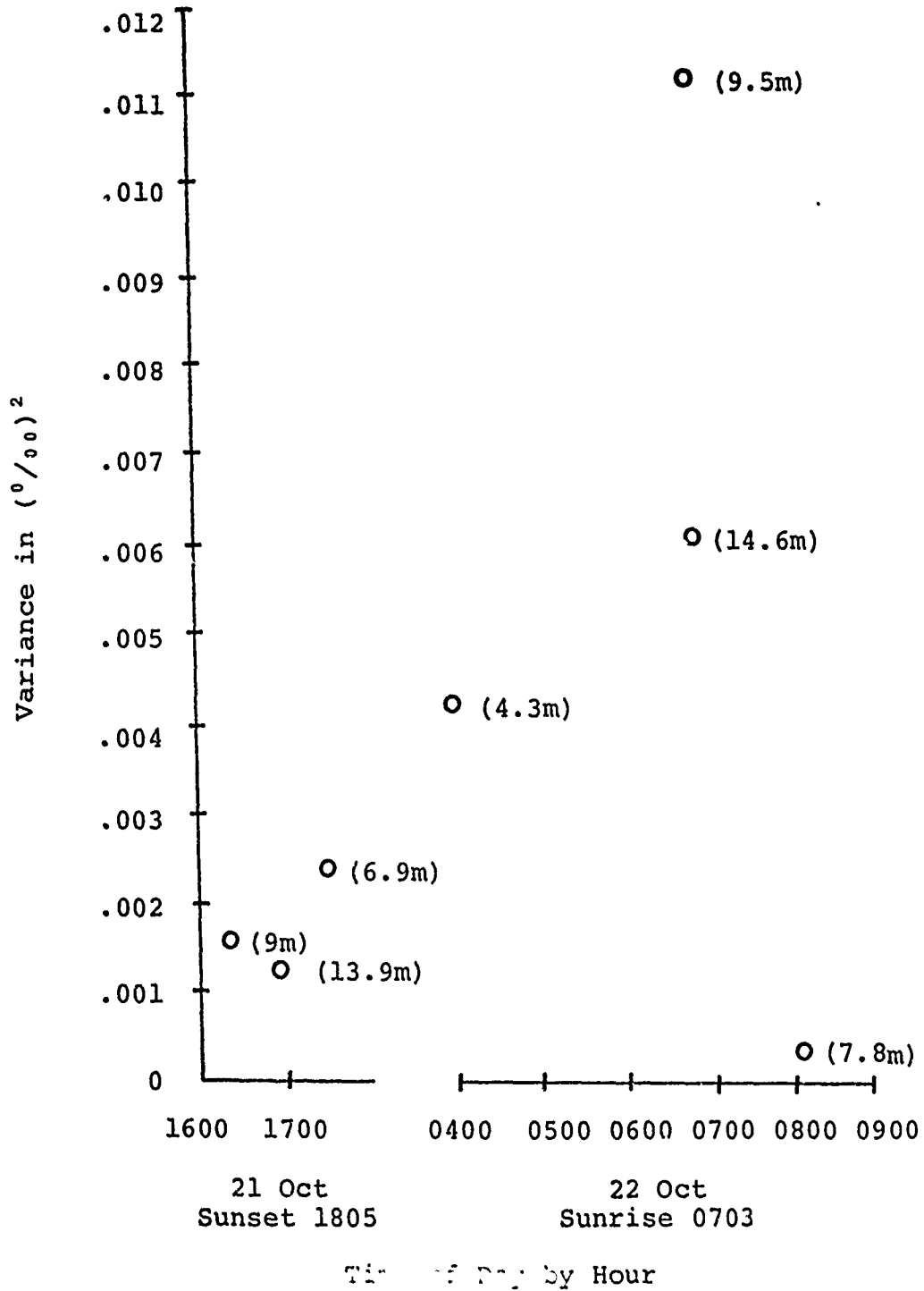
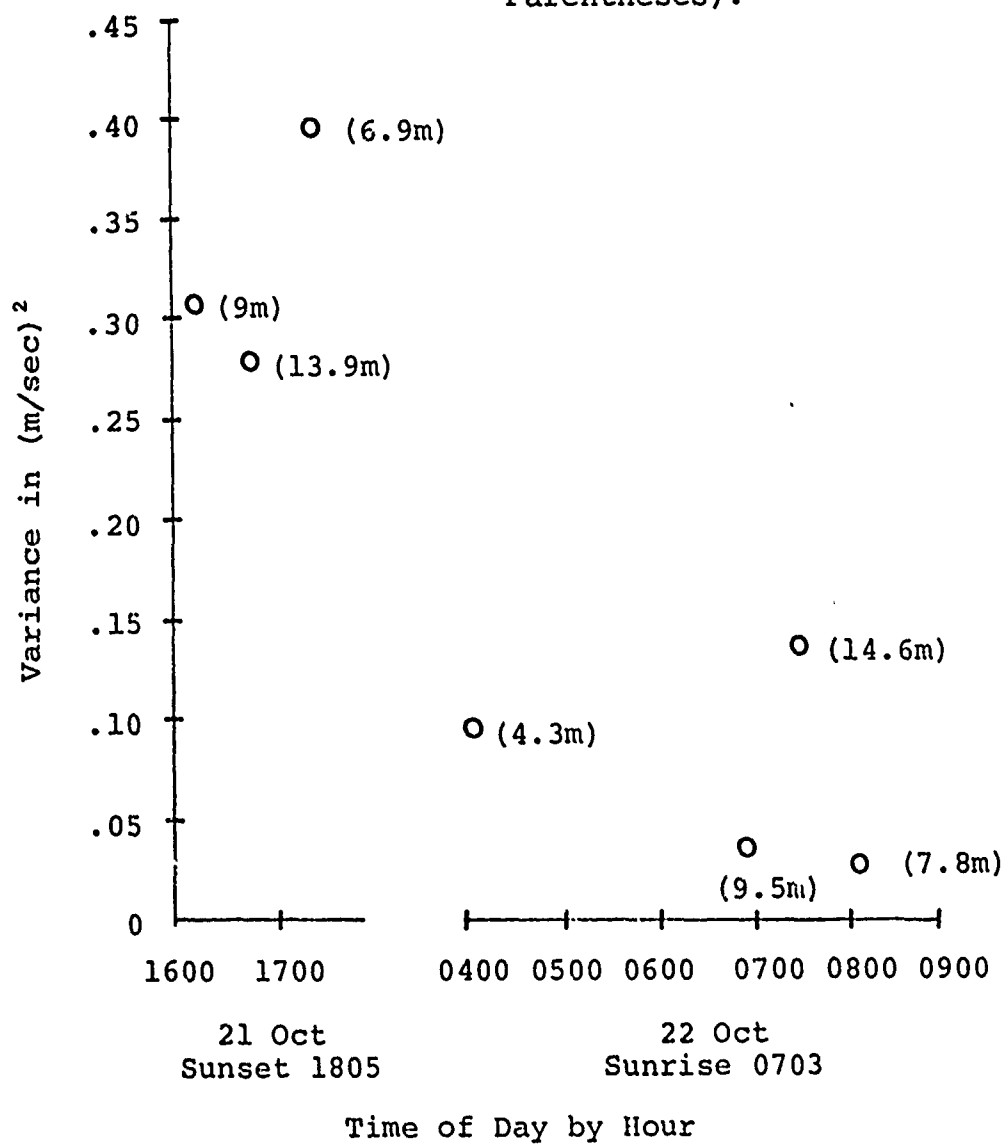


FIGURE 15.

Plot of Sound Velocity
Variance Versus Time
of Day (Depth in
Parentheses).



This behavior could possibly have been caused by the "convective lag" phenomenon. James [Ref. 9] describes this behavior as occurring in the early morning just after sunrise. Insolation increases to the point where it is equal to the outgoing heat loss from the water. However heat loss occurs exclusively at the surface, with consequential continued cooling of the surface. As insolation increases in the hours just after sunrise, surface cooling continues while the lower levels are slowly heated. Eventually, of course, the lag is overcome and surface heating begins causing growth of small cells with large fluctuations near the surface and large cells of small fluctuations at greater depths, as described by Deacon.

4. Variance of Salinity Fluctuations

The analysis of the plots of salinity variance versus time showed a decrease in salinity fluctuations with depth during the late afternoon period. The fluctuations were smaller during the period just prior to sunset than just after sunrise (assuming that the 7.8m reading is in error). The decrease in variance of salinity with increasing depth in the late afternoon was expected since a stronger salinity gradient would exist in the surface layer where evaporation was initiated. However, it is speculated that convective mixing caused a more nearly isohaline condition to exist in the water column by sunset than existed just after sunrise thereby accounting for the difference in magnitudes of variances at those two times of the day.

In the section "Parametric Interrelations Between Salinity, Temperature, and Sound Velocity" the theoretical calculation of sound velocity variance is discussed, and further analysis of the difference between theoretical and experimental results is made.

5. Probability Density Function Results

Salinity and sound velocity information were put into Program B in order to establish the type of distribution of the populations sampled. In all cases the distributions were Gaussian in nature. Figures 16 and 17 are examples of the distributions.

6. Normalized Autocorrelation Function

The normalized autocorrelation functions of the oceanographic parameters (see Appendix D) indicated a long correlation time for temperature data thereby indicating relatively well mixed thermal structure. Conversely the relatively low degree of correlation for both salinity and sound velocity indicated an inhomogeneous medium with respect to those two parameters. The peaks and troughs found on the salinity and sound velocity autocorrelation plots indicated the presence of patches of higher and lower salinity water as well as patchy areas of water yielding higher and lower values of sound velocity.

7. Power Spectral Density

Plots were made of power spectral densities of salinity, temperature, and sound velocity fluctuations (see Appendix E).

of Occurrences of Particular Variance Value in (.01v²) Band

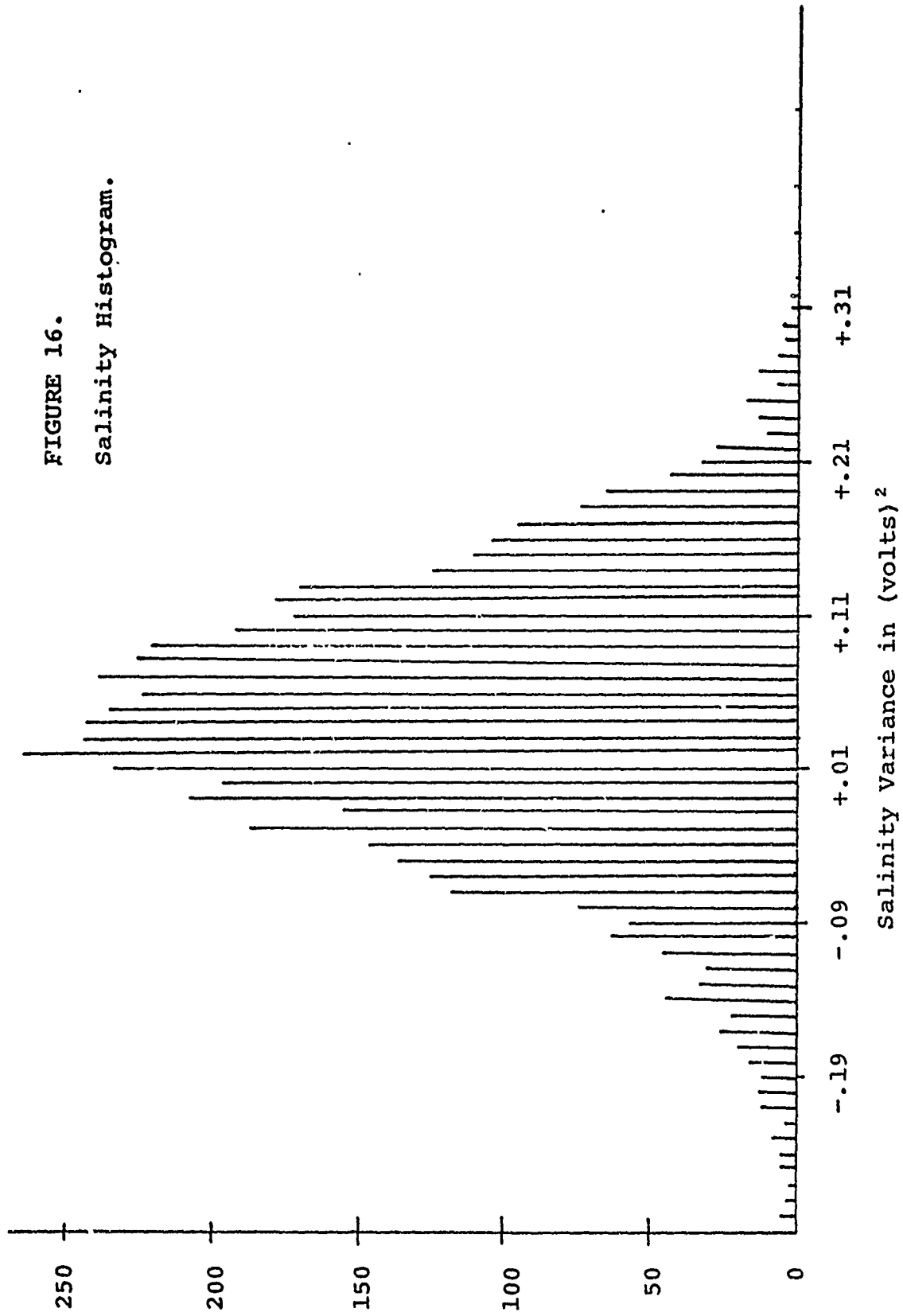


FIGURE 16.
Salinity Histogram.

of Occurrences of Particular Variance Value in (.01v²) Band

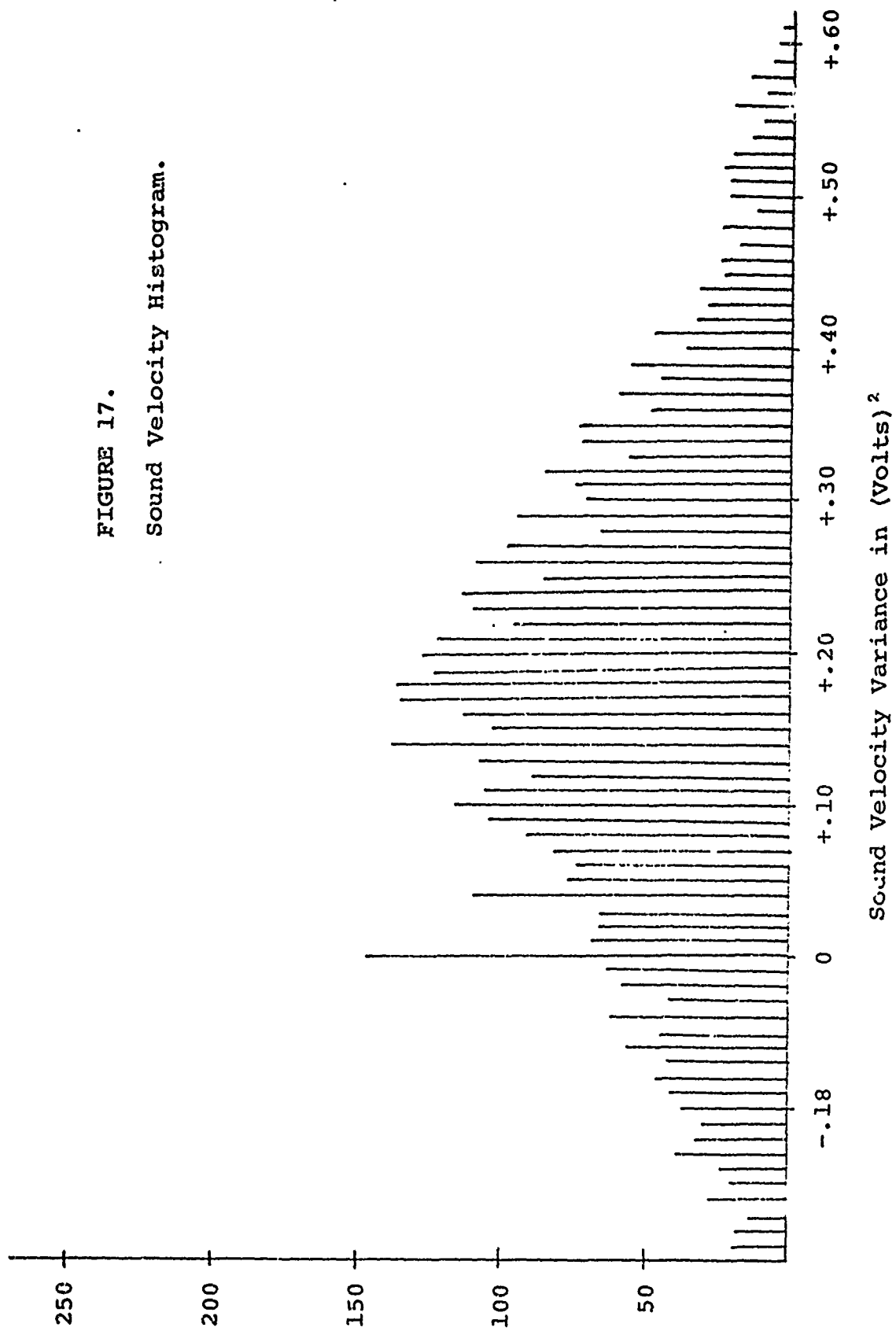


FIGURE 17.
Sound Velocity Histogram.

The nature of the plots indicated peaks of "energy" centered about frequencies of 0.17 and 0.08 Hertz. This coincided with the dominant wave frequencies existing at the time of the experiment.

VI. PARAMETRIC INTERRELATIONS BETWEEN SALINITY, TEMPERATURE,
AND SOUND VELOCITY

A. INTRODUCTION

With hopes of shedding light on possible heretofore unknown variables capable of affecting sound velocity a comparison was made between sound velocity variance derived from Wilson's sound speed equation and that measured experimentally with the Ramsay Velocimeter.

B. DERIVATION OF THEORETICAL SOUND VELOCITY VARIANCE FROM WILSON'S EQUATION

1. Wilson's Equation

$$C(t) = 1449.2 + 4.623 T(t) - .0546 T^2(t) \\ + 1.391 (S(t) - 35)$$

2. Computation of Variance

$$\text{var } C = 0 + (4.623)^2 \text{ var } T - (.0546)^2 \text{ var } (T^2) \\ + (1.391)^2 \text{ var } (S)$$

3. Dropping the Term, var (T²), as Negligible Yields
the Final Result

$$\text{var } C = 21.372 \text{ var } T + 1.935 \text{ var } S$$

The utilization of the above formula yielded the following results, with the velocimeter results shown for comparison:

RUN	VARIANCE C_{theory}	VARIANCE $C_{velocimeter}$
3	.3095 (m/sec.) ²	-
4	.2770 (m/sec.) ²	.0293 (m/sec.) ²
5	.3979 (m/sec.) ²	.0003 (m/sec.) ²
6	.0968 (m/sec.) ²	.0072 (m/sec.) ²
8	.0437 (m/sec.) ²	.0021 (m/sec.) ²
9	.1371 (m/sec.) ²	-
10	.0273 (m/sec.) ²	-

It was hoped that the results would indicate a theoretical variance slightly smaller than experimental variance thereby implying the presence of other parameters such as bubble presence to which the 3 MHz acoustic velocimeter would have been insensitive. However, as seen above, the experimental variance was much smaller than that calculated from the variances of temperature and salinity. Analysis of the wide discrepancy led to the conclusion that since all sensors appeared to have operated in an optimum manner, and salinity and temperature signals were strong and yielded good results, the sound velocity signal was suspect. The signal had been filtered and amplified and conceivably could have been altered, or else a mistake made in the data reduction settings. In order to determine which values of the variance of sound velocity should be used for the remainder of the analysis a final check of the results of both methods was conducted. Part of the experiment involved the measurement of sound amplitude modulation (see NPS thesis of LCDR

W. J. Smith, Jr., December 1971). Stone and Mintzer [Ref. 10] define the coefficient of variation (CV) as:

$$CV = \frac{\overline{|\Delta P|^2}}{\overline{P}^2}$$

where ΔP is the variation of the acoustic pressure relative to the mean value \overline{P} . In his experiment LCDR Smith measured σ_s which he shows is related to CV by:

$$(CV)^2 = 40 \sigma_s^2$$

Chernov [Ref. 11] formulated the relationship:

$$(CV)^2 = \sqrt{\pi} \overline{v}^2 K_0^2 aL$$

where,

$$K_0 = \frac{2\pi}{\lambda}$$

λ = acoustical wave length

\overline{v}^2 = variance of sound velocity

a = correlation length (Gaussian correlation function assumed)

L = distance between transducer and receiver

This relationship combined with the measured values of CV and sound velocity variance, allowed for the calculation of the correlation length:

RUN	DEPTH (m)	a (from var C_{theory}) (cm)	a (from var C_{expt}) (cm)
5	6.9	175.0	2.699×10^5
3	9.3	157.5	-
4	13.9	452.5	4279.9

The values of "a" calculated from velocimeter data are unreasonably large. For this reason the theoretical sound velocity variances are used throughout the remainder of the analysis. A graphical plot of theoretical sound velocity variances versus time of day with depths in parentheses are shown in Fig. 15.

It is interesting to observe that Skudrzyk [Ref. 12] also found patch sizes, which increased approximately linearly with depth in approximately the same manner as shown above. However, Skudrzyk's patch sizes were much larger than reported here, probably due to his acoustic range being much greater than in this experiment.

VII. CONCLUSIONS

A. Although the near surface regime is one of complex and high variability, several conclusions can be made:

1. Temperature fluctuations decrease with depth during the period just prior to sunset.
2. Temperature fluctuations increase with depth just after sunrise, but are smaller in magnitude than the fluctuations just prior to sunset.
3. Salinity fluctuations decrease with depth but are larger in magnitude in the period after sunrise.
4. Sound velocity fluctuations normally follow the trend of temperature variations. However, the importance of salinity fluctuations cannot be neglected. In one instance the salinity fluctuations had as much an effect on sound velocity fluctuations as did temperature fluctuations.
5. The maximum energy spectra of salinity and temperature fluctuations occurred at frequencies that agreed with dominant surface wave frequencies.
6. The sizes of patches of sound velocity fluctuations were calculated from the statistics of sound amplitude, temperature and salinity fluctuations. The implied patch sizes increased approximately linearly with increasing depth.

VIII. RECOMMENDATIONS FOR FURTHER STUDY

A. While the medium was described in terms of temperature and salinity, a major question remains, "Are there other variables that could affect the propagation of sound in sea water?" In order to best achieve an answer to this question one should ensure that a correct experimental value of sound velocity is measured for comparison with sound velocity computed theoretically. LCDR Smith's and Rautmann's thesis work indicated the presence of bubbles in the medium that could have a marked affect on sound velocity.

B. In order to complete the description of the medium, an analysis of the size of the "patches" of temperature and salinity should be performed by use of arrays of sensors. Application of knowledge of the drift velocity, in addition to the procedures used in the present experiment, would also enable patch size determination.

APPENDIX A

GENERAL DESCRIPTION OF BISSETT-BERMAN MODEL 9006 SALINITY, TEMPERATURE AND DEPTH MEASURING SYSTEM [Ref. 13]

The model 9006 STD is comprised of underwater sensors and deck equipment whose functions are to furnish power to the sensors and process data received from same.

In situ measurement of salinity is determined by measuring conductivity, temperature and pressure. An inductively-coupled sensor enables detection of conductivity, which is also compensated for temperature and pressure effects, thereby producing an output totally dependent upon salinity. The output shifts the frequency of a PARALOC signal providing an FM analog of salinity.

The temperature sensor uses a platinum resistance thermometer and a PARALOC which provides an FM analog of temperature.

The depth sensor utilized a pressure transducer into which is incorporated a strain-gauge bridge circuit. The changes in resistance are converted to a frequency analog in the PARALOC.

The signal mixer receives and regulates power from the deck equipment and sends it onto the underwater sensors. It then multiplexes and amplified the FM signals from the sensor and sends them to the deck equipment.

The distribution amplifier amplifies the FM signal from the underwater units, and separates data signals from

the DC power which enters the distribution amplifier from the power supply rack.

Each underwater sensor has a separate discriminator which separates the mixed data signal into an individual channel for recording availability. The discriminator filters the desired signal and rejects others. The accepted signal is amplified, squared, and converted to a 10 millivolt DC level which is the output of the recorder. Dial readouts enable continual monitoring of this signal.

The Power Supply is a model 8600 and provides a constant voltage of 26.5 volt DC to the deck units, and a constant current of 150 milliamps at a maximum of 140 volts DC to the underwater units. The underwater rack is stainless steel. The sensors and mixer are mounted in individual shock-absorbent brackets.

A single conductor cable provides for physical connection between sensors and deck equipment.

APPENDIX B

DATA CUMULATION AND RUN DESCRIPTION

The output DC voltage from the oceanographic sensors was recorded on the Sangamo magnetic tape recorder as explained in "Experimental Configuration" section. The runs during which data were collected are described below:

RUN	DEPTH	DATE	START TIME	STOP TIME
1	4.3m	21 Oct	1419	1429
2	4.2m	21 Oct	1530	1550
3	9.0m	21 Oct	1616	1636
4	13.9m	21 Oct	1648	1708
5	6.9m	21 Oct	1728	1748
6	4.3m	22 Oct	0354	0448
7	4.3m	22 Oct	0546	0622
8	9.5m	22 Oct	0650	0715
9	14.6m	22 Oct	0725	0749
10	7.8m	22 Oct	0802	0821
11	8.2m	22 Oct	0832	0852
12	5.7m	22 Oct	0929	0945

SENSITIVITY SETTINGS

Run 3

salinity	50 millivolts/millimeter
thermistor 1	100 millivolts/millimeter
thermistor 2	100 millivolts/millimeter

Run 4

salinity	50 millivolts/millimeter
thermistor 2	100 millivolts/millimeter
sound velocity	50 millivolts/millimeter

Run 5

salinity	50 millivolts/millimeter
thermistor 1	100 millivolts/millimeter
thermistor 2	50 millivolts/millimeter
sound velocity	20 millivolts/millimeter

Run 6

salinity	50 millivolts/millimeter
thermistor 1	100 millivolts/millimeter
sound velocity	50 millivolts/millimeter

Run 8

salinity	100 millivolts/millimeter
thermistor 1	100 millivolts/millimeter
sound velocity	100 millivolts/millimeter

Run 9

salinity	100 millivolts/millimeter
thermistor 1	100 millivolts/millimeter

Run 10

salinity	50 millivolts/millimeter
thermistor 1	100 millivolts/millimeter

In addition to Bissett-Berman salinity measurements, Nansen casts were taken during each run in order to monitor the calibration correction which had to be applied to the dial readout of the base value of salinity (see Table III). The correction factor was (-) 5.1 ppt. While this was a high correction factor, pre-experiment checks on the STD led to the assumption that the system was operating correctly in the measurement of fluctuations and was consequently used for that purpose.

Run	Depth (Meters)	Time	Date	Salinity (%)
2	4.2	1530	21 Oct	33.520
3	9.0	1636	21 Oct	33.512
6	4.3	0357	22 Oct	33.506
6	4.3	0410	22 Oct	33.478
6	4.3	0425	22 Oct	33.489
6	4.3	0442	22 Oct	33.464
7	4.3	0552	22 Oct	33.506
7	4.3	0559	22 Oct	33.480
8	9.5	0654	22 Oct	33.459
8	9.5	0659	22 Oct	33.438
8	9.5	0715	22 Oct	33.471
9	14.6	0725	22 Oct	33.469
10	7.8	0810	22 Oct	33.455
10	7.8	0817	22 Oct	33.463
11	8.2	0839	22 Oct	33.453
11	8.2	0852	22 Oct	33.455
12	5.7	0934	22 Oct	33.440

TABLE III

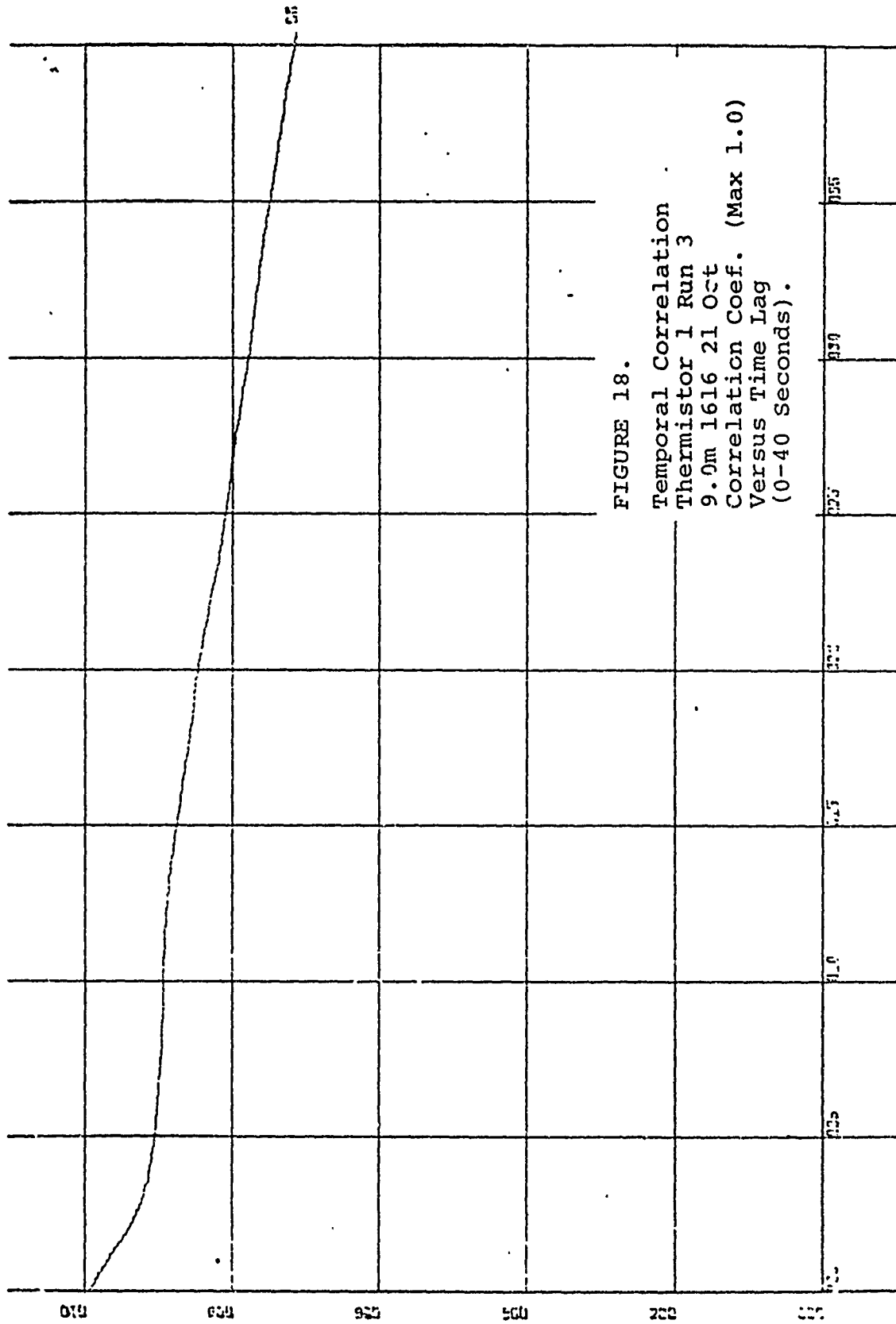


FIGURE 18.
 Temporal Correlation
 Thermistor 1 Run 3
 9.9m 1616 21 Oct
 Correlation Coef. (Max 1.0)
 Versus Time Lag
 (0-40 Seconds).

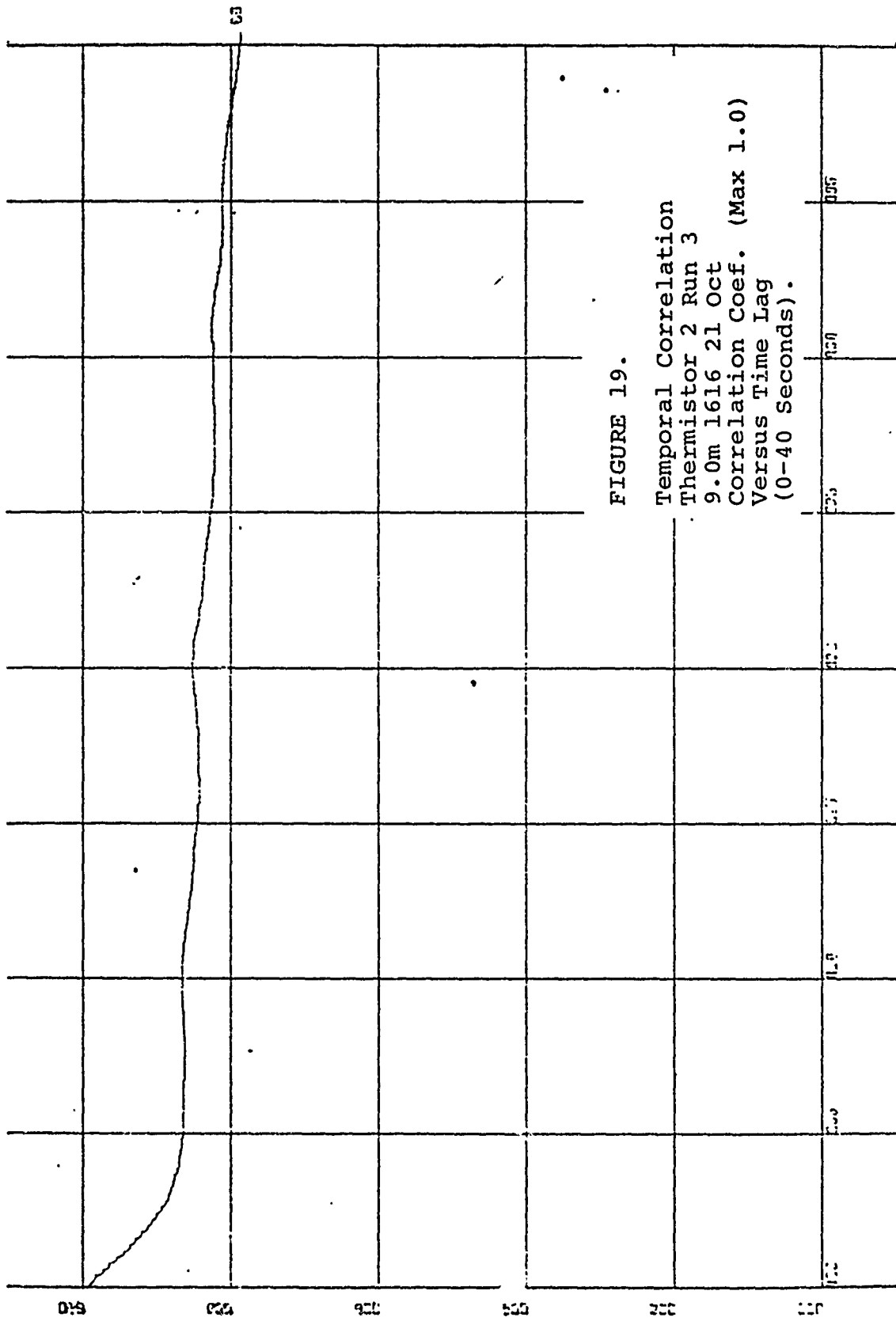
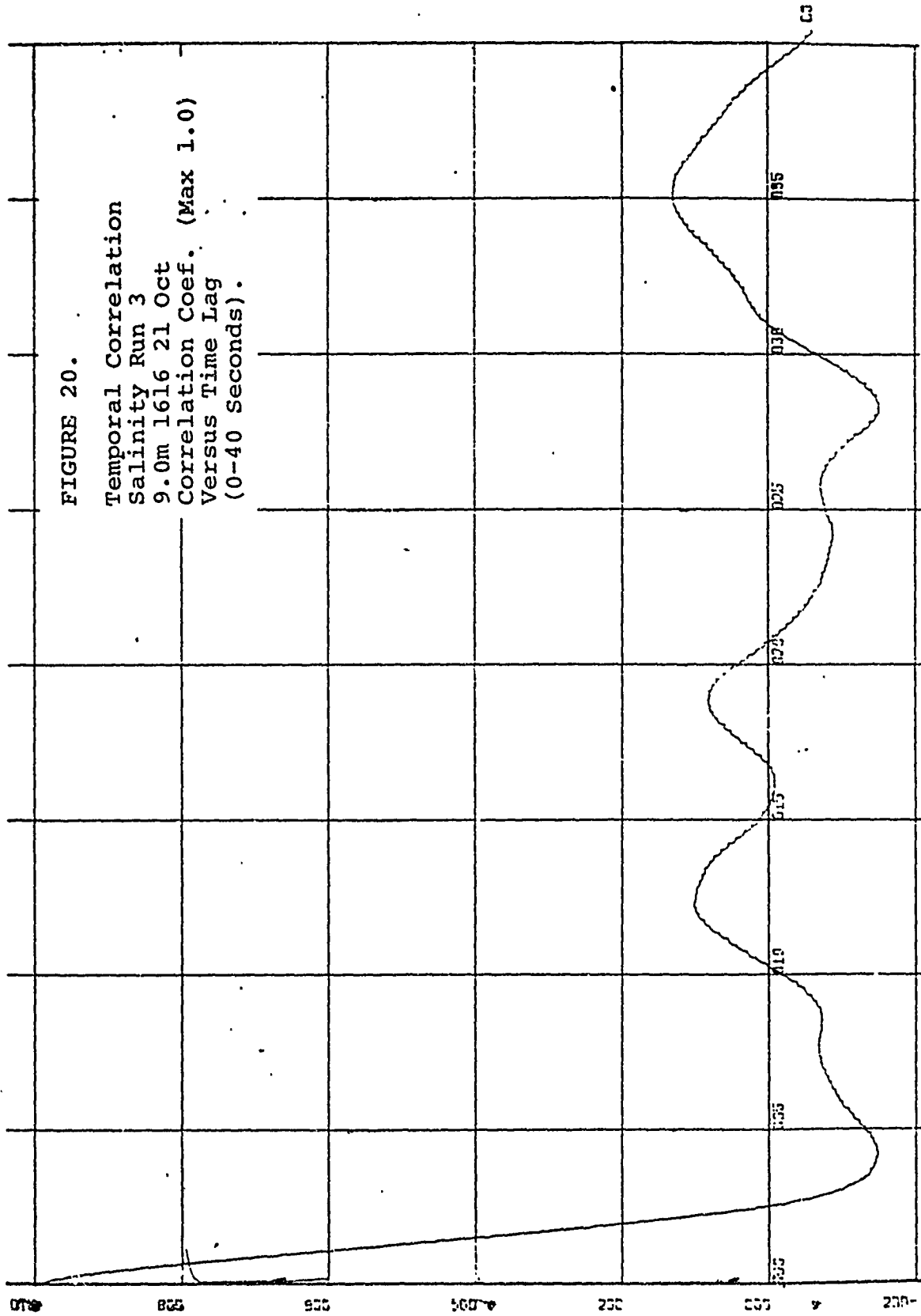


FIGURE 19.
 Temporal Correlation
 Thermistor 2 Run 3
 9.0m 1616 21 Oct
 Correlation Coef. (Max 1.0)
 Versus Time Lag
 (0-40 Seconds).

FIGURE 20.

Temporal Correlation
Salinity Run 3
9.0m 1616 21 Oct
Correlation Coef. (Max 1.0)
Versus Time Lag
(0-40 Seconds).



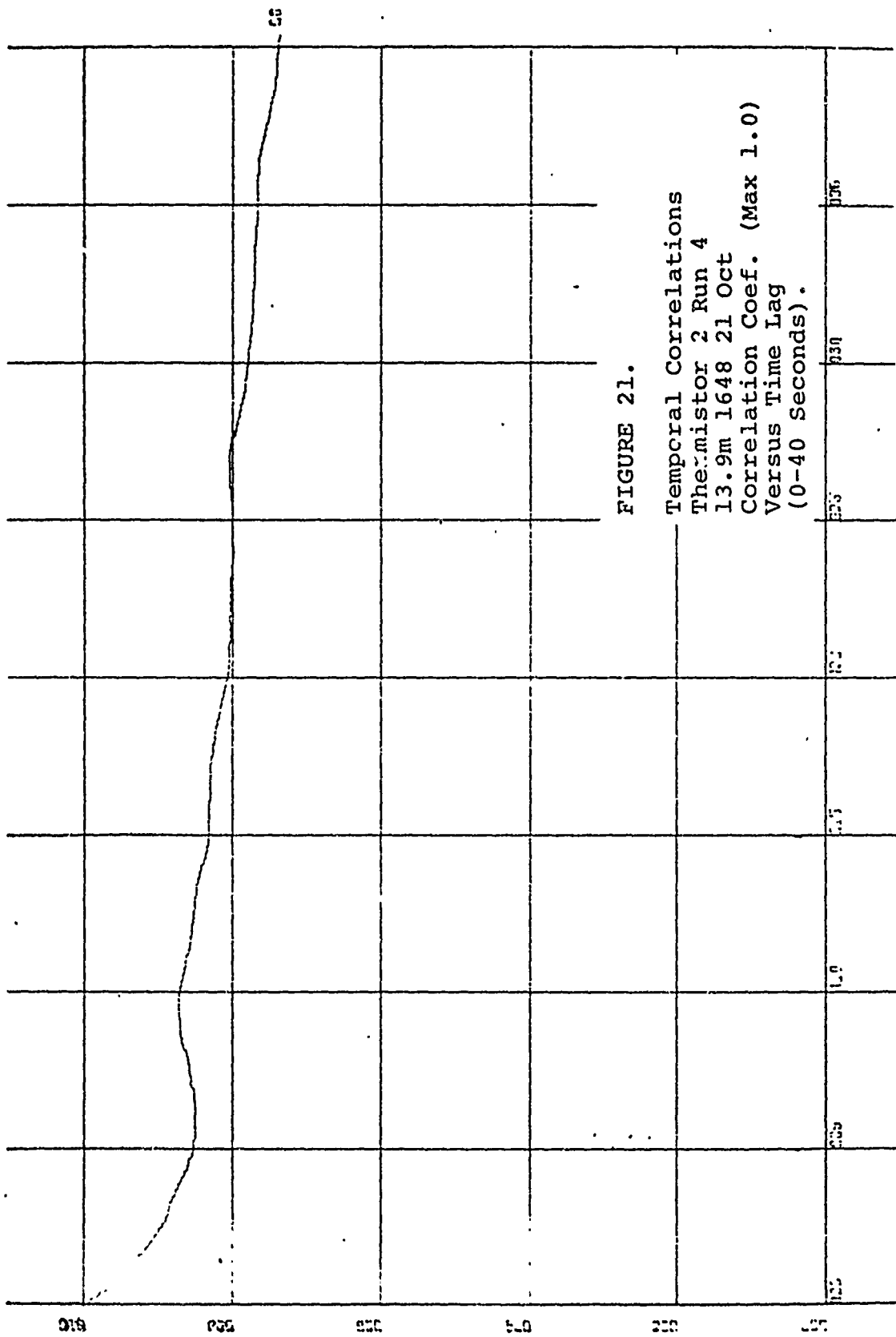


FIGURE 21.

Temporal Correlations
 Thermistor 2 Run 4
 13.9m 1648 21 Oct
 Correlation Coef. (Max 1.0)
 Versus Time Lag
 (0-40 Seconds).

FIGURE 22.

Temporal Correlation
Salinity Run 4
13.9m 1648 21 Oct
Correlation Ccoef. (Max 1.0)
Versus Time Lag
(0-40 Seconds).

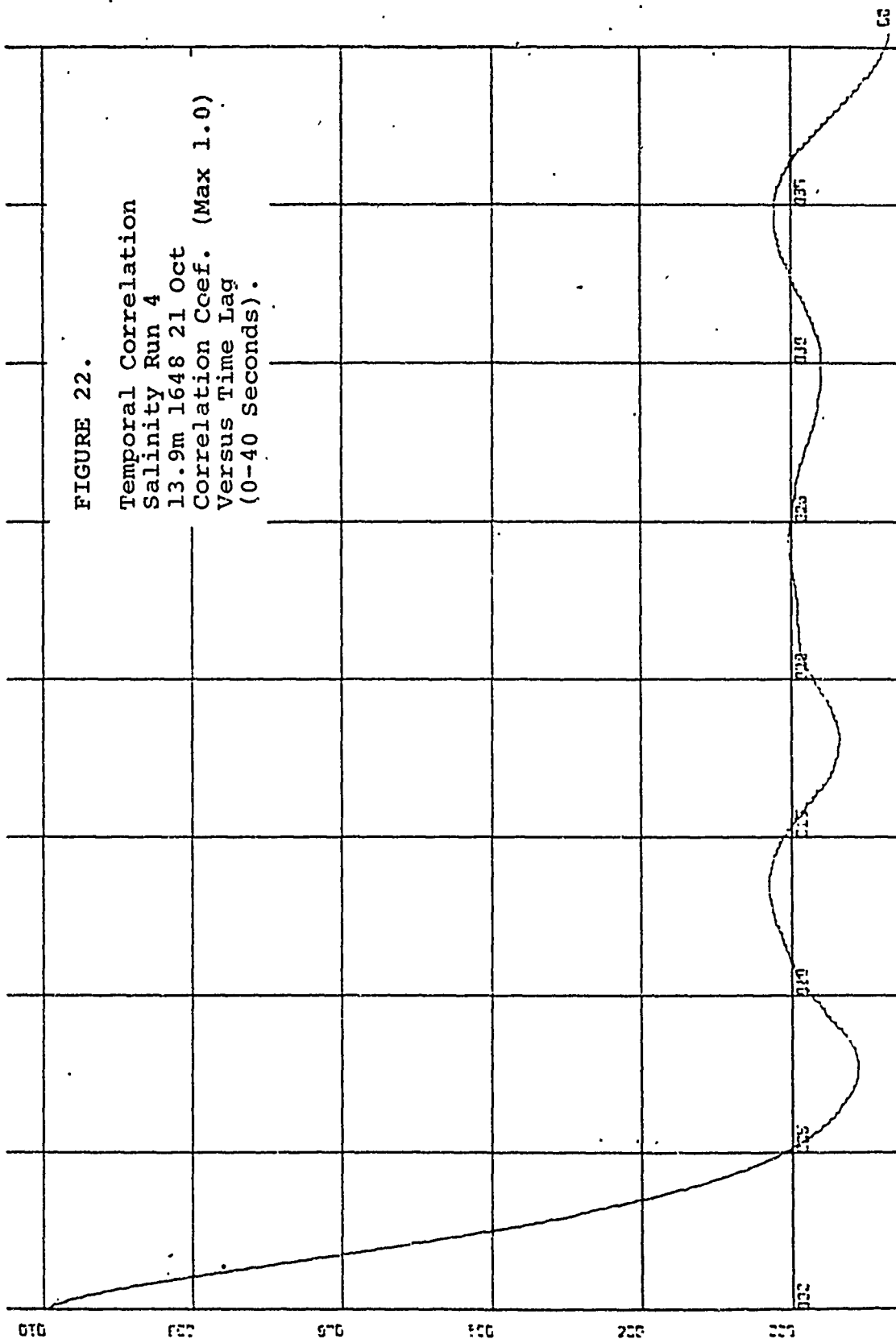


FIGURE 23.

Temporal Correlation
Sound Velocity Run 4
13.9m 1648 21 Oct
Correlation Coef. (Max 1.0)
Versus Time Lag
(0-40 Seconds).

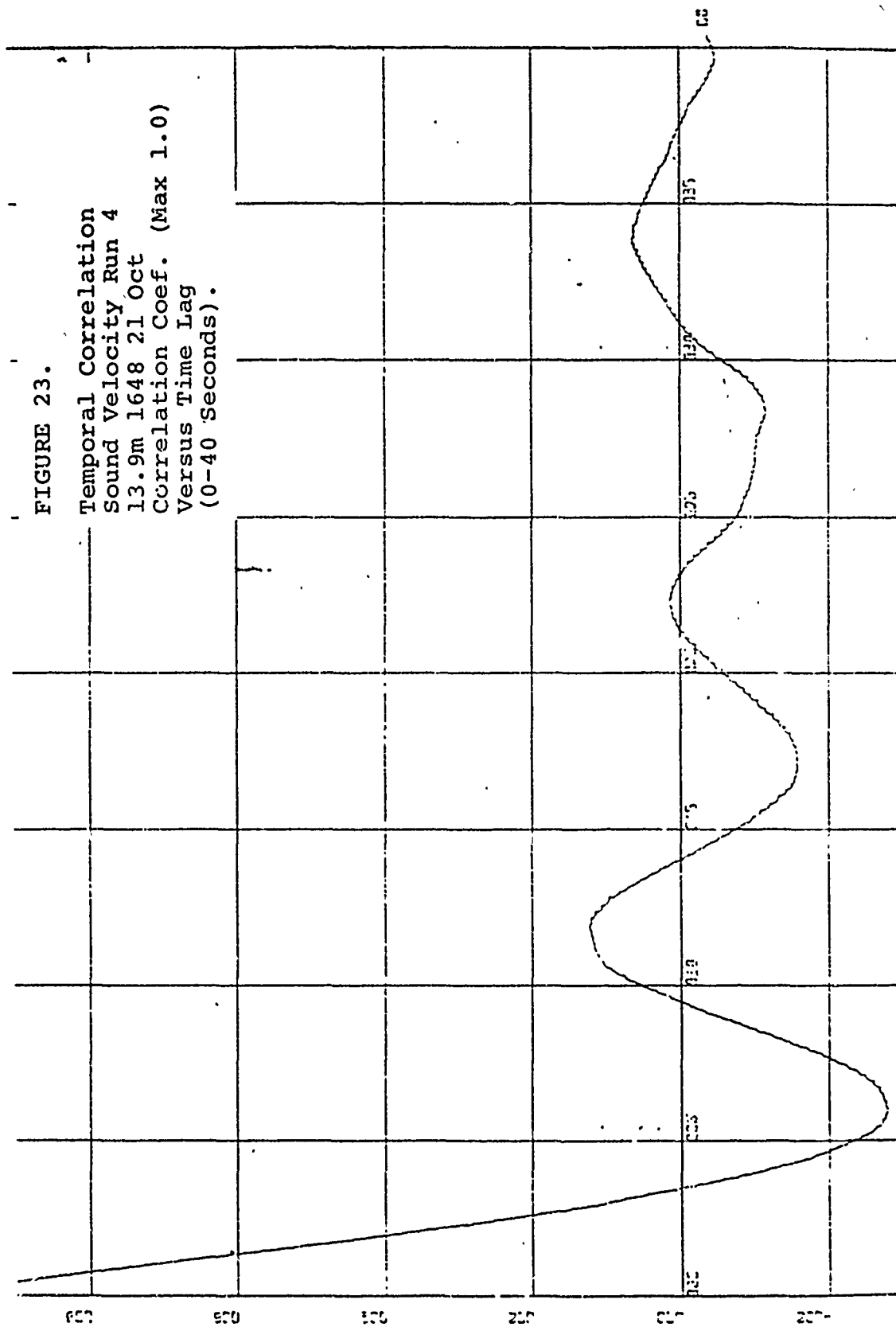


FIGURE 24.

Temporal Correlation
Thermistor 1 Run 5
6.9m 1728 21 Oct
Correlation Coef. (Max 1.0)
Versus Time Lag
(0-40 Seconds).

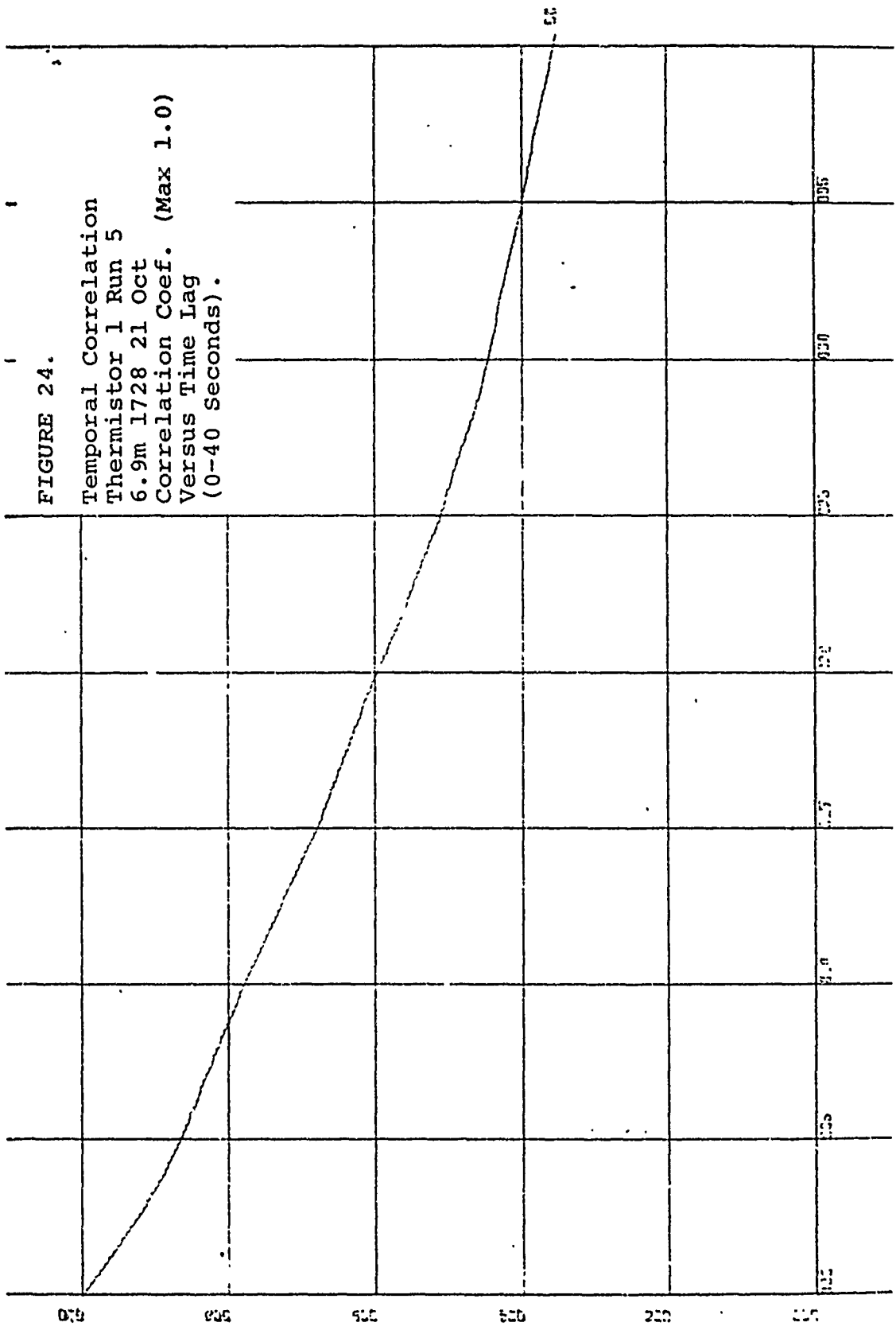


FIGURE 25.
 Temporal Correlation
 Thermistor 2 Run 5
 6.9m 1728 21 Oct
 Correlation Coef. (Max 1.0)
 Versus Time Lag
 (0-40 Seconds).

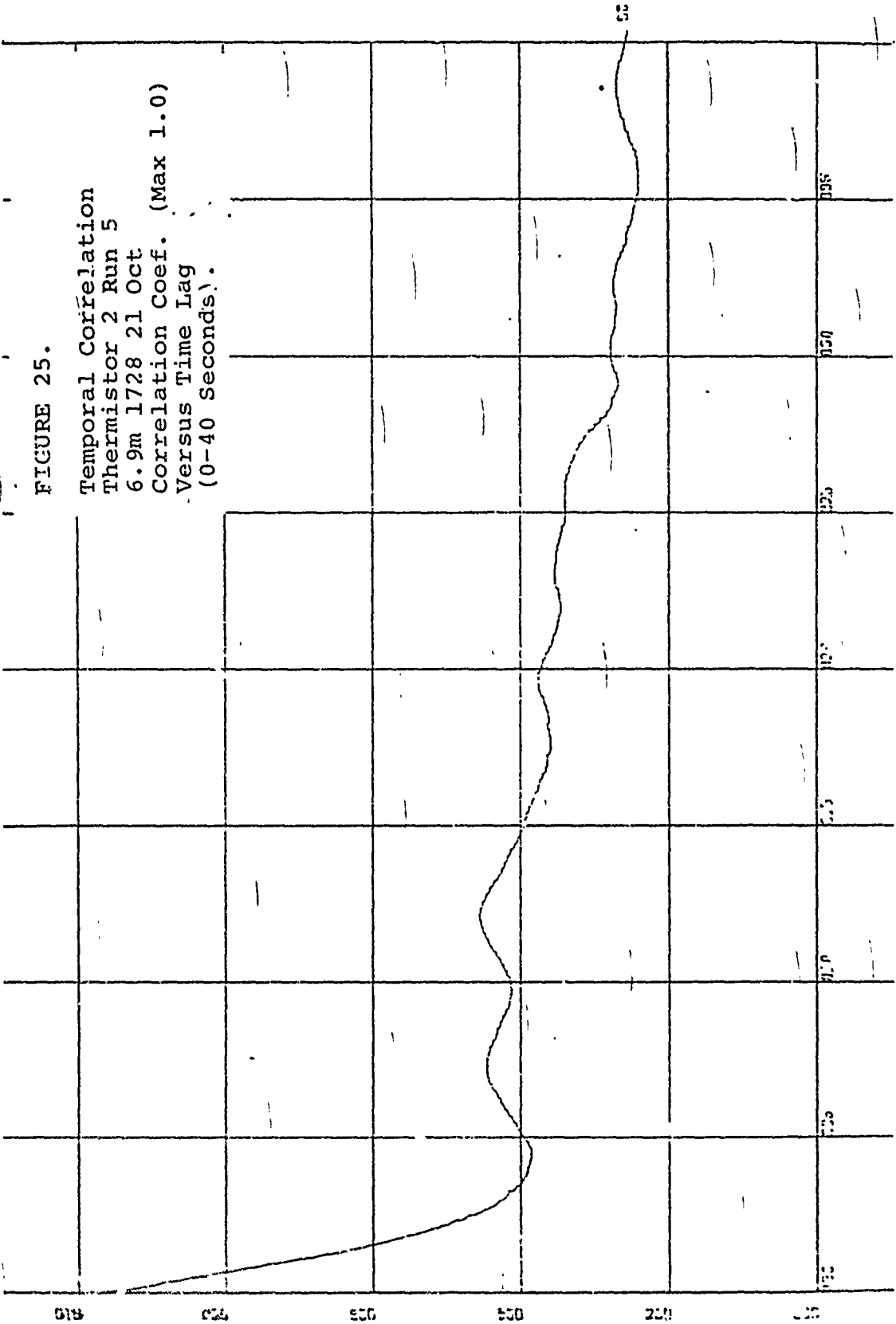


FIGURE 26.

Temporal Correlation
Salinity Run 5
6.9m 1728 21 Oct
Correlation Coef. (Max 1.0)
Versus Time Lag
(0-40 Seconds).

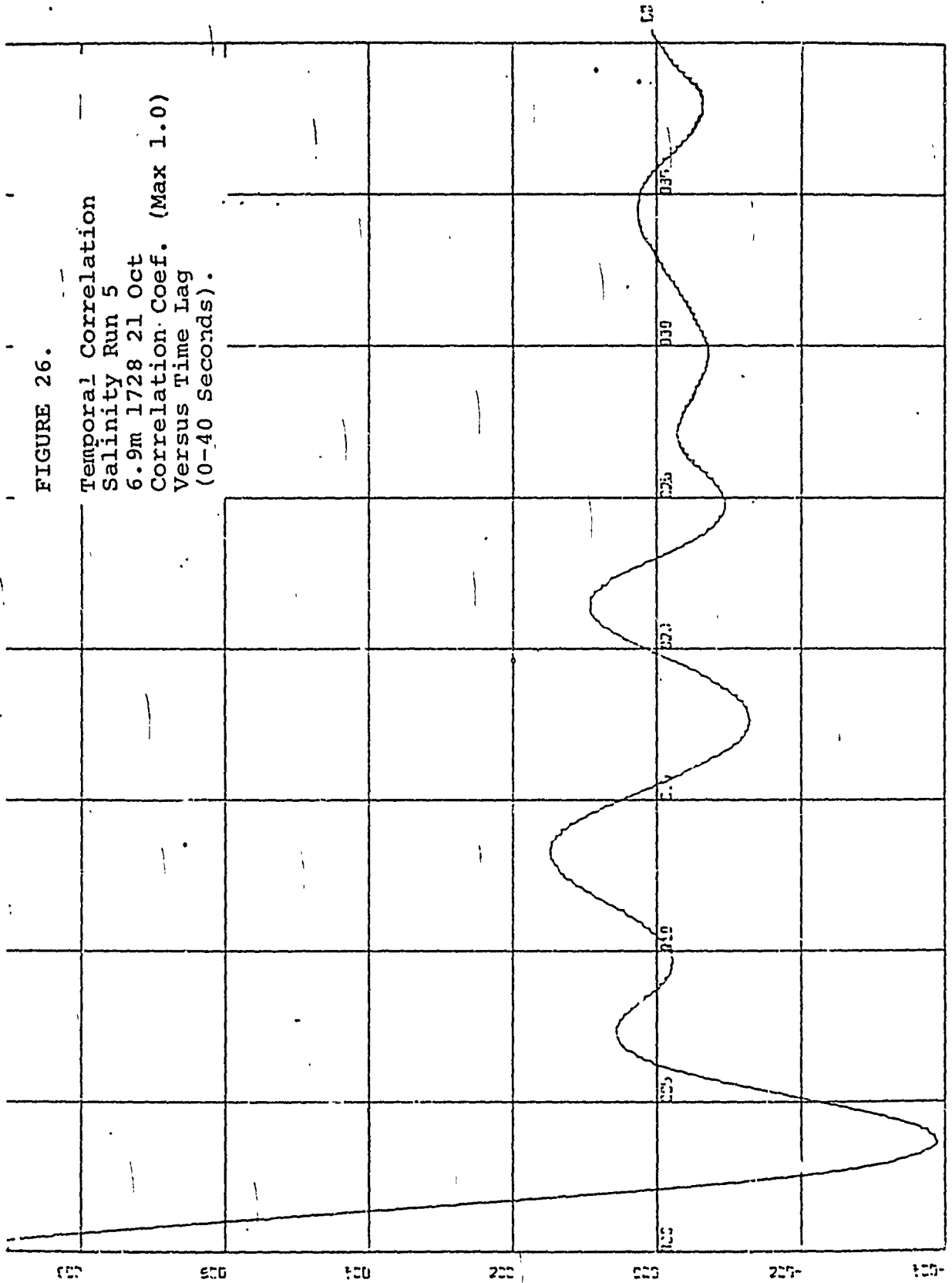


FIGURE 27.
 Temporal Correlation
 Sound Velocity Run 5
 6.9m 1728 21 Oct
 Correlation Coef. (Max 1.0)
 Versus Time Lag
 (0-40 Seconds).

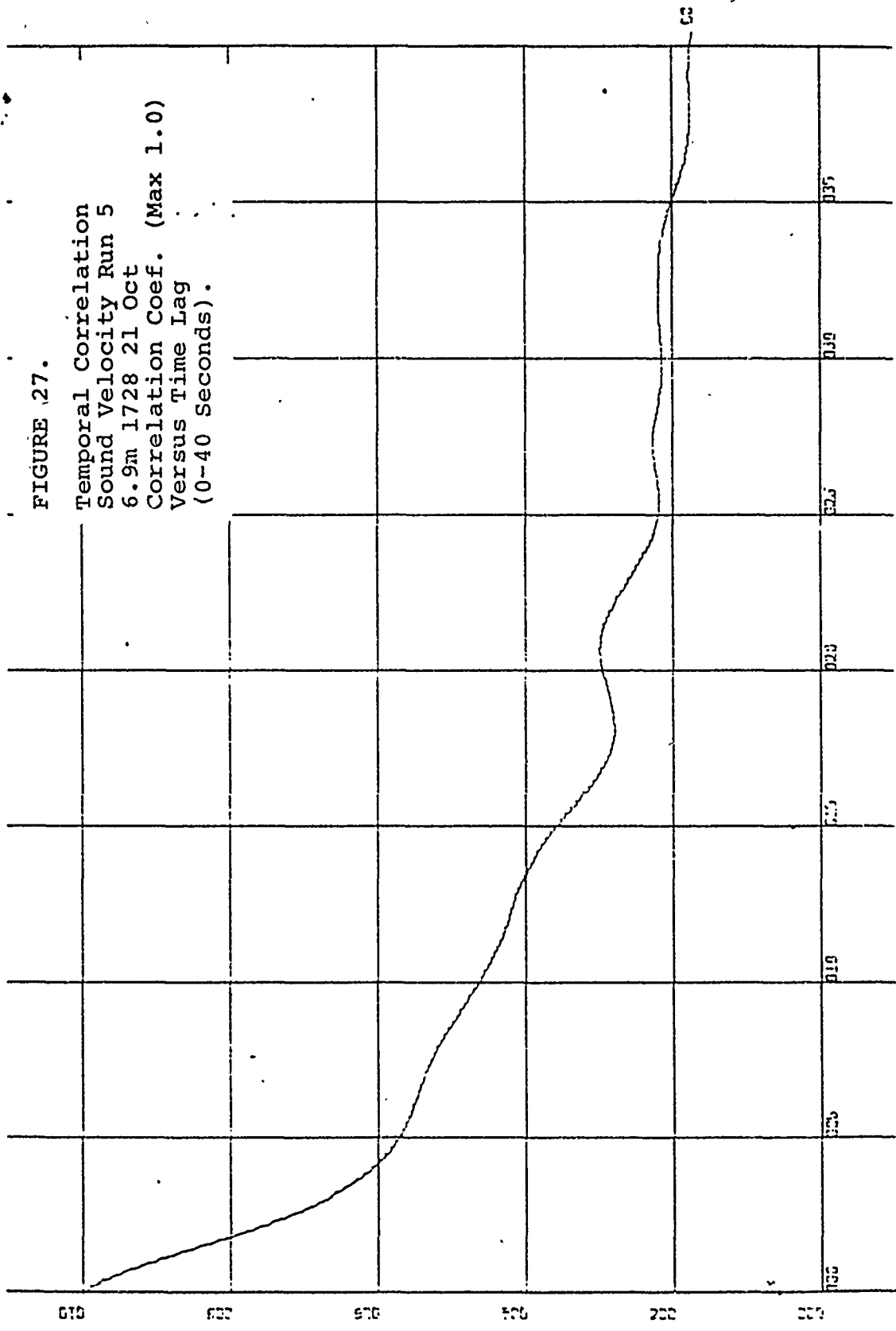


FIGURE 28.

Temporal Correlation
Thermistor 1 Run 6
4.3m 0354 22 Oct
Correlation Coef. (Max 1.0)
Versus Time Lag
(0-40 Seconds).

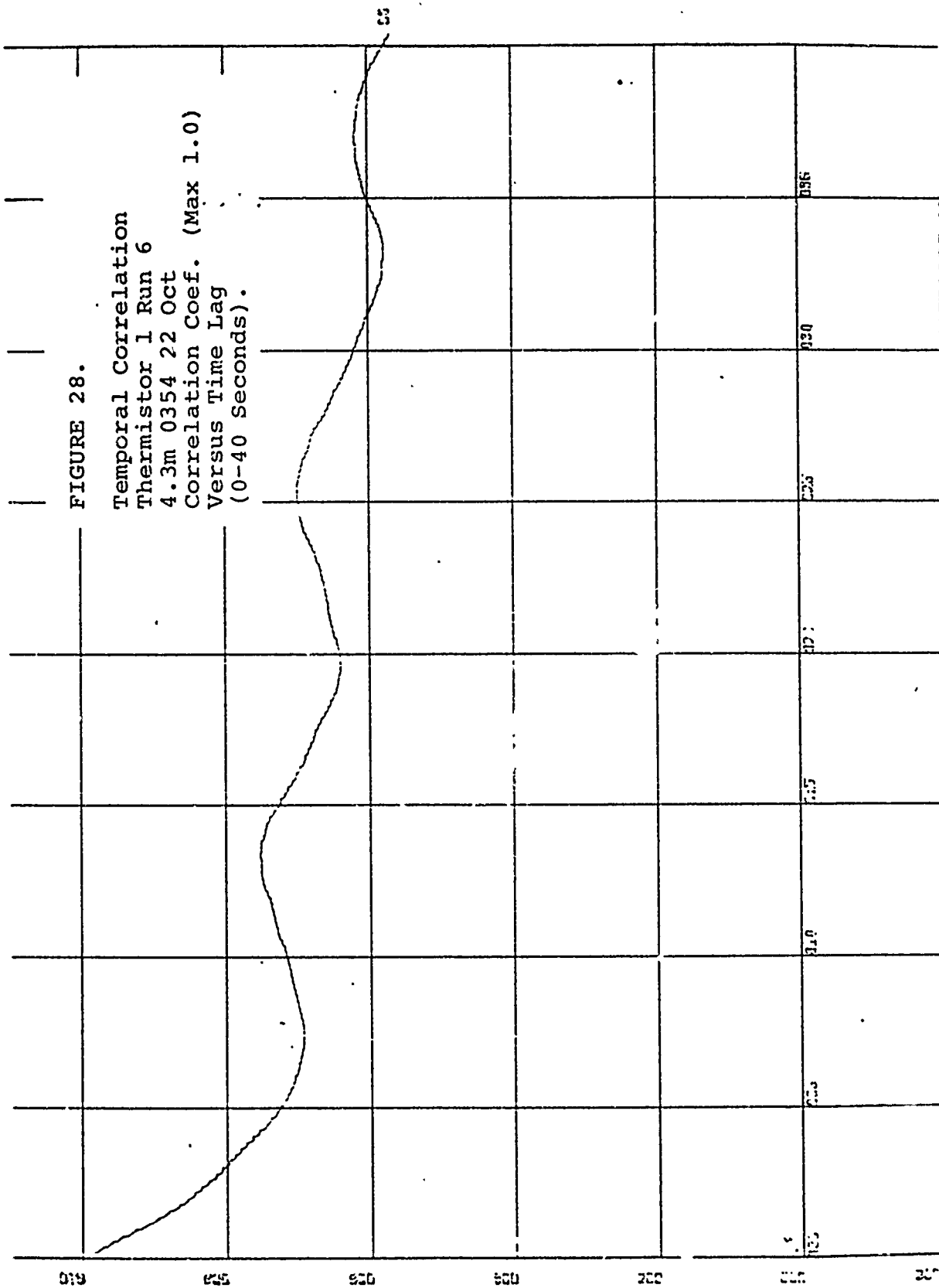


FIGURE 29.
 Temporal Correlation
 Salinity Run 6
 4.3m 0354 22 Oct
 Correlation Coef. (Max 1.0)
 Versus Time Lag
 (0-40 Seconds).

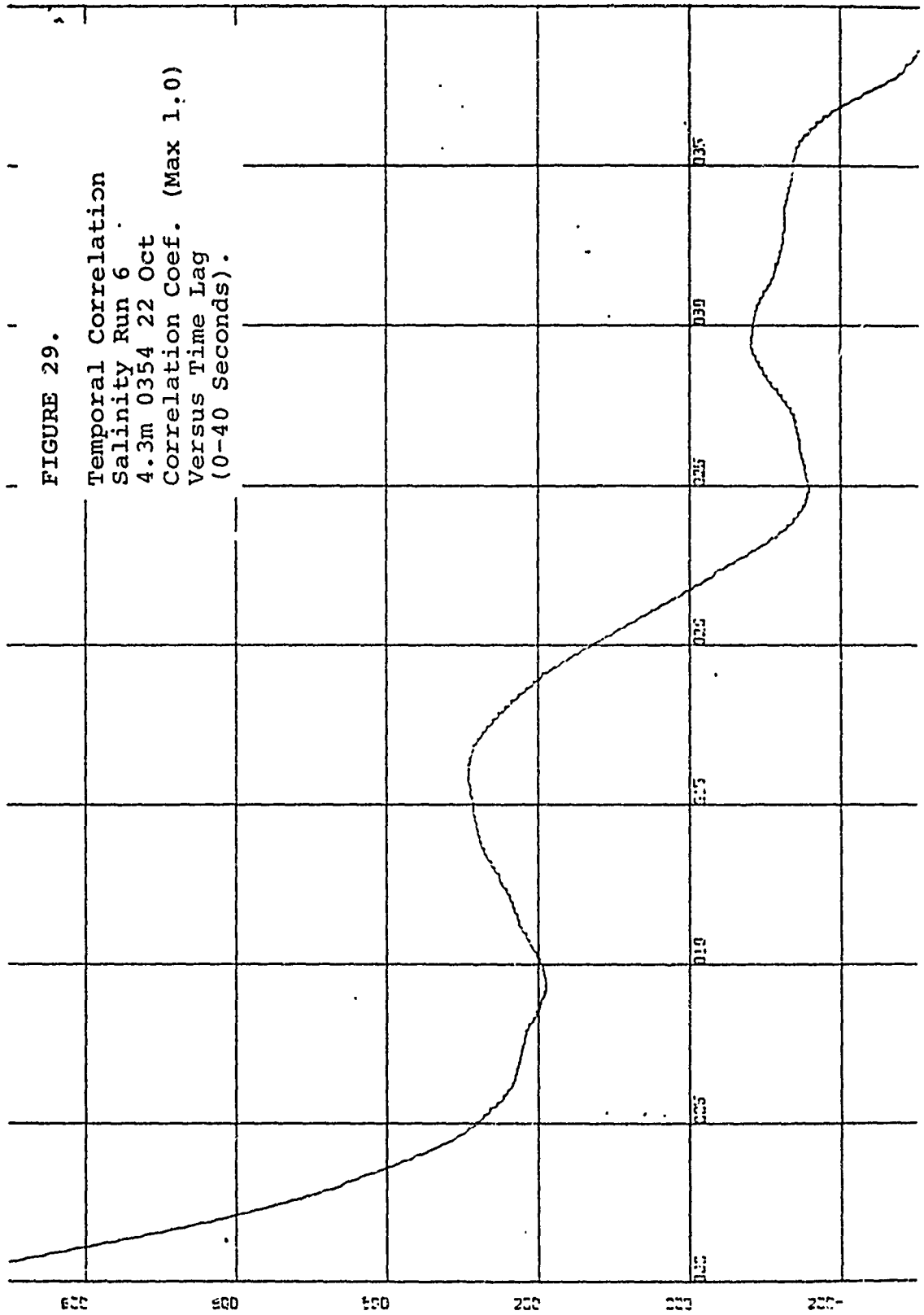
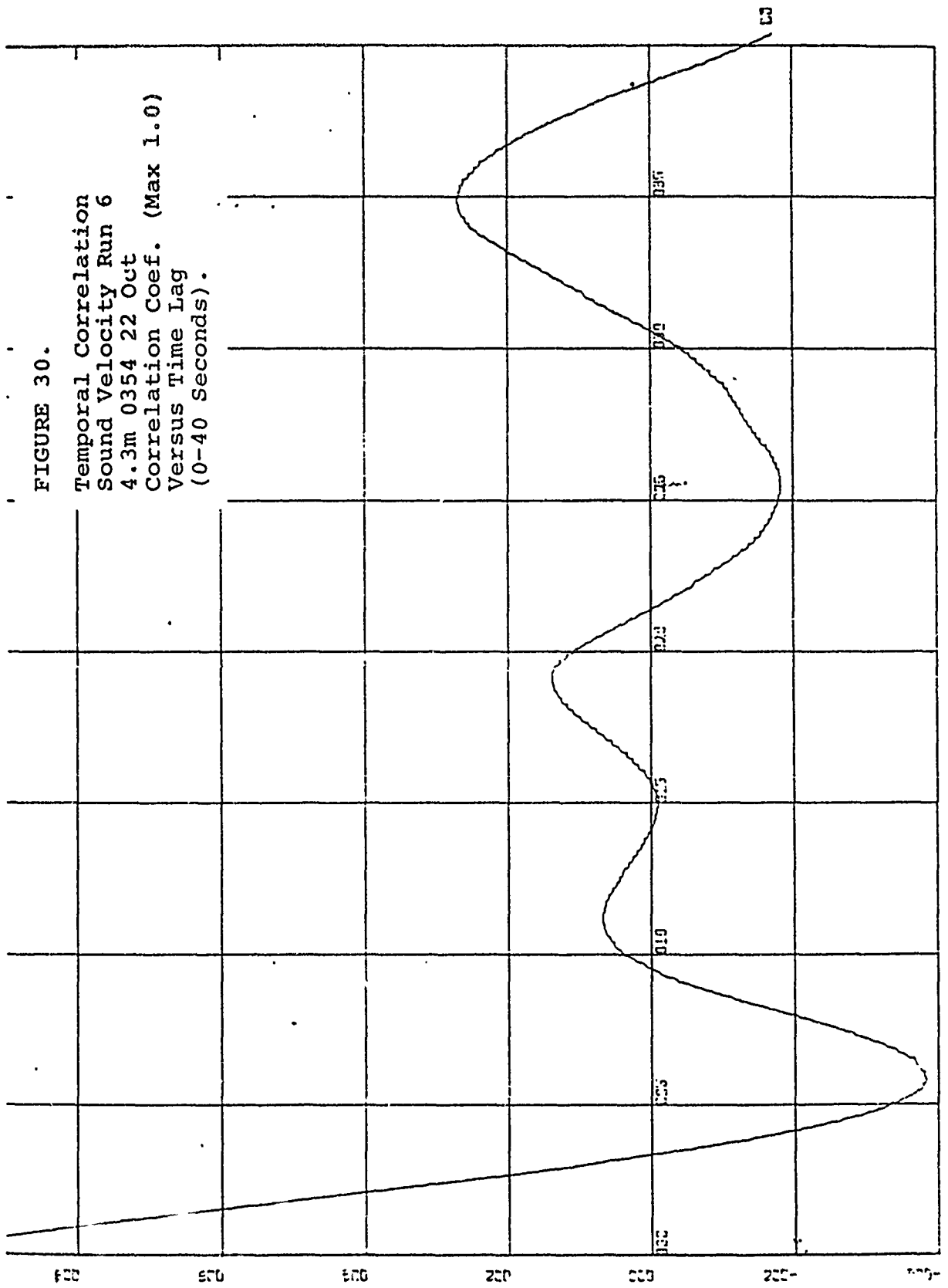


FIGURE 30.

Temporal Correlation
Sound Velocity Run 6
4.3m 0354 22 Out
Correlation Coef. (Max 1.0)
Versus Time Lag
(0-40 Seconds).



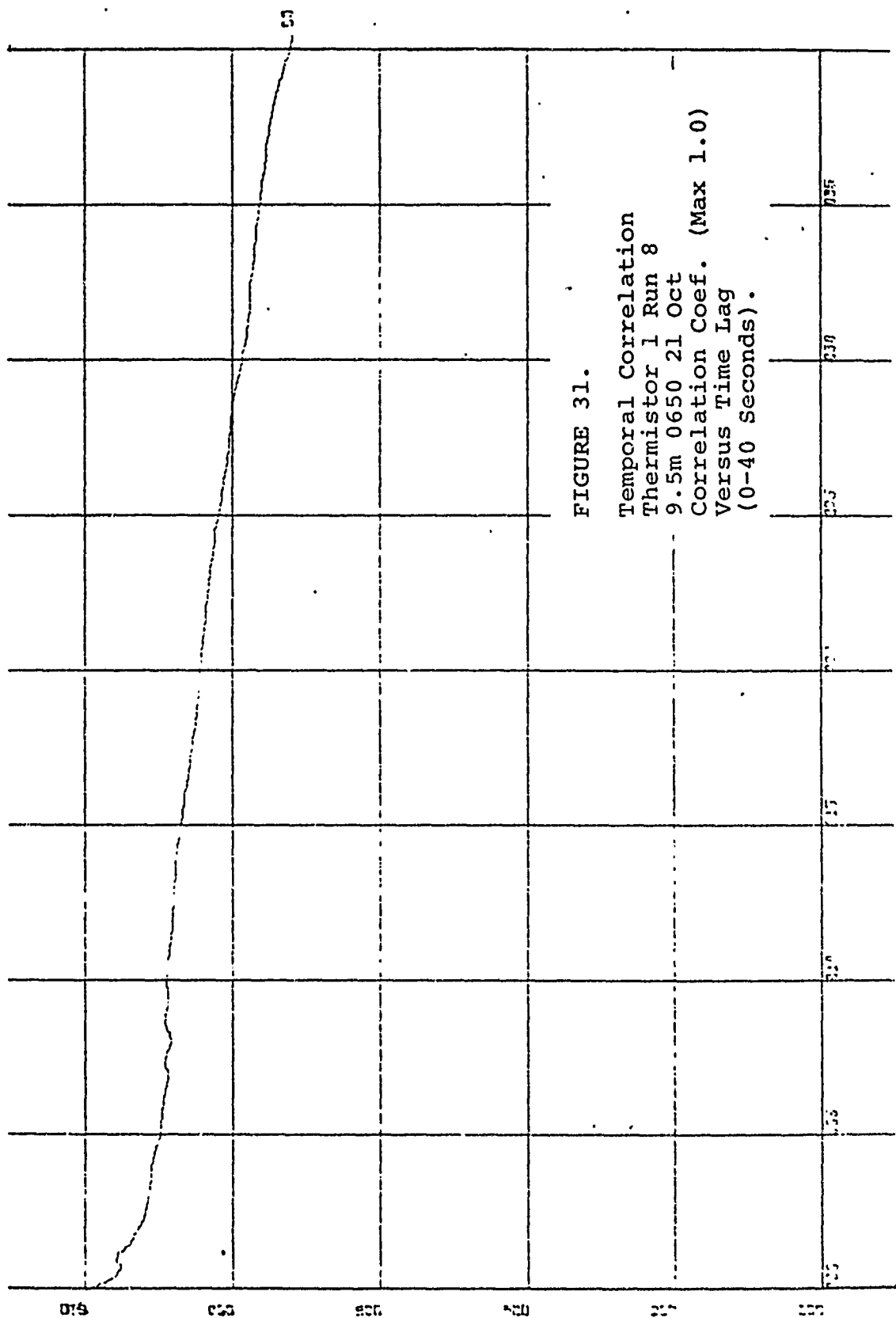


FIGURE 31.
 Temporal Correlation
 Thermistor 1 Run 8
 9.5m 0650 21 Oct
 Correlation Coef. (Max 1.0)
 Versus Time Lag
 (0-40 Seconds).

FIGURE 32.
 Temporal Correlation
 Salinity Run 8
 9.5m 0650 22 Oct
 Correlation Coef. (Max 1.0)
 Versus Time Lag
 (0-40 Seconds).

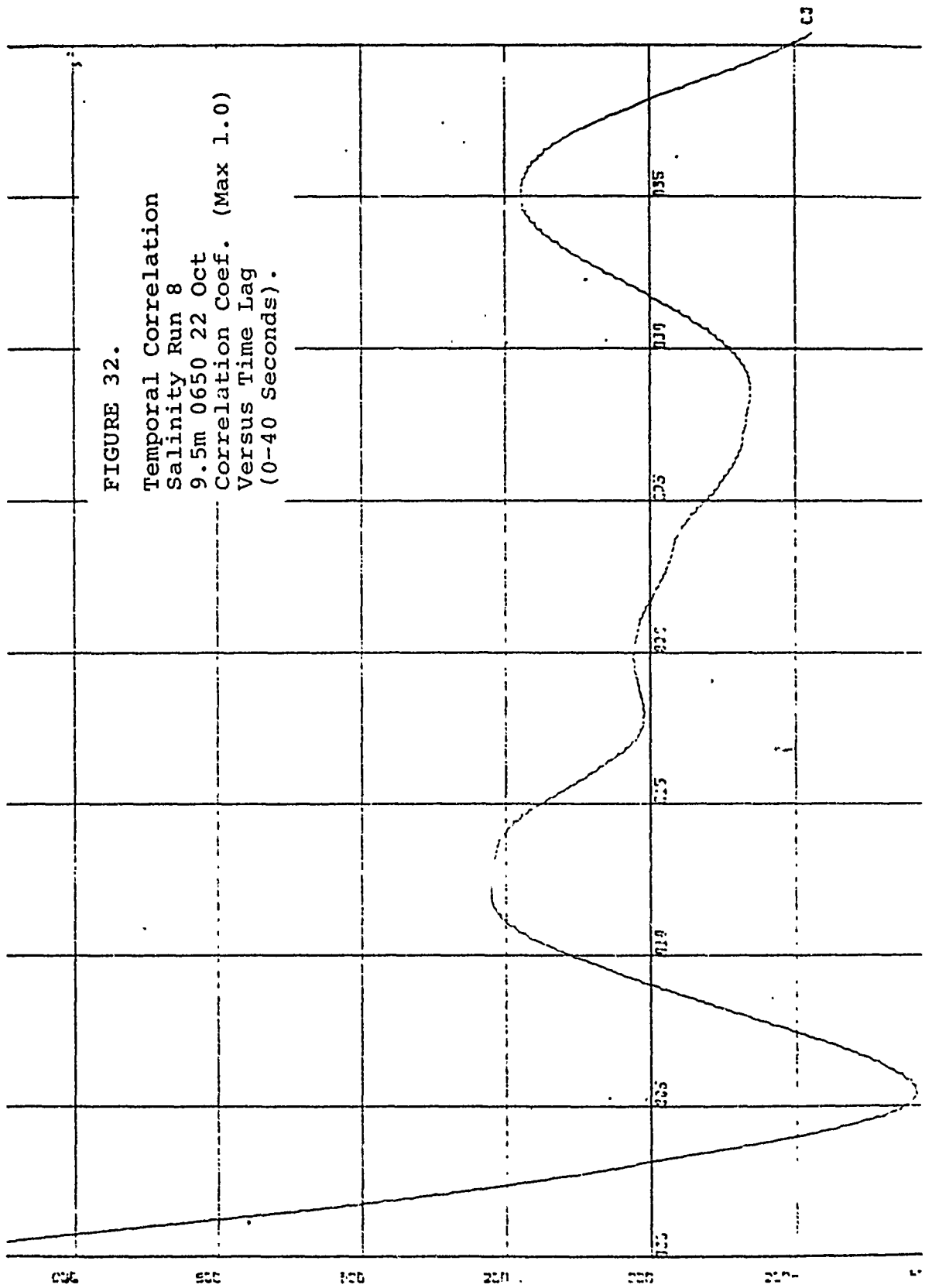
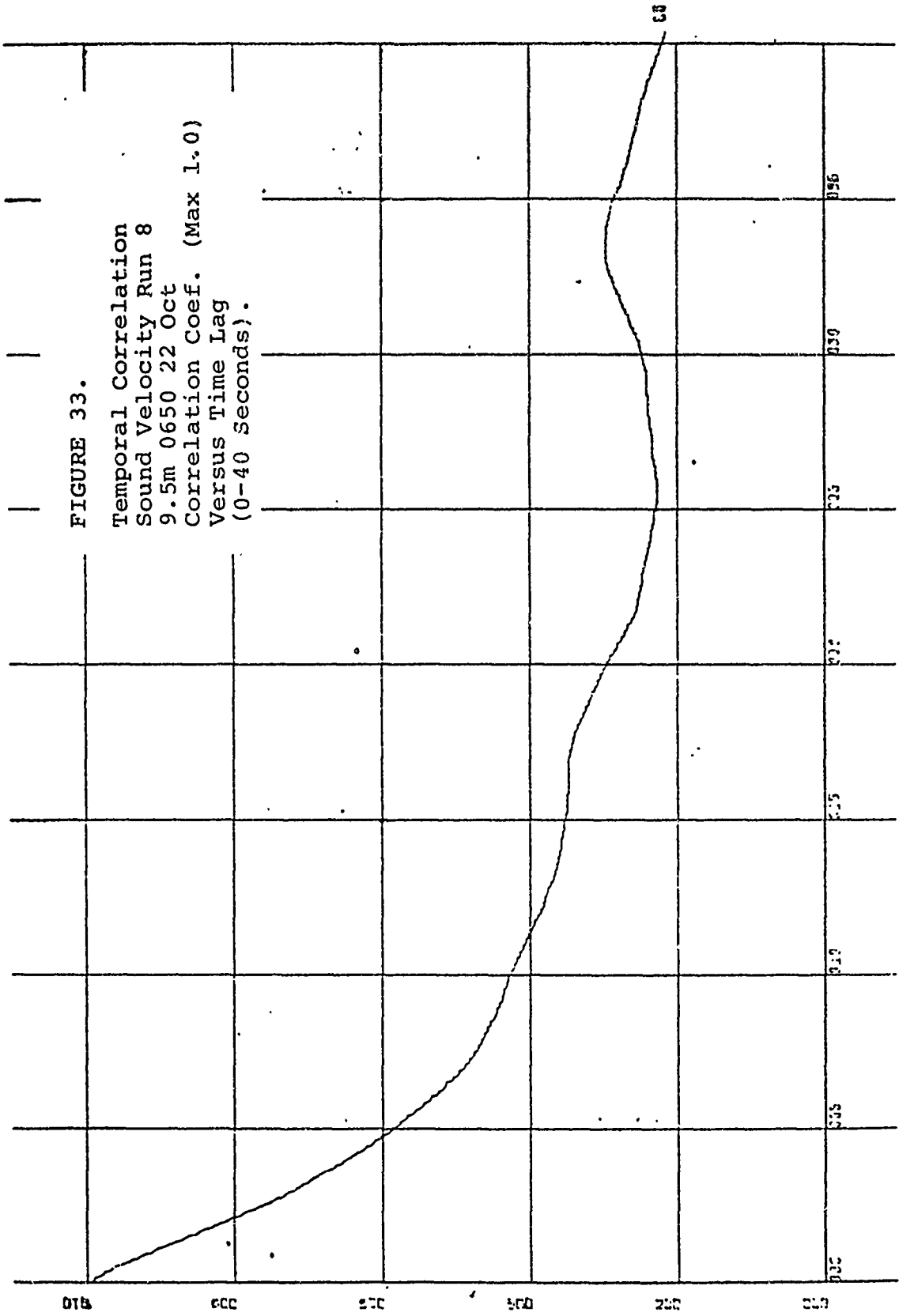


FIGURE 33.
 Temporal Correlation
 Sound Velocity Run 8
 9.5m 0650 22 Oct
 Correlation Coef. (Max 1.0)
 Versus Time Lag
 (0-40 Seconds).



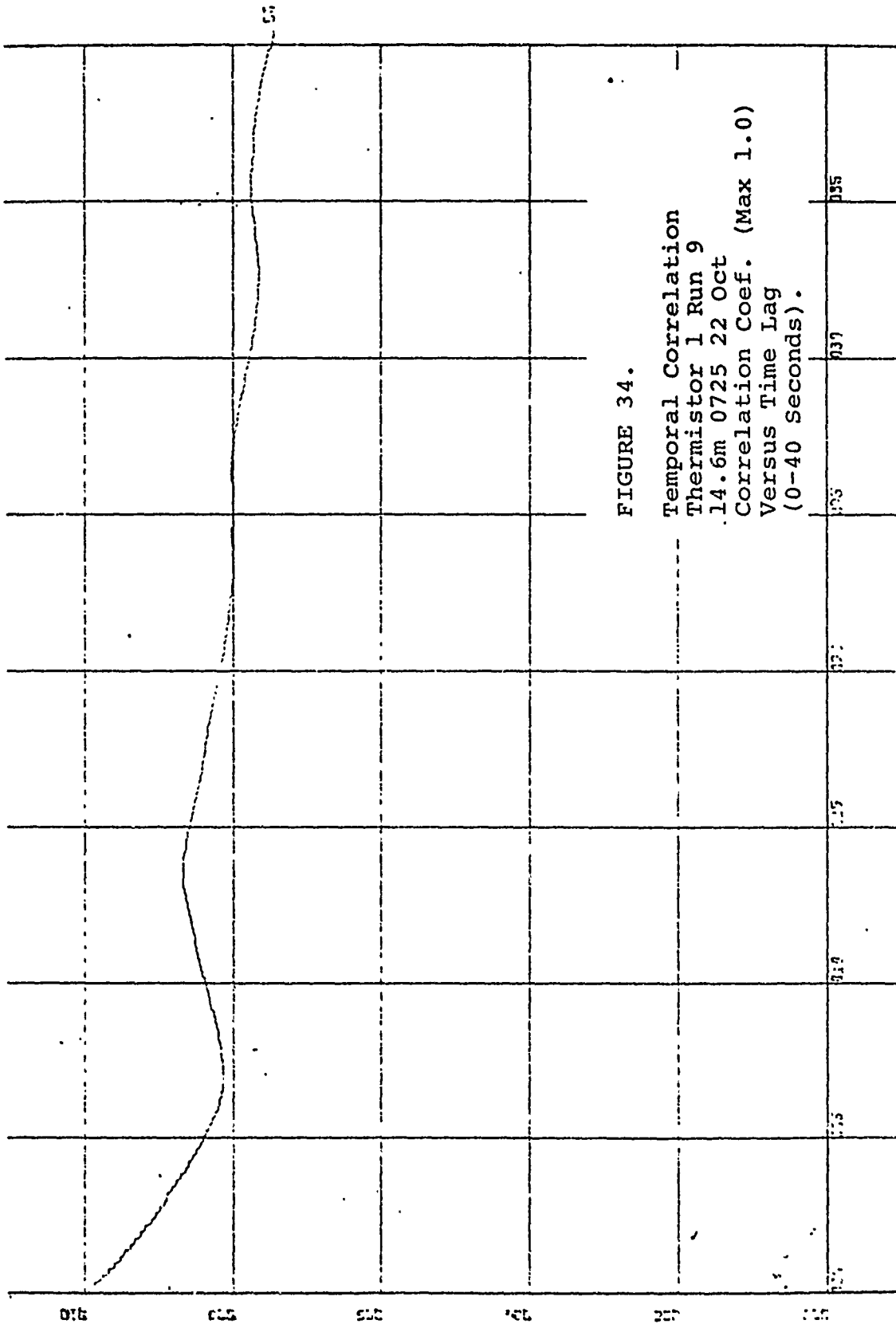


FIGURE 34.

Temporal Correlation
 Thermistor 1 Run 9
 14.6m 0725 22 Oct
 Correlation Coef. (Max 1.0)
 Versus Time Lag
 (0-40 Seconds).

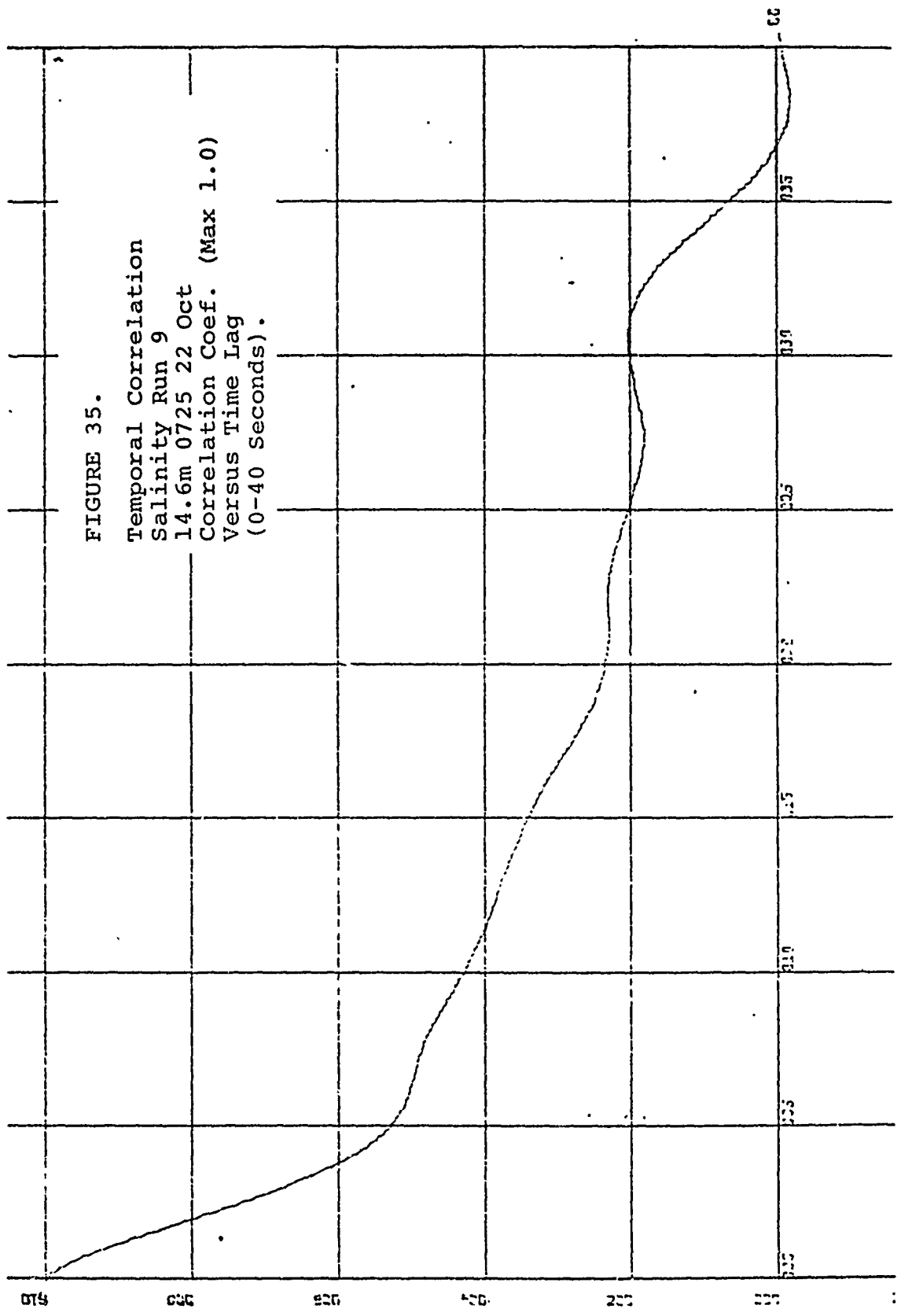


FIGURE 35.
 Temporal Correlation
 Salinity Run 9
 14.6m 0725 22 Oct
 Correlation Coef. (Max 1.0)
 Versus Time Lag
 (0-40 Seconds).

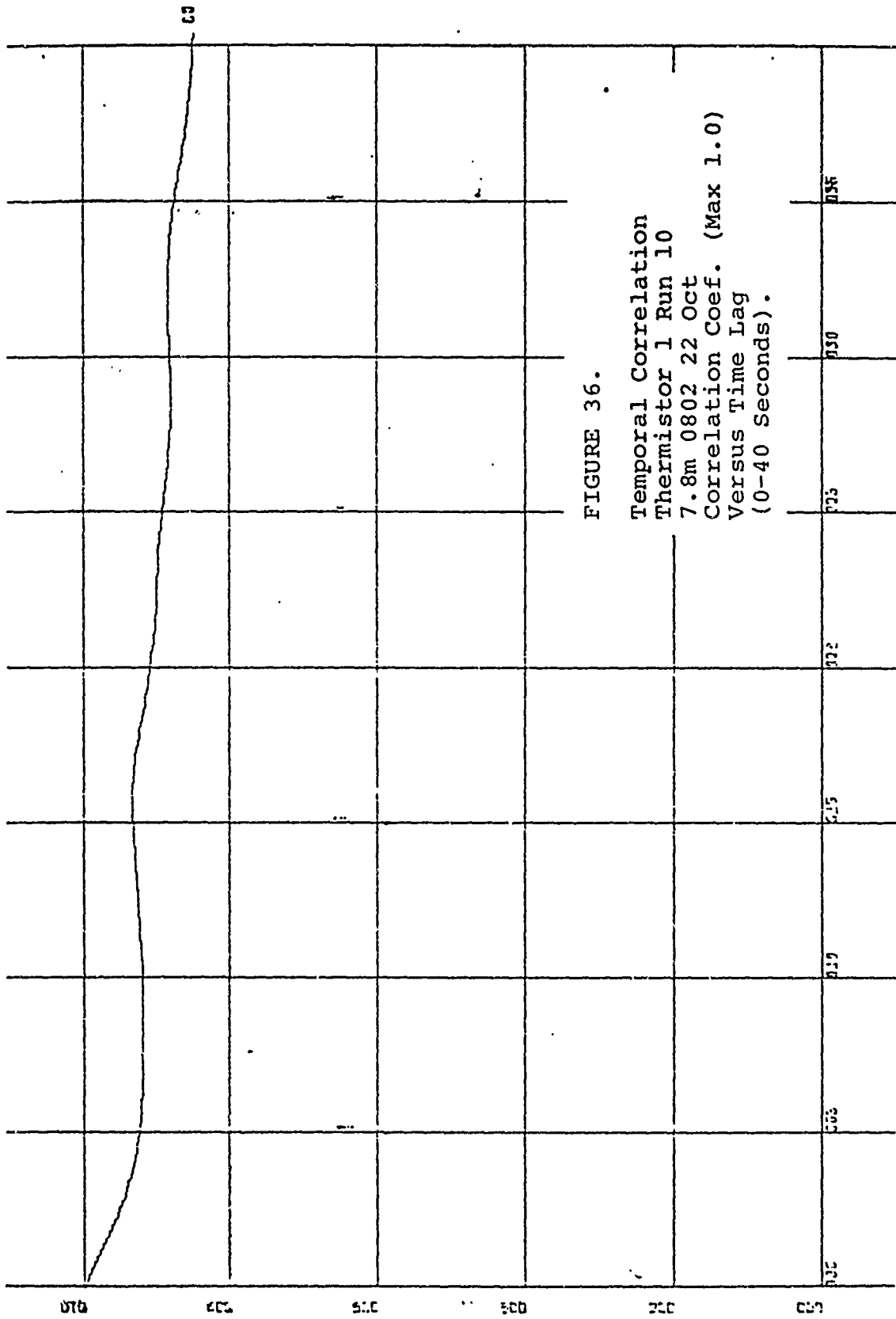


FIGURE 36.
 Temporal Correlation
 Thermistor 1 Run 10
 7.8m 0802 22 Oct
 Correlation Coef. (Max 1.0)
 Versus Time Lag
 (0-40 Seconds).

FIGURE 37.

Temporal Correlation
Salinity Run 10
7.8m 0802 22 Oct
Correlation Coef. (Max 1.0)
Versus Time Lag
(0-40 Seconds).

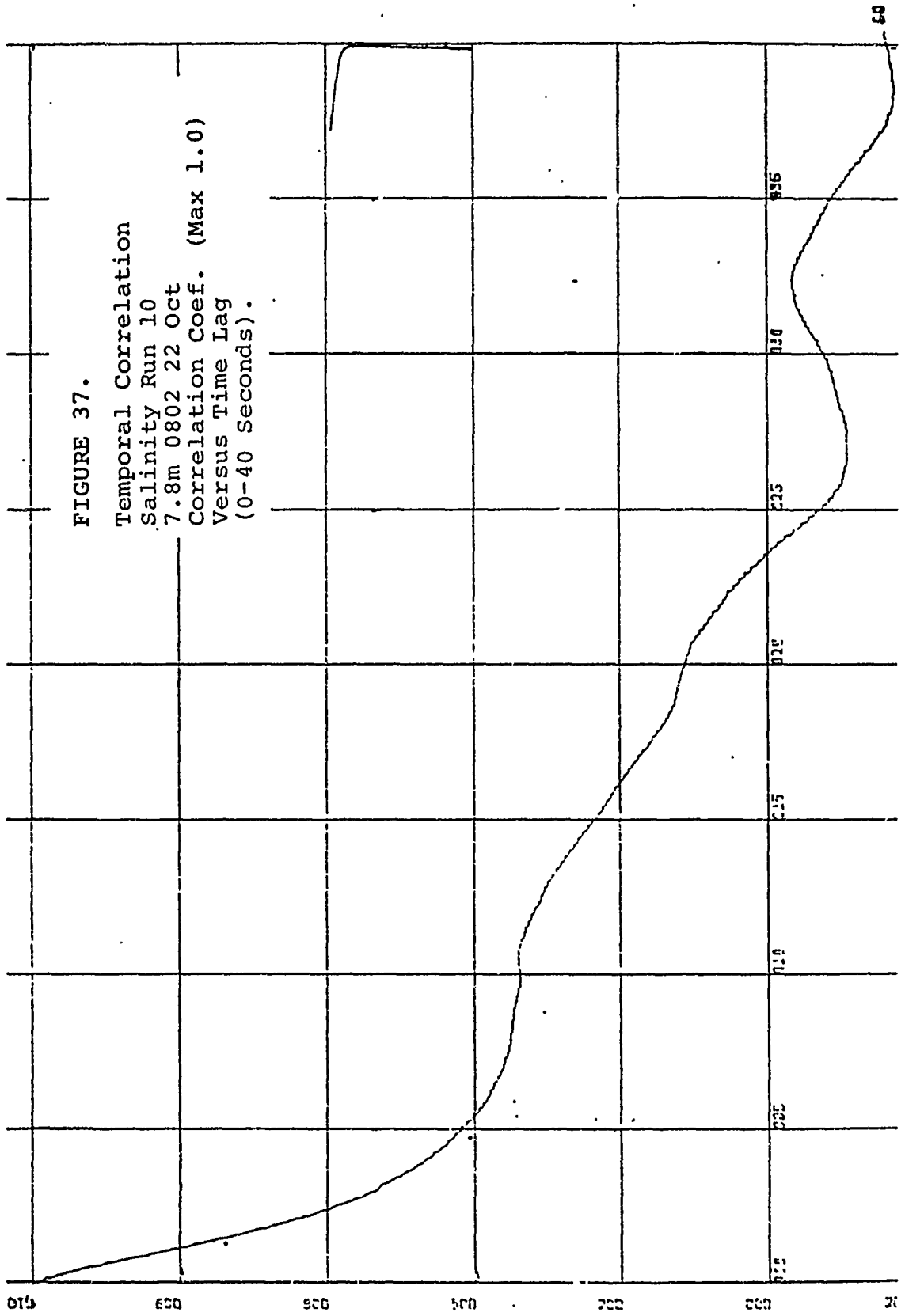


FIGURE 38.

Power Spectral Density
Thermistor 1 Run 3
9.0m 1616 21 Oct
Spectrum ($^{\circ}\text{C}$)²/HZ
Versus Frequency (0-2.5 HZ).

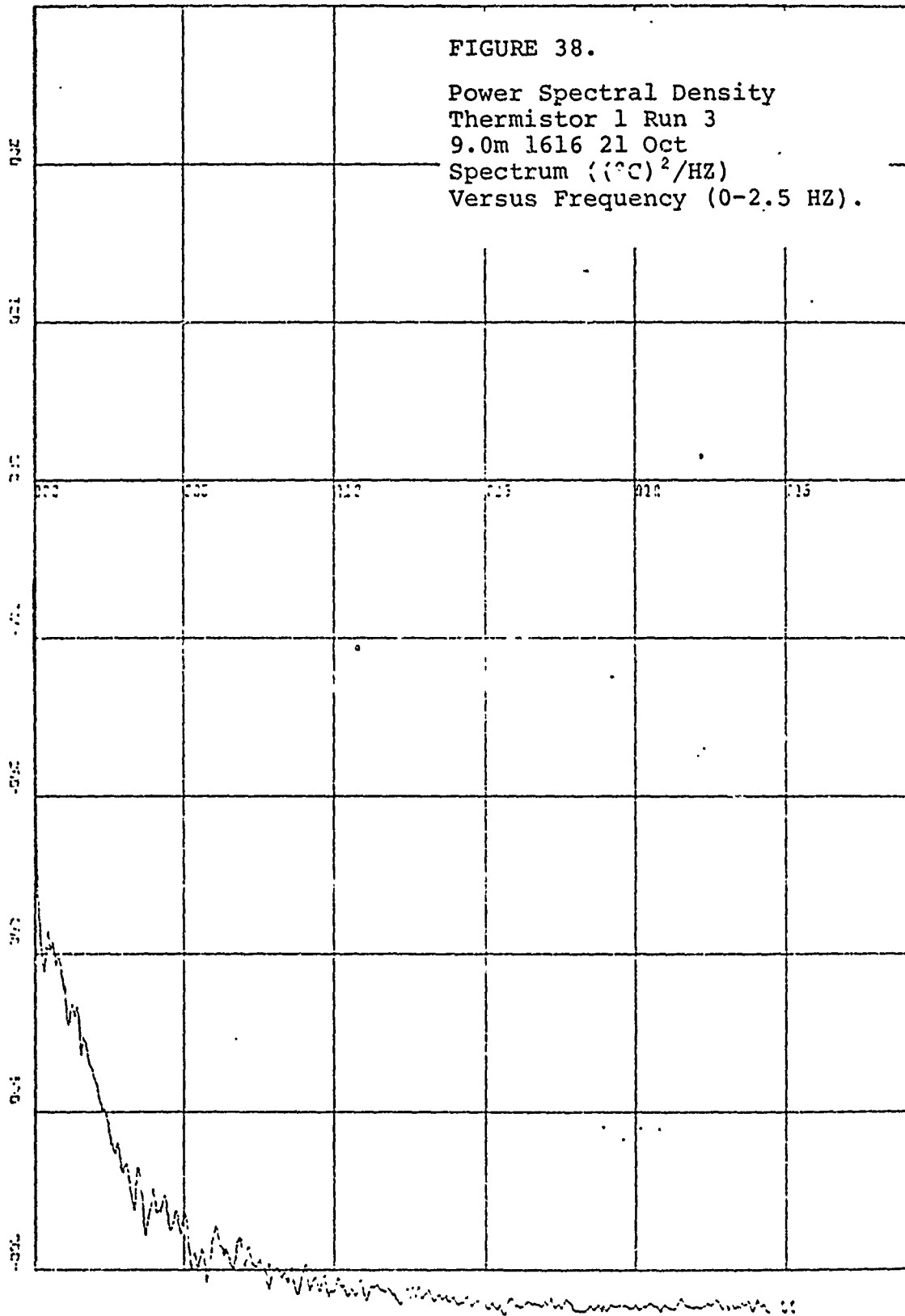
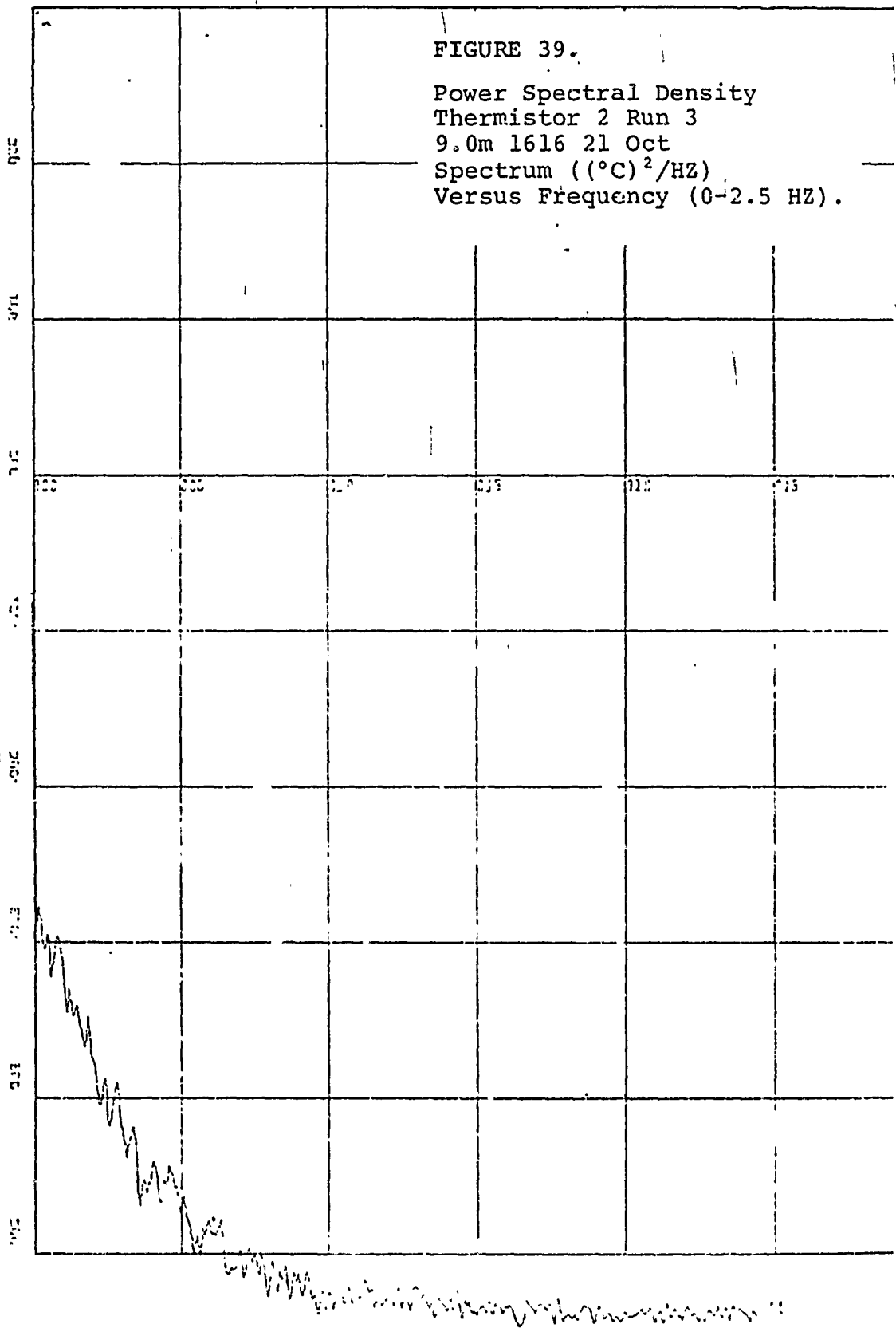


FIGURE 39.

Power Spectral Density
Thermistor 2 Run 3
9.0m 1616 21 Oct
Spectrum ($^{\circ}\text{C}$)²/HZ
Versus Frequency (0-2.5 HZ).



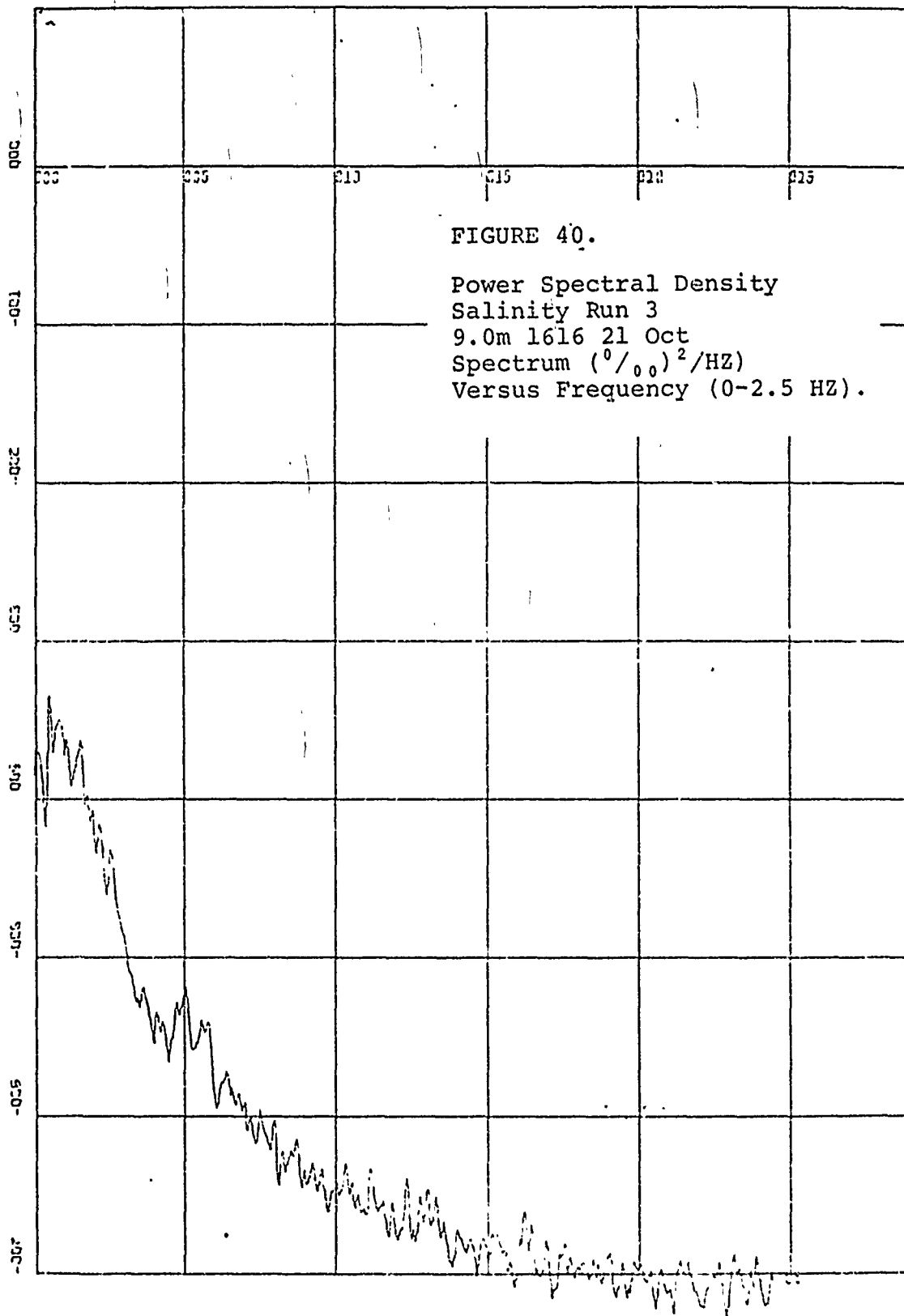
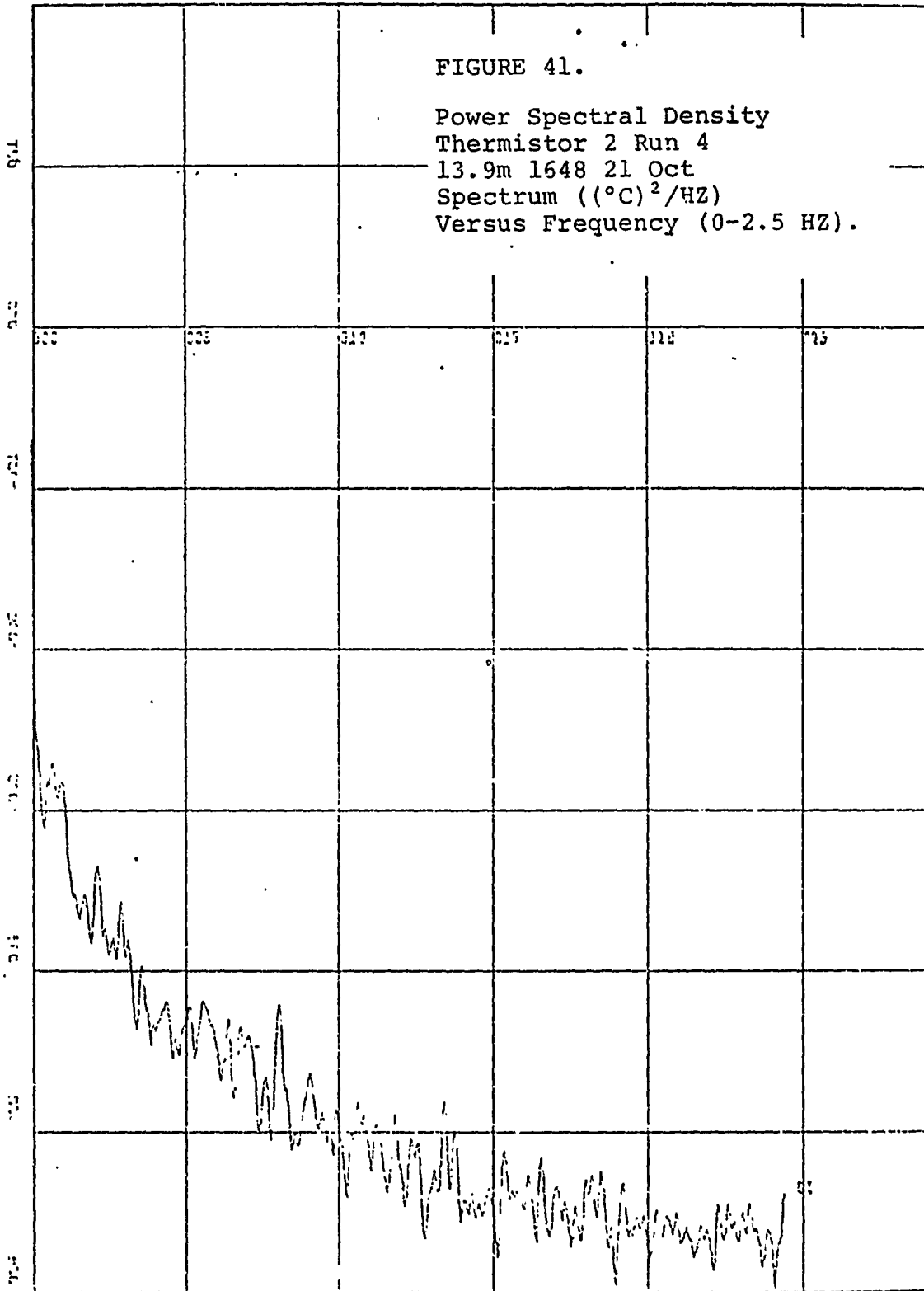


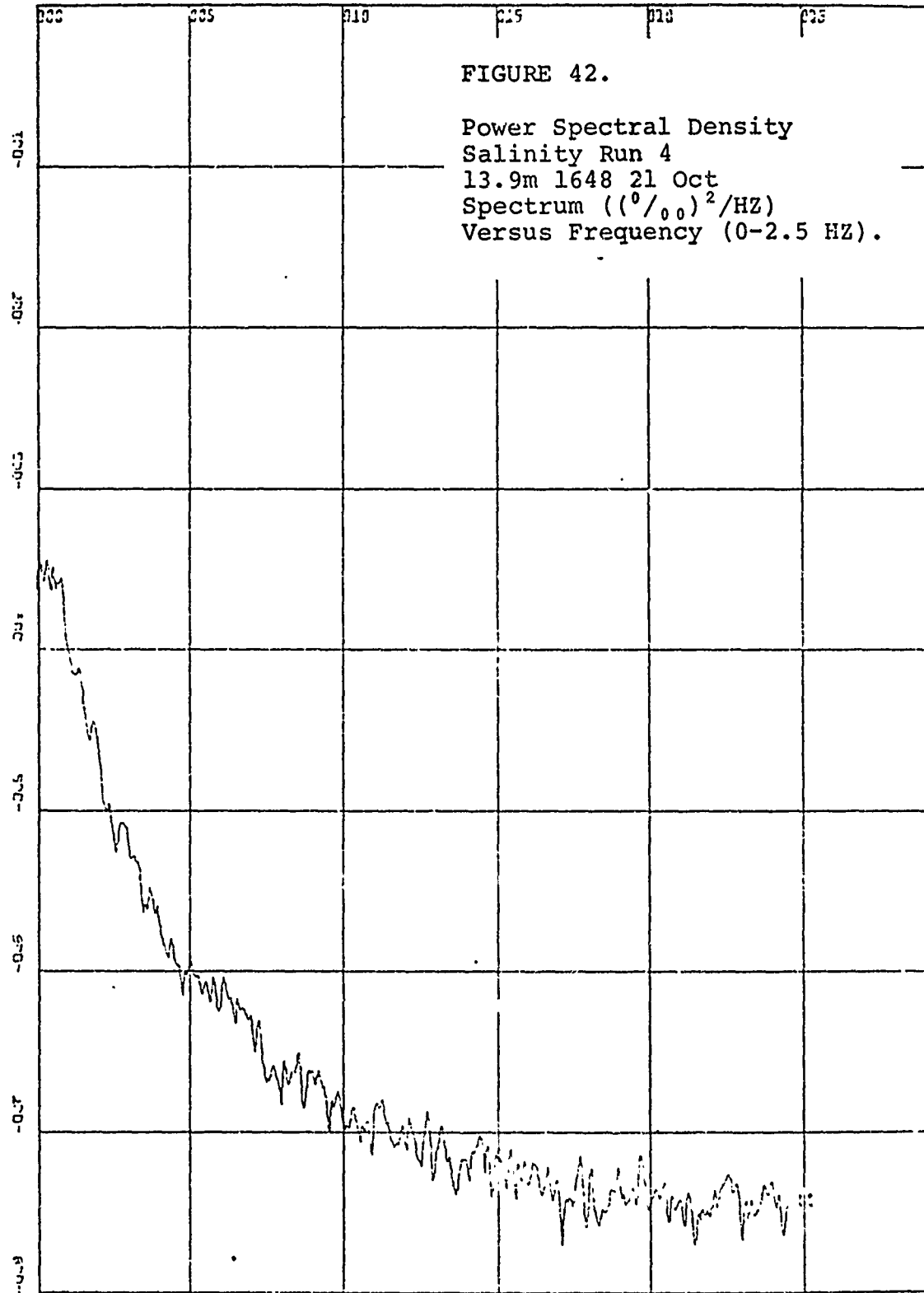
FIGURE 40.

Power Spectral Density
 Salinity Run 3
 9.0m 1616 21 Oct
 Spectrum $(\text{‰})^2/\text{HZ}$
 Versus Frequency (0-2.5 HZ).

FIGURE 41.

Power Spectral Density
Thermistor 2 Run 4
13.9m 1648 21 Oct
Spectrum $(^{\circ}\text{C})^2/\text{HZ}$
Versus Frequency (0-2.5 HZ).





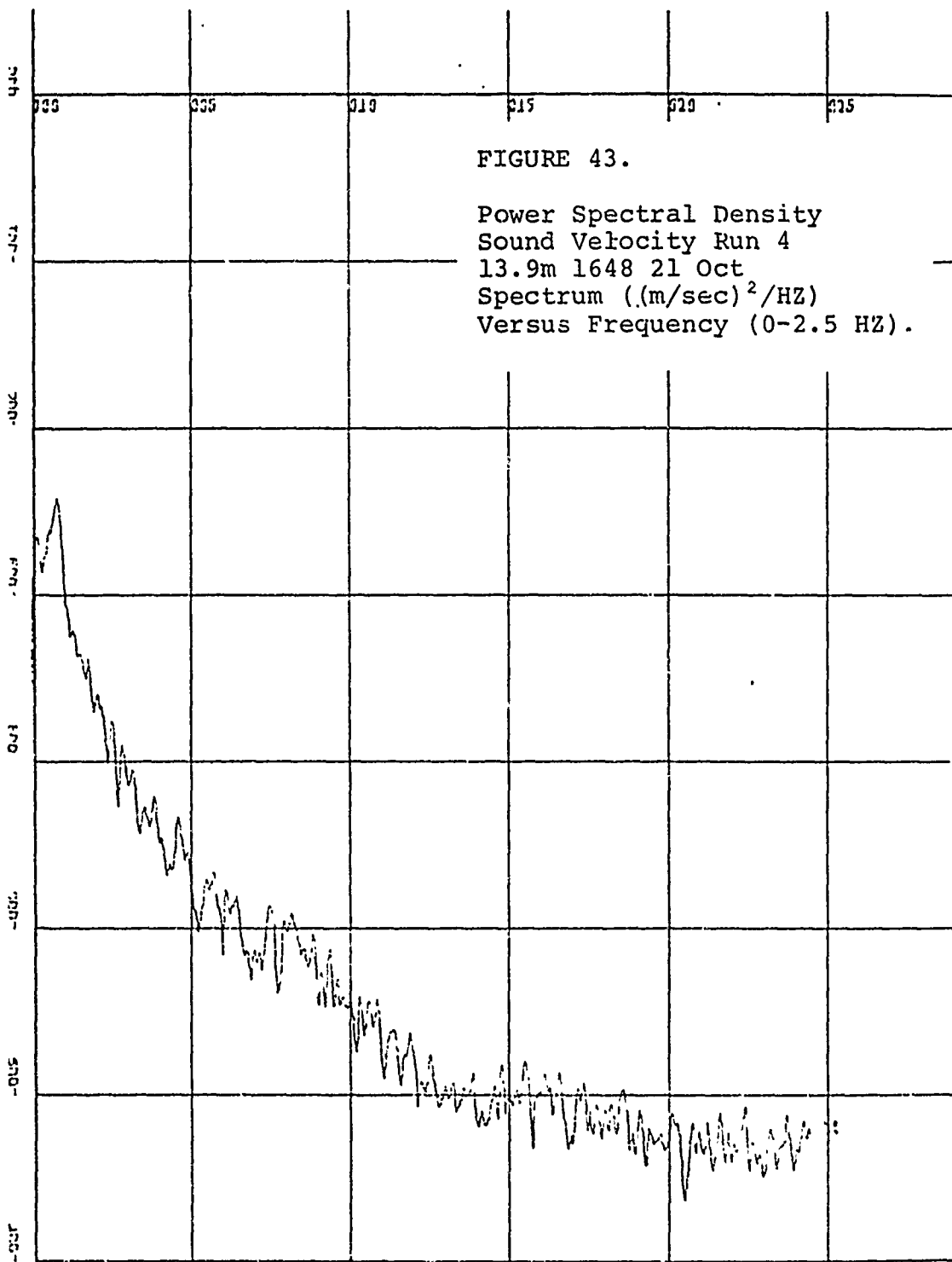


FIGURE 43.

Power Spectral Density
 Sound Velocity Run 4
 13.9m 1648 21 Oct
 Spectrum $((m/sec)^2/HZ)$
 Versus Frequency (0-2.5 HZ).

FIGURE 44.

Power Spectral Density
Thermistor 1 Run 5
6.9m 1728 21 Oct
Spectrum $(\frac{\circ}{\circ\circ})^2/\text{HZ}$
Versus Frequency (0-2.5 HZ).

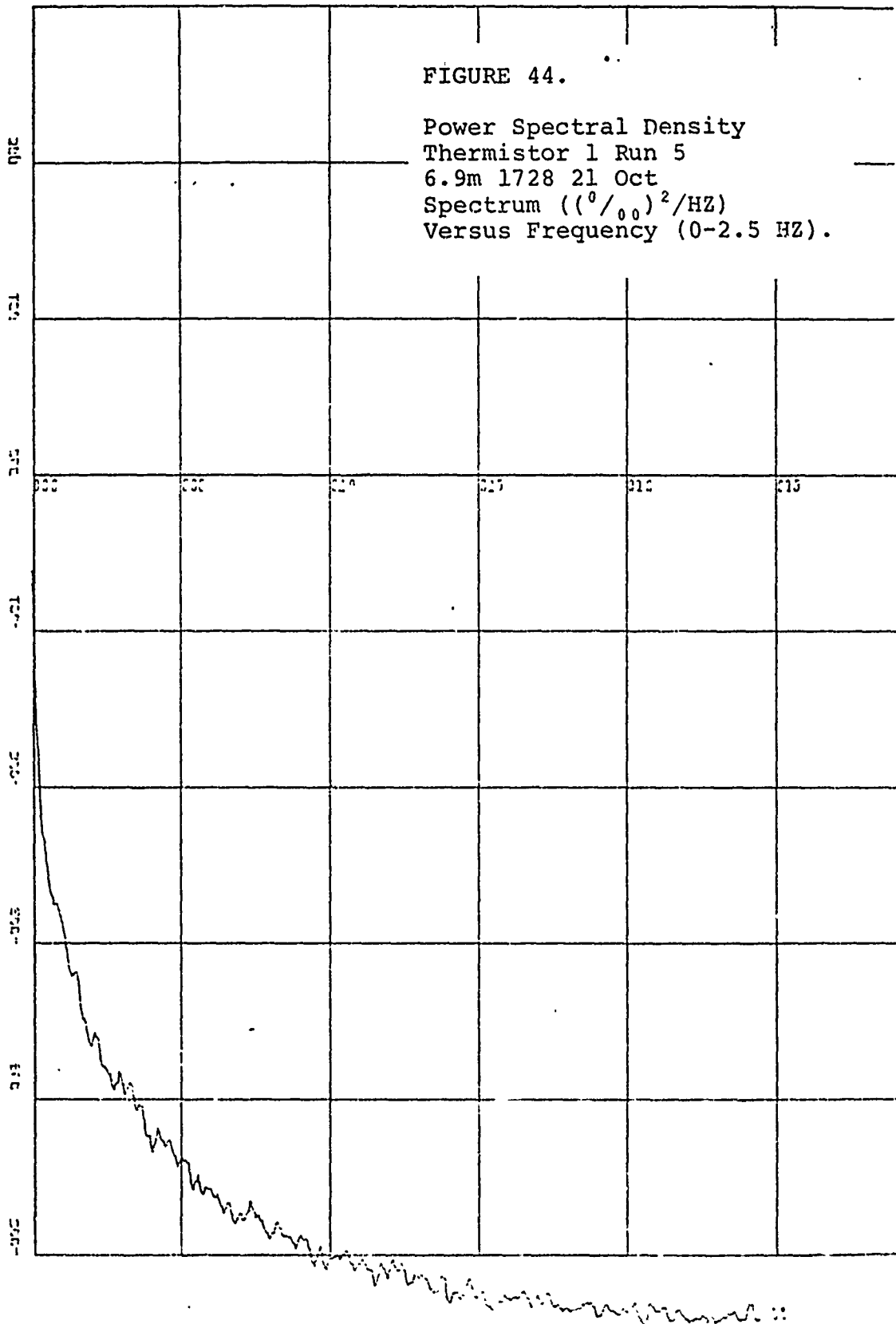


FIGURE 45.

Power Spectral Density
Thermistor 2 Run 5
6.9m 1728 21 Oct
Spectrum ($^{\circ}\text{C}$)²/HZ
Versus Frequency (0-2.5 HZ).

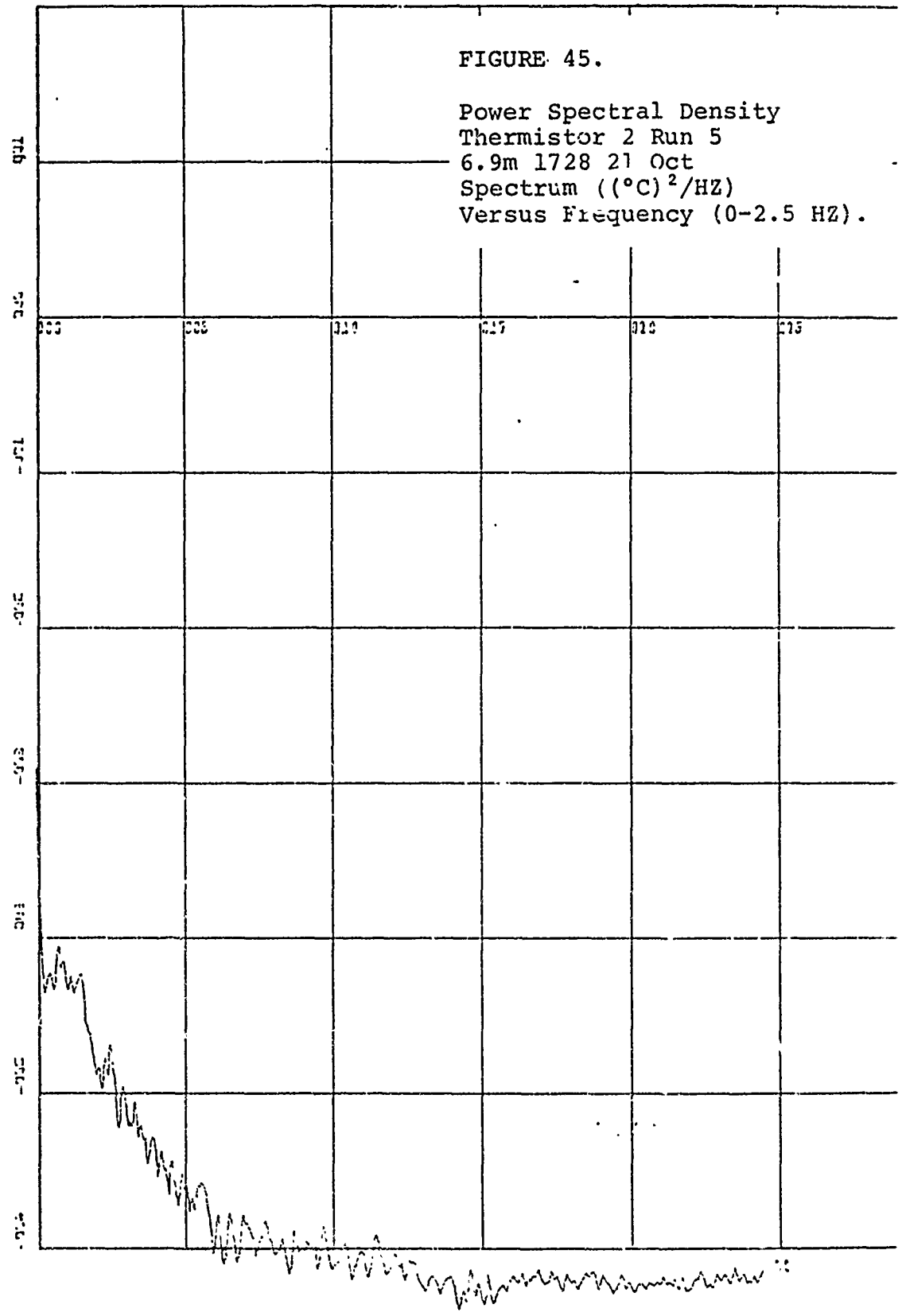


FIGURE 46.

Power Spectral Density
Salinity Run 5
6.9m 1728 21 Oct
Spectrum $(\text{‰})^2/\text{HZ}$
Versus Frequency (0-2.5 HZ).

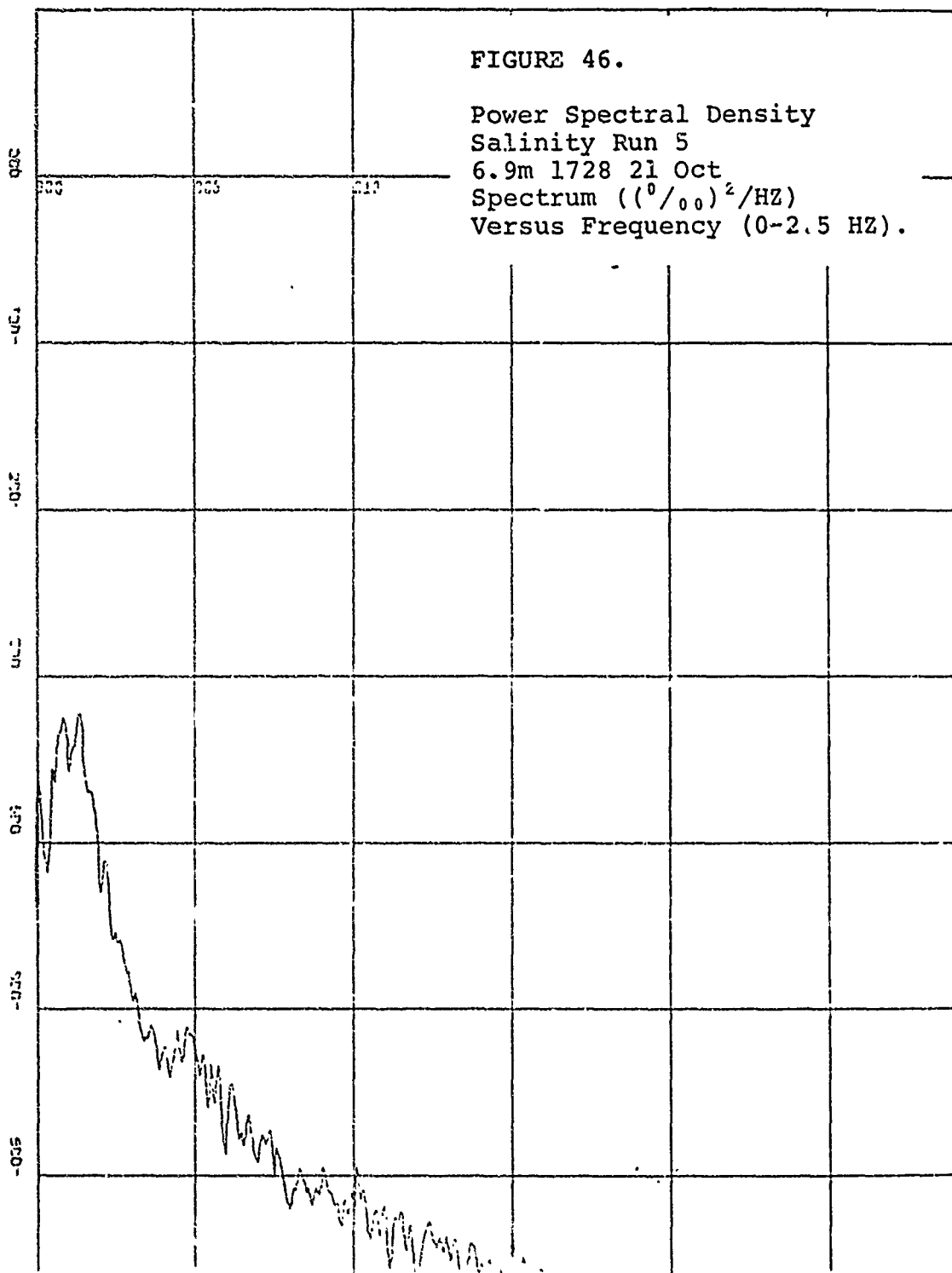


FIGURE 47.

Power Spectral Density
Sound Velocity Run 5
6.9m 1728 21 Oct
Spectrum $(\text{m/sec})^2/\text{HZ}$
Versus Frequency (0-2.5 HZ).

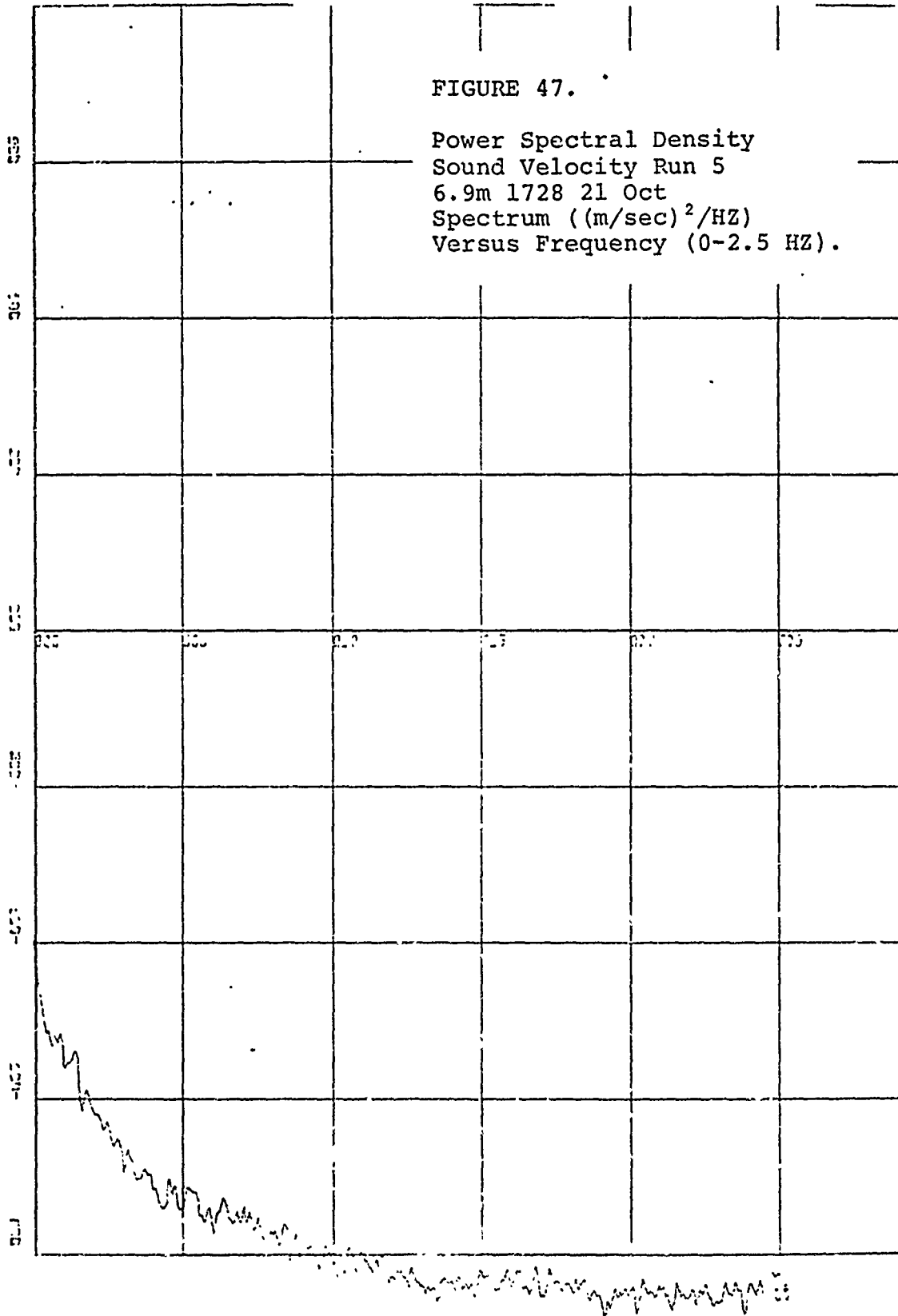
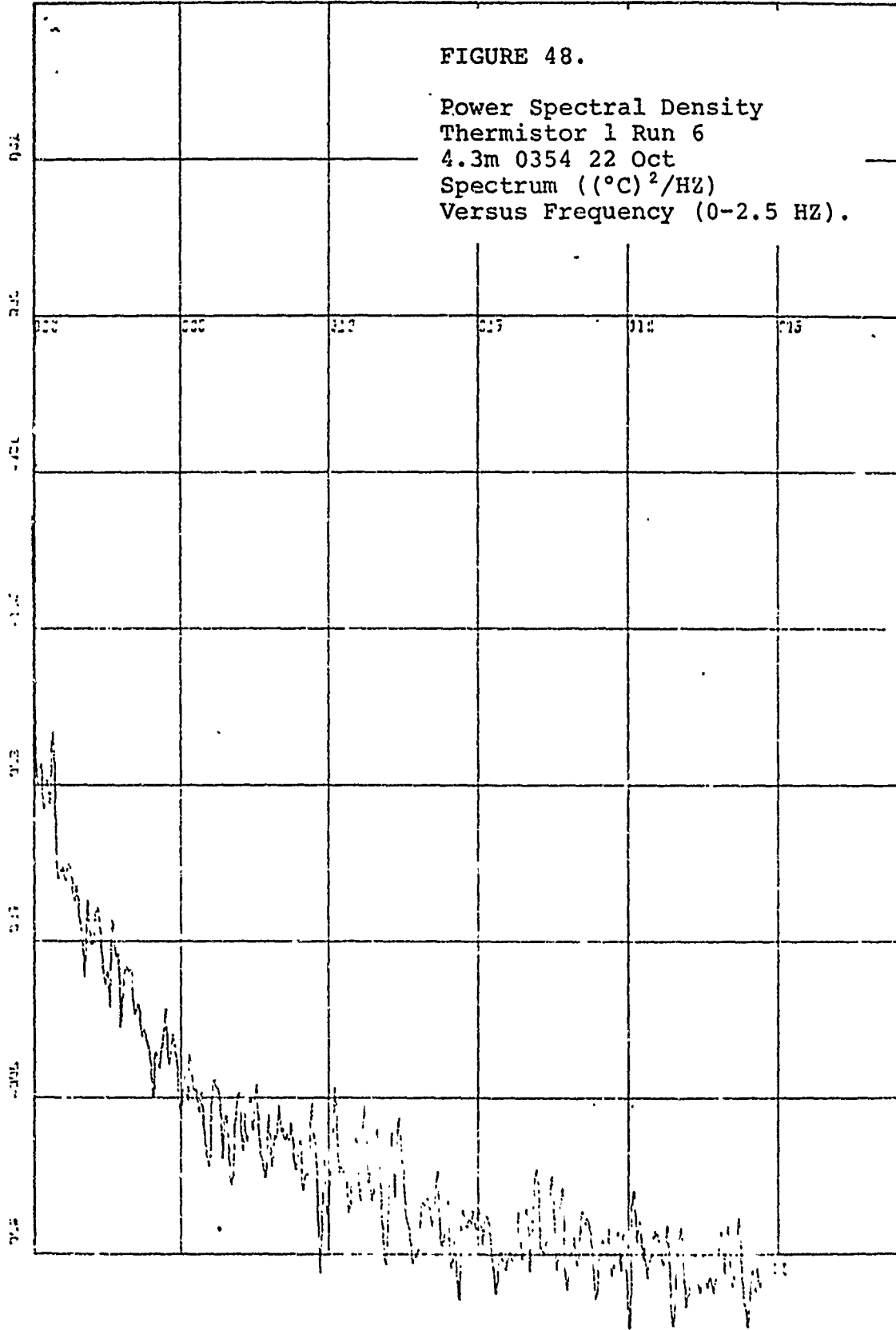
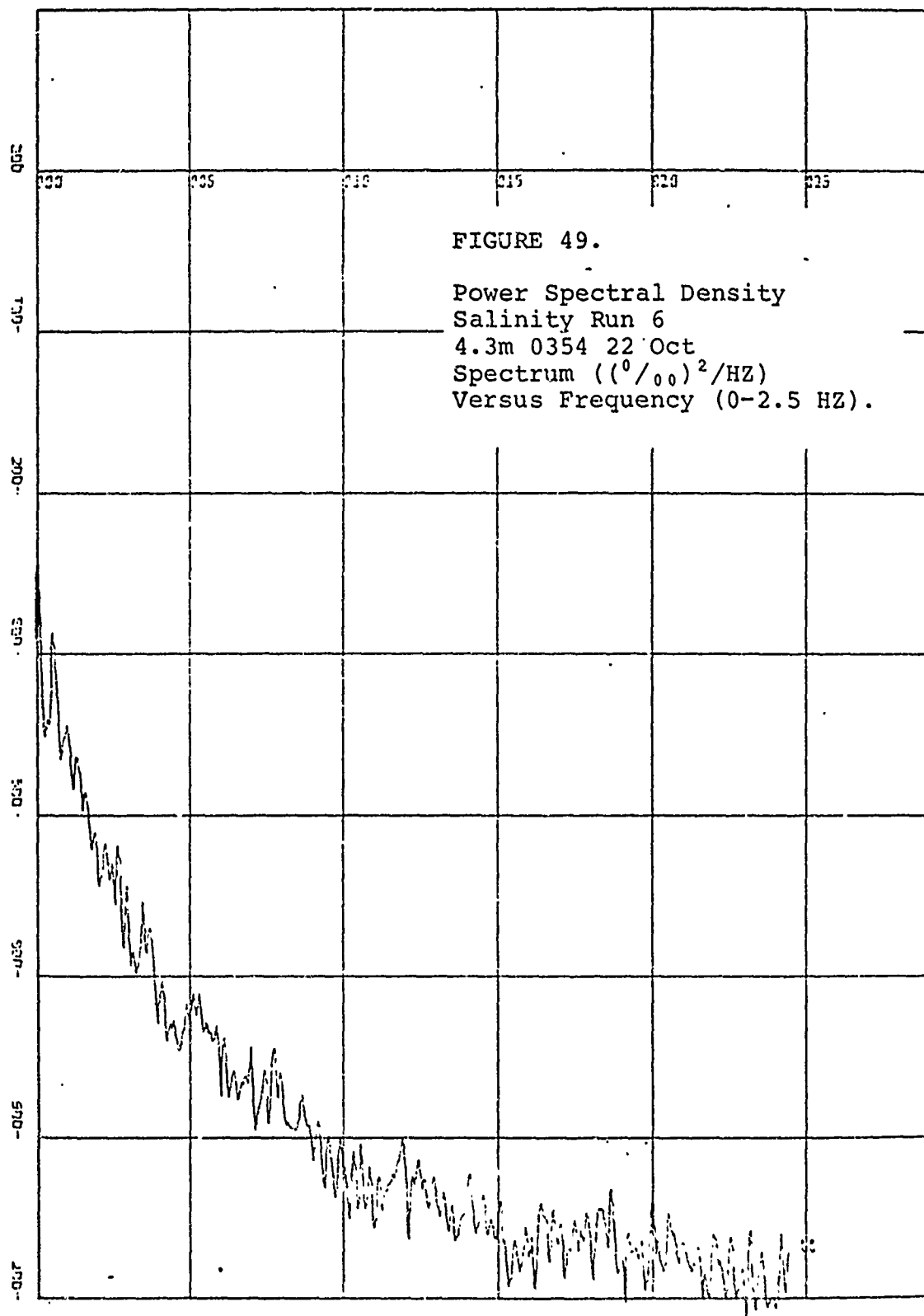


FIGURE 48.

Power Spectral Density
Thermistor 1 Run 6
4.3m 0354 22 Oct
Spectrum ($^{\circ}\text{C}$)²/HZ)
Versus Frequency (0-2.5 HZ).





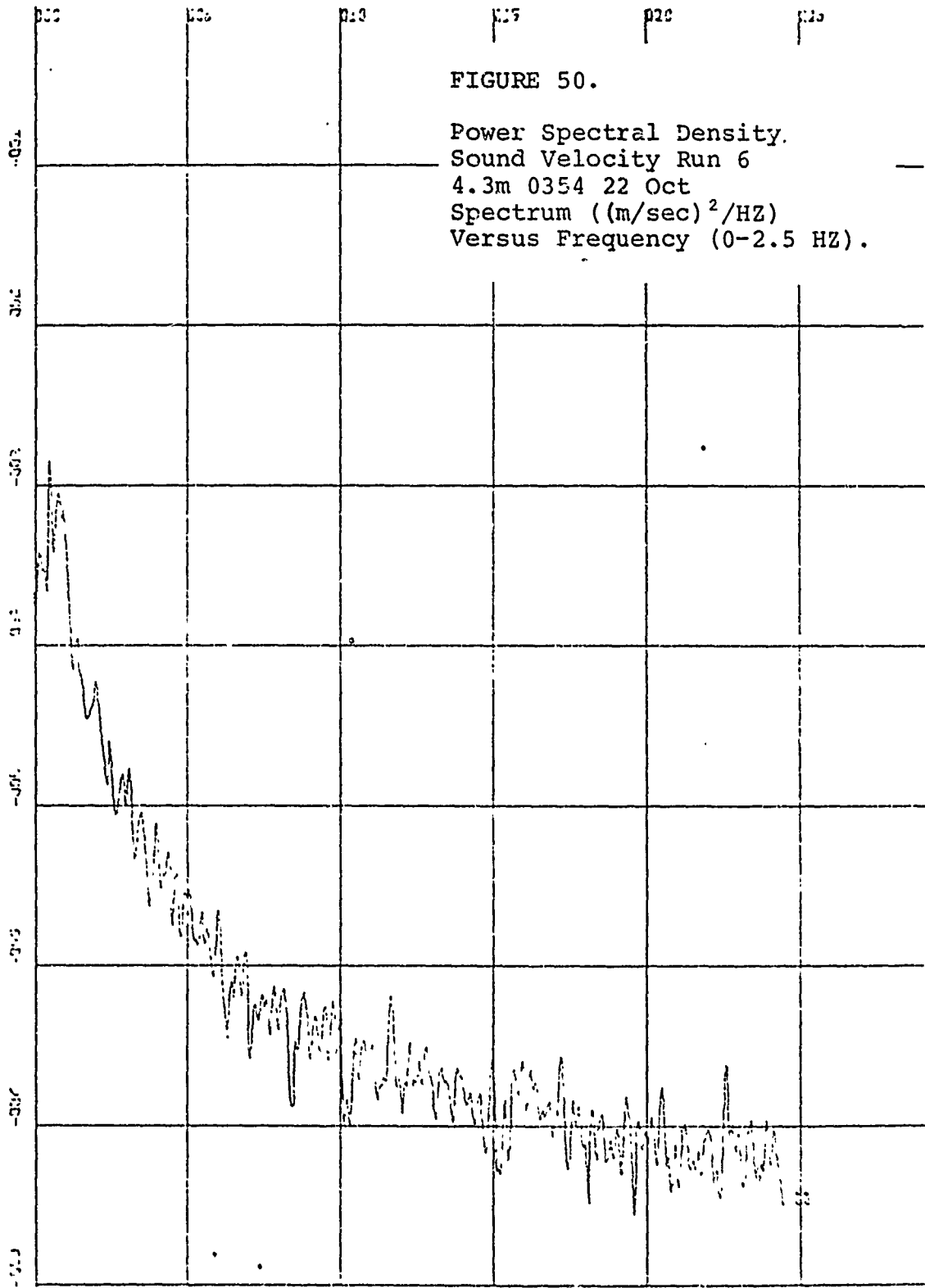
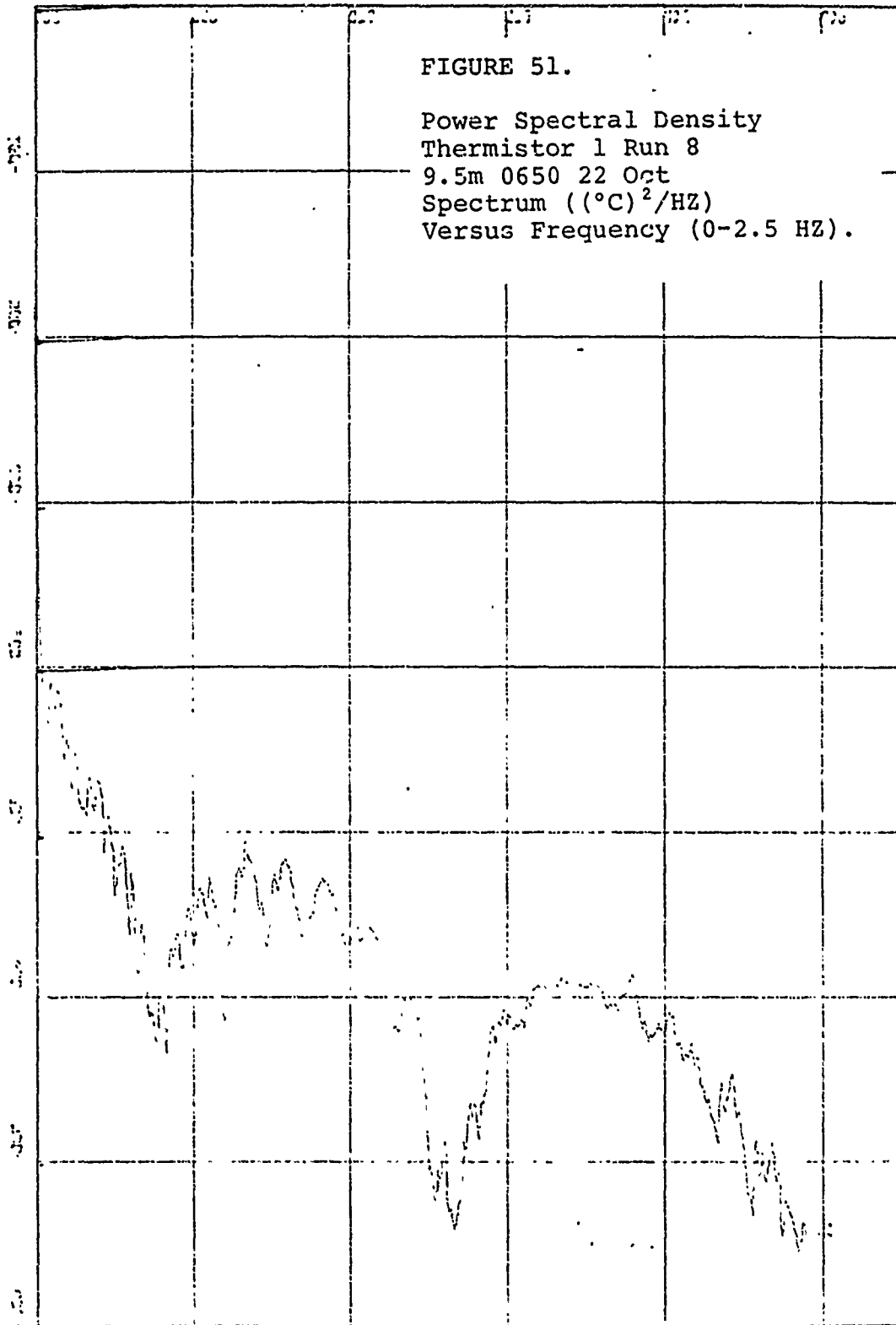
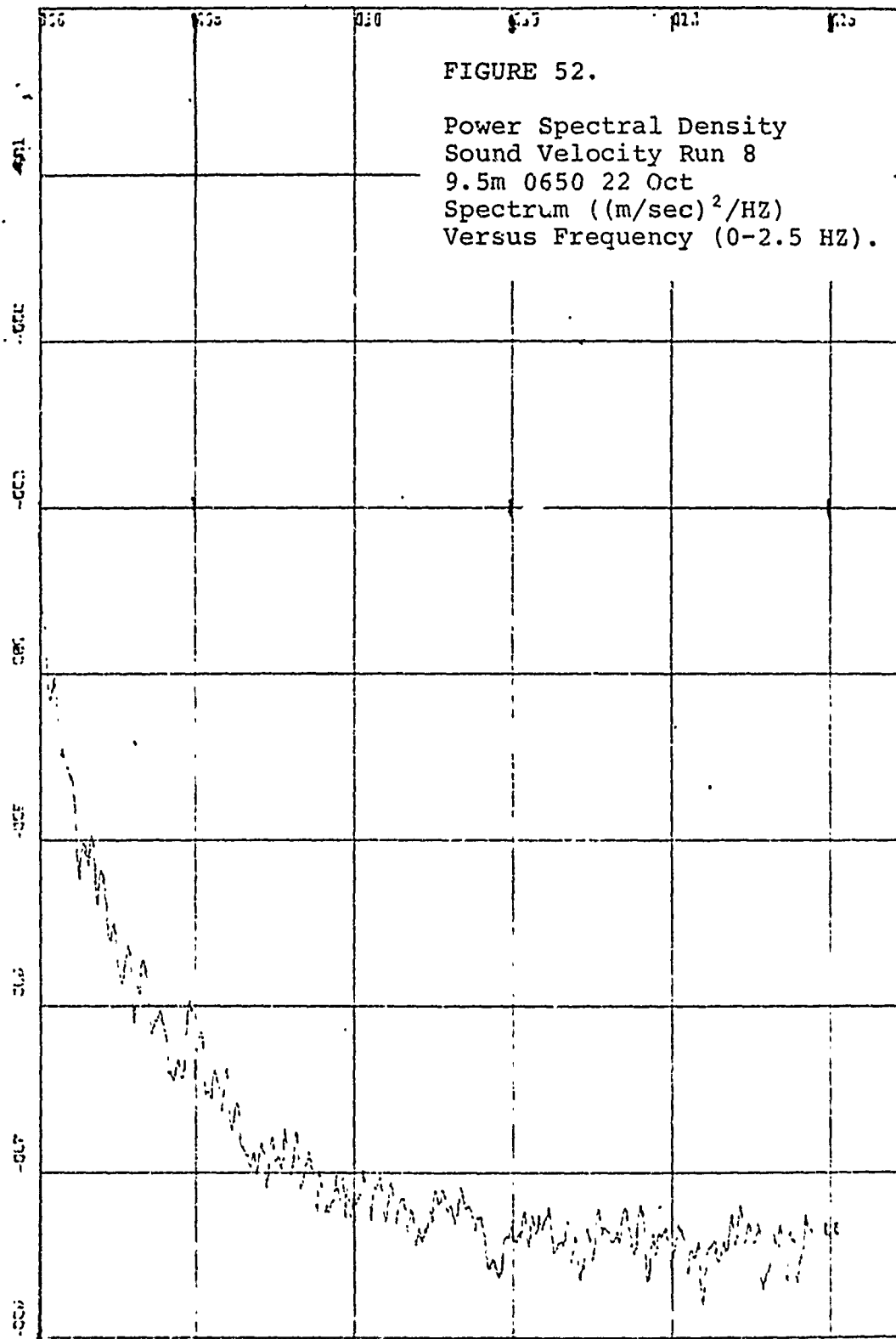


FIGURE 50.

Power Spectral Density.
 Sound Velocity Run 6
 4.3m 0354 22 Oct
 Spectrum $(\text{m/sec})^2/\text{HZ}$
 Versus Frequency (0-2.5 HZ).





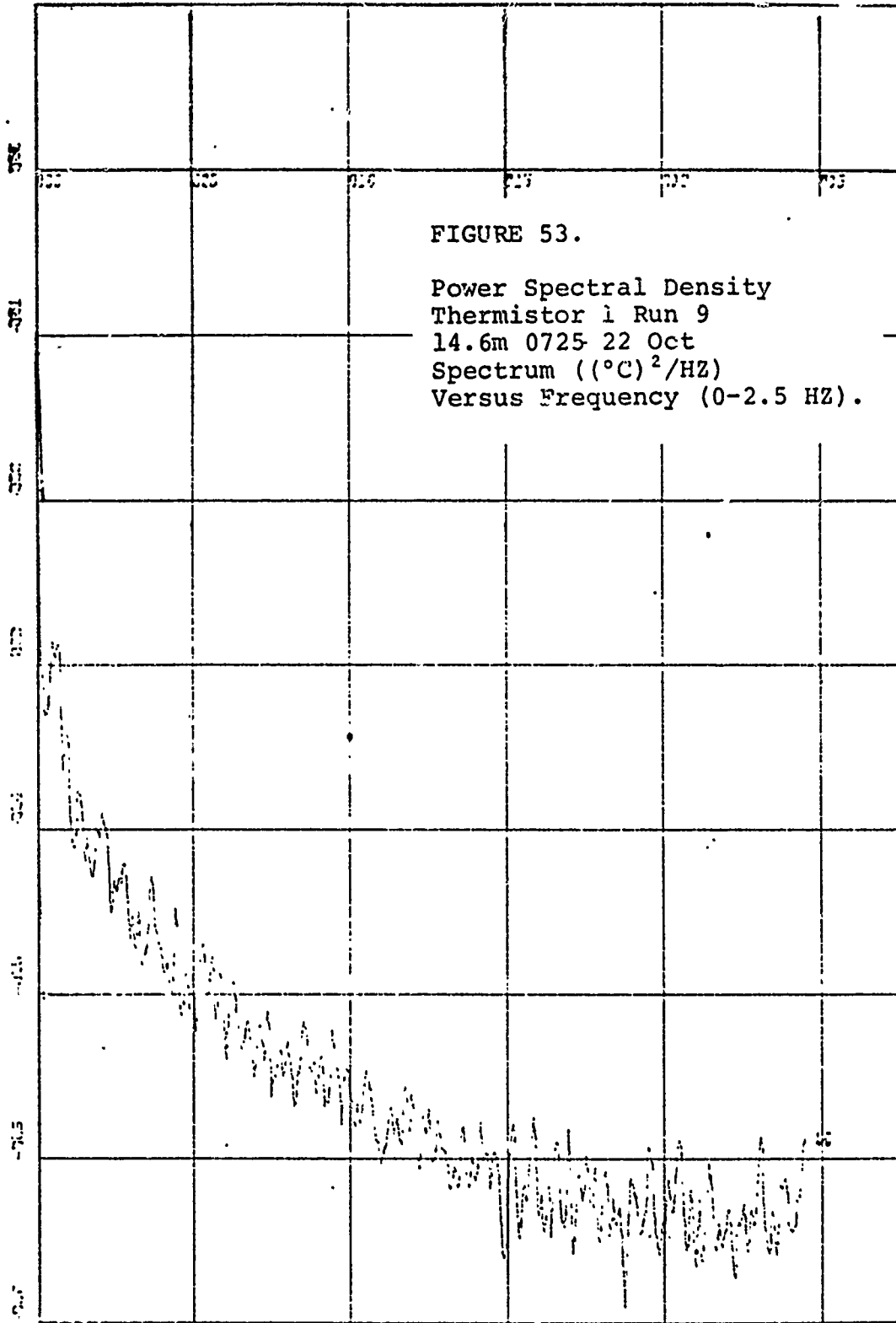


FIGURE 53.

Power Spectral Density
 Thermistor i Run 9
 14.6m 0725 22 Oct
 Spectrum ($^{\circ}\text{C}$)²/HZ
 Versus Frequency (0-2.5 HZ).

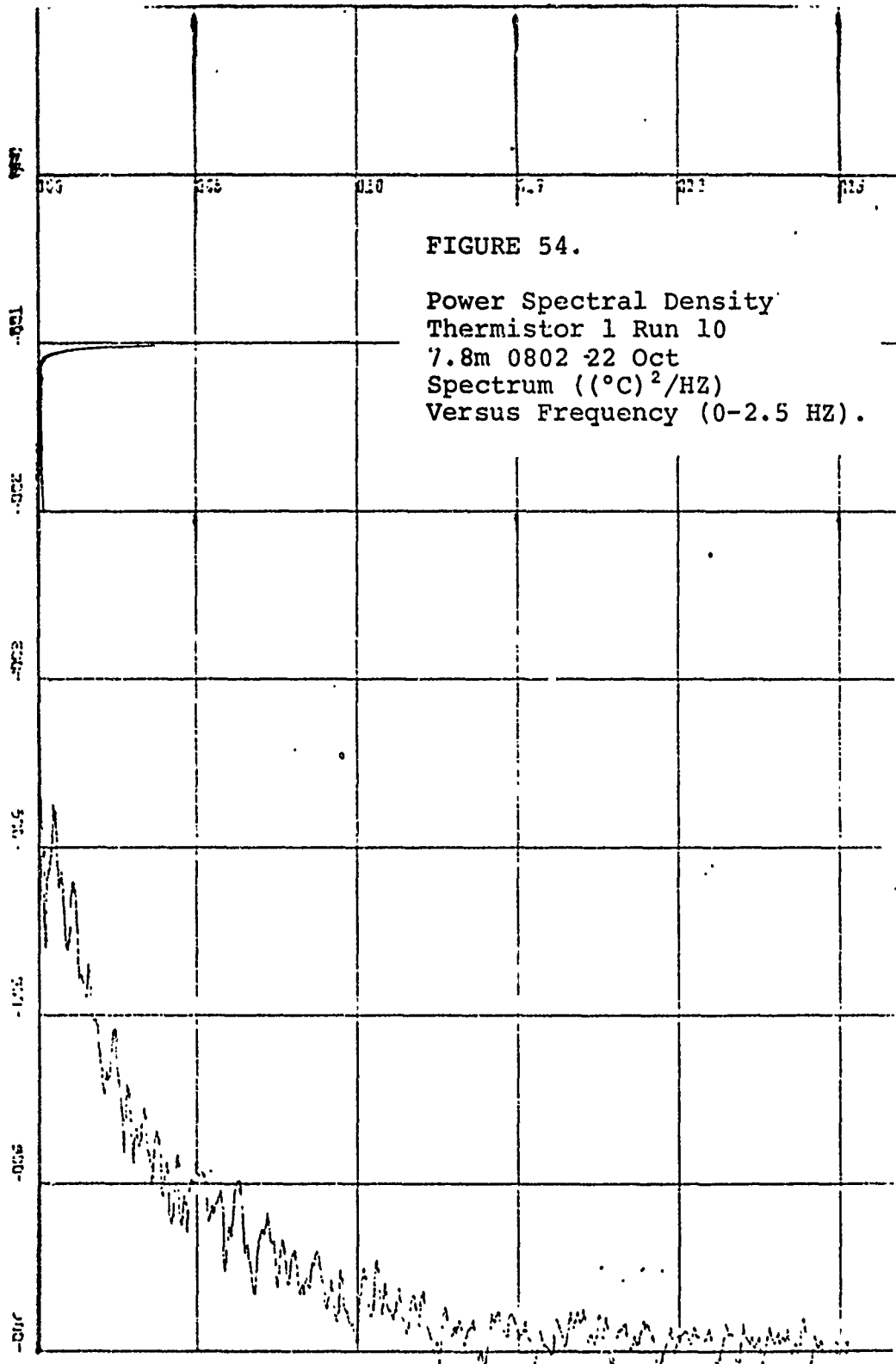
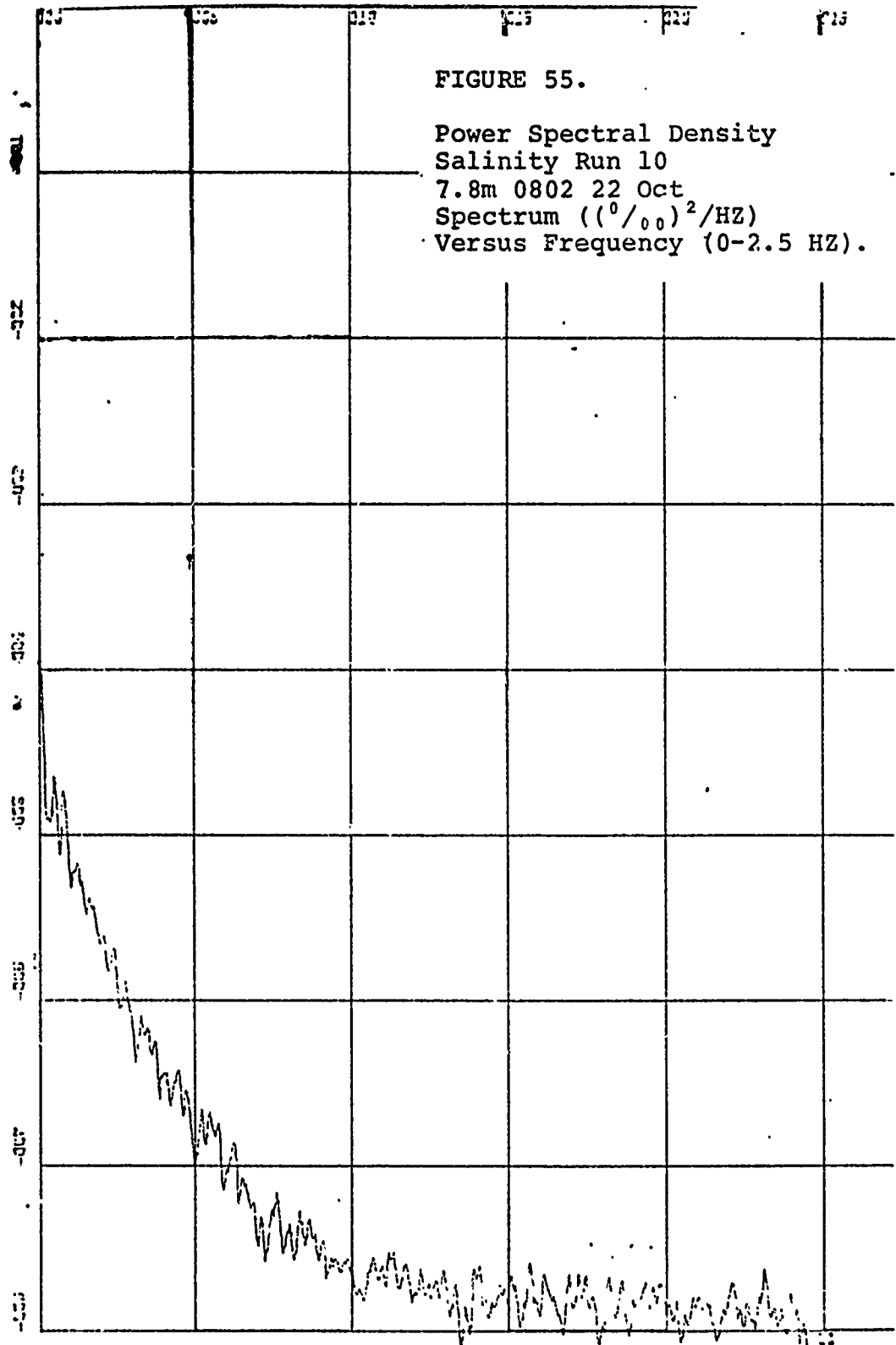


FIGURE 54.

Power Spectral Density
 Thermistor 1 Run 10
 7.8m 0802 22 Oct
 Spectrum ((°C)²/HZ)
 Versus Frequency (0-2.5 HZ).




```

2  CALX2 = ,F10.8//, H = ,F10.3//, X2 = ,F10.3//)
99  FORMAT (2I6,5F10.8)
801  FORMAT (6F10.5)
803  FORMAT (40H LONG WAVE STUDY OF MONTEREY BAY ,5X,7H DATE ,2A
14,10H HOUR 2A4//,5X,10A4//)
C BAND WIDTH FREQUENCIES OF TOTAL ENERGY FLUX- CMIN,CMAX
CMAX = 0.2

```

```

C COMPUTING POWER SPECTRUM
PI=3.14159265
FB = FBHZ*2.0*PI
DE = DHZ*2.0*PI
FMIN = 2.0*PI*CMIN
FMAX = 2.0*PI*CMAX
FORMAT(14F5.2)
READ(5,900)(F1(I),I=1,NTS)
WRITE(6,901)(F1(I),I=1,NTS)
FORMAT(14F7.2)
CALL TRNDF(F1,NTS,DT,CALX1)
CALL AVER(F1,NTS,DT)
DO 10 I=1,MLAG
SUM=0.0
NMAX=NTS-M+1
DO 8 I=1,NMAX
NN=M+I-1
SUM=SUM+F1(I)*F1(NN)
XMAX=SUM
XX=M-1
TAU(M)=XX*DT
PHI(M)=SUM/XNMAX
PHN(M)=PHI(M)/PHI(1)
CONTINUE
CALL PARZ(MLAG,PHI)
FORMAT(1,PHI(0))=,F10.4//)
NFR=50*(FB-FB)/DF+0.1
DO 14 N=1,NFR
XN=N
FREQ(N)=(XN-1.0)*DF+FB
CYCL(N)=FREQ(N)/(2.0*PI)
PER(1)=0.0
DO 15 N=2,NFR
PER(N)=1.0/CYCL(N)
MLAGM1=MLAG-1
XMLAG=MLAG
DO 50 N=1,NFR
SUM=0.5*(PHI(1)+PHI(MLAG)*COS(FREQ(N)*TAU(MLAG)))

```

Reproduced from
 best available copy.

```

C1=COS(FREQ(N)*DT)
S1=STN(FREQ(N)*DT)
CC=1.0
DO 49 N=2,MLAGM1
CT=CC#C1-SC*SI
ST=SC#C1+CC*SI
CC=CT
SC=ST
SUM=SUM+PHI(M)*CC
SPEC(N)=SUM#2.C/XMLAG
I(N,FLAGP) 741,741,742
742 CONTINUE
CALL PRESS(FREQ,SPEC,NFREQ,H,X2,DF,FB,FMAX)
741 CONTINUE
MD=3.14159265/(DF*DT*XMLAG)+0.1
DC = DF/(2.0*PI)
SUM = 0.0
DO 650 N=1,NFREQ
SUM = SUM + SPEC(N)
WRITE(6,651) SUM VARIANCE OF SPECTRUM//,3X,16H VARIANCE = ,F10.
651 FORMAT (25H //)
WRITE(6,106)(TAU(M),PHN(M),M=1,MLAG)
DO 9988 I=1,INUM
SPEC(I)=10*ALOG10(SPEC(I))
9988 CONTINUE
105 FPKMAT (10X,24H ENERGY SPECTRAL DENSITY//,5X,10H FREQUENCY,5X,13H
106 FORMAT (5X,F10.5,6X,F10.5)
WRITE(6,106) (CYCL(M),SPEC(M) ,M=1,NFREQ)
GO TO 200
888 STOP
END

C SUBROUTINE PRESS(FREQ,SPEC,NFREQ,H,X2,DF,FB,FMAX)
C DIMENSION FREQ(NFREQ),SPEC(NFREQ),SPECF(NFREQ)
NMAX = (FMAX-FB)/DF+1.0
DO 1 I=1,NMAX
C CALCULATE LINEAR WAVE LENGTH BY NEWTONS METHOD
1 FREQ(I)=0.00001) 8.7E-80
IF(XKHO=6.3) 5,1,1
1 XKH = XKHO

```

```

5 GO TO 9
3 XKH = SORT(XKHO)
  SH = SINH(XKH)
  CH = COSH(XKH)
  EPS = XKHO - XKH*SH/CH
  SLOPE = -XKH/CH**2 - SH/CH
  DXKH = -EPS/SLOPE
  IF (ABS(DXKH/XKH) - 0.0001) 9,9,4
4 XKH = XKH + DXKH
  GC TO 3
8 RESPE = 1.00
9 GO TO 11
  XKH/H = COSH(XK*H)/(COSH(XK*(H-X2)))
  RESPE = COSH(XK*H)/(COSH(XK*(H-X2)))
  IF (RESPE - 10.0) 11,11,12
  SPEC(I) = RESPE*RESPE*SPEC(I)
11 RETURN
12 END

```

```

SUBROUTINE TREND(FX,NTS,DT,CALXX)
DIMENSION FX(NTS)
C ALIBRA 104 I=1,NTS
104 FX(I) = FX(I)*CALXX
C COMPUTING THE LINEAR TREND
  NTS = NTS
  SUMF = 0.0
  DO 101 I=1,NTS
101 SUMF = SUMF + FX(I)
  DO 102 I=1,NTS
  XI = I
102 SUMF1 = SUMF1 + XI*FX(I)
  XNMI = NTS-1
  XNPI = NTS+1
  XM = (1.0/DT)*(FNTS*XNMI*XNPI) - 6.0*SUMF/(XNMI*FNTS)
  BMEAN = SUMF/FNTS
  FMEAN = SUMF/FNTS
  WRITE(6,9) FMEAN,XM,B
9 FORMAT(6,9) FMEAN,XM,B
1 = F10.5,9H SLOPE = ,F10.5,3X,13H INTERCEPT
  DO 103 I=1,NTS
  XI = I
103 FX(I) = FX(I) - (B+XM*XI*DT)
  RETURN
  END

```

```

SUBROUTINE SMD(MD, X1, X2, NFREQ)
DIMENSION X1(MD), X2(MD)
DO I = 1, MD
  NA = N + MD
  NN = NFR - Q - N + 1
  NB = NN - MD
  X2(N) = 0.25*(X1(1) + X1(NA)) + 0.5*X1(N)
  X2(NN) = 0.5*(X1(NN) + X1(NB))
  X2(MD+1)
  ME = NN - 1
  DC 2 N = MB, ME
  NA = N + MD
  NB = N - MD
  X2(N) = 0.25*(X1(NA) + X1(NB)) + 0.5*X1(N)
RETURN
END

```

```

SUBROUTINE AVER (FX, NTS, DT)
DIMENSION FX(NTS)

```

```

U2 = 0.0
SUMU2 = 0.0
DO I = 1, NTS
  U2 = FX(I)*FX(I)
  SUMU2 = SUMU2 + U2

```

```

CONTINUE
FNTS = NTS
U2 = SUMU2/FNTS
URMS = SQRT(U2)
WRITE(6, 152) U2, URMS
FORMAT (3X, 6H H2 = , F10.5, 3X, 8H HRMS = , F10.5, 5H M )
COMPUTING AVERAGE PERIOD, T
COUNTS THE TOTAL ZERO UP-CROSSINGS
USUM = 0.0
K = 1

```

```

68 N = K
69 IF(FX(N)) 73, 69, 69
73 K = N

```

```

71 K = K + 1
IF(FX(K)) 71, 71, 80
USUM = USUM + 1.0
IF(NTS - K) 83, 83, 68
T = FNTS*DT/USUM
83 WRITE(6, 82) T
82 FORMAT (3X, 18H AVERAGE PERIOD = , F10.5, 4H SEC//)
RETURN
END

```

151

152
COUNTS

68

69

73

71

80

83

82

```

C
SUBROUTINE PARZ (MLAG, PHI)
PARZ SUBROUTINE PARZEN FILTERS AUTO-CORRELATION FUNCTION
DIMENSION PHI (MLAG)
XMLAG = MLAG
MLAGH1 = XMLAG/2.0-0.1
DO 31 M=1, MLAGH1
MM = M-1
R = MM
RM = R/XMLAG
UM = 1.0-6.C*RM*RM*(1.0-RM)
PHI(M) = PHI(M)*UM
CONTINUE
DO 32 M = MLAGH1, MLAG
MM = M-1
R = MM
RM = R/XMLAG
RM1 = (1.0-RM)
UM = 2.0*RM1*RM1*RM1
PHI(M) = PHI(M)*UM
CONTINUE
RETURN
END
31
32

```

PROGRAM B

```
PROGRAM TO OUTPUT VALUES FROM WHICH A HISTOGRAM CAN BE PLOTTED
DIMENSION X(5399),BO(98),FREQ(98)
READ(5,1100) (X(I),I),I=1,5399)
FORMAT(14F5.2)
1100 XXX=C.58
DO 999 I=1,98
BO(I)=XXX
FREQ(I)=0.
XXX=XXX-0.01
999 CONTINUE
DO 998 I=1,5399
DO 997 J=1,98
IF(X(I),I).LT.80(J)) GO TO 997
FREQ(J)=FREQ(J)+1.
GO TO 998
997 CONTINUE
998 CONTINUE
995 WRITE(6,995) (BO(I),FREQ(I),I=1,98)
FORMAT(5X,F4.2,F10.0)
STOP
END
```

BIBLIOGRAPHY

1. Wilson, W. D., "Speed of Sound in Distilled Water as a Function of Temperature and Pressure," The Journal of the Acoustical Society of America, v. 31, p. 1067 - 1072, August 1959.
2. Wilson, W. D., "Speed of Sound in Sea Water as a Function of Temperature, Pressure, and Salinity," The Journal of the Acoustical Society of America, v. 32, p. 541 - 644, June 1960.
3. Mackenzie, K. V., "A Decade of Experience with Velocimeters," The Journal of the Acoustical Society of America, v. 50, p. 1321 - 1332, November 1971.
4. Del Grosso, V. A., "Sound Speed in Pure Water and Sea Water," The Journal of the Acoustical Society of America, v. 47, p. 947 - 949, March 1970.
5. Leroy, C. C., "Development of Simple Equations for Accurate and More Realistic Calculation of the Speed of Sound in Seawater," The Journal of the Acoustical Society of America, v. 46, p. 216 - 226, June 1968.
6. Liebermann, L., "The Effect of Temperature Inhomogeneities in the Ocean on the Propagation of Sound," The Journal of the Acoustical Society of America, v. 23, p. 563 - 570, September 1951.
7. Kadis, A. L. and Shonting, D. H., "The Thermiprobe. A System for Measuring Thermal Microstructure in the Sea," Instrument Society of America, Marine Sciences Instrumentation, v. 4, p. 652 - 660, Plenum Press, 1968.
8. Sagar, F. H., "Acoustic Intensity Fluctuations and Temperature Microstructure in the Sea," Journal of the Acoustical Society of America, v. 32, p. 112 - 121, January 1960.
9. James, R. W., Ocean Thermal Structure Forecasting, p. 105, U.S. Government Printing Office, 1966.
10. Mintzer, D. and Stone, R. G., "Transition Regime for Acoustic Fluctuations in a Randomly Inhomogeneous Medium," Journal of the Acoustical Society of America, v. 38, p. 843 - 846, November 1965.
11. Chernov, L. S., Wave Propagation in a Random Medium, McGraw - Hill, 1960.

12. Skudrzyk, E. J., "Thermal Microstructure in the Sea and Its Contribution to Sound Level Fluctuations," Chapter 12, Underwater Acoustics, V.M. Albers, ed., p. 199 - 233, Plenum Press, New York, 1963.
13. Smith, W. J., Jr., Amplitude Modulation of an Acoustic Wave Propagating Near the Ocean Surface, MS Thesis, United States Naval Postgraduate School, Monterey, 1971.
14. Rautmann, J., Sound Dispersion and Phase Fluctuations in the Upper Ocean, MS Thesis, United States Naval Postgraduate School, Monterey, 1971.
15. Duchock, C. J., The Measurement and Correlation of Sound Velocity and Temperature Fluctuations Near the Sea Surface, MS Thesis, United States Naval Postgraduate School, Monterey, 1972.
16. Bordy, M. W., Spectral Measurement of Water Particle Velocities Under Waves, MS Thesis, United States Naval Postgraduate School, Monterey, 1972.